The p+^{24}Mg Interaction in the Energy Range 20 to 50 MeV

D. K. Hasell

A thesis written in partial fulfilment of the requirements for a M.Sc. degree from the Physics Department at the University of Manitoba. 1978

The $p+{}^{24}Mg$ Interaction in the Energy Range 20 to 50 Mev

BY

DOUGLAS KENNETH HASELL

A dissertation submitted to the Faculty of Graduate Studies of the University of Manitoba in partial fulfillment of the requirements of the degree of

MASTER OF SCIENCE

Acknowledgements

I would like to thank Dcctors N. E. Davison, A. M. Sourkes, and B. T. Murdoch for their assistance and helpful suggestions during the experiment described in this thesis. Also, I am indebted to Dr. R. Abegg, and Dr. S. Datta for many useful discussions concerning the theory of the coupled channels calculations and for their aid with the computer codes used in these calculations.

Finnally, I wish to express my gratitude to my thesis advisor, Dr. W. T. H. van Oers, for his patience, guidance and support throughout the past few years.

It has been a pleasure learning from you.

Douglas Hasell

Abstract

Using the University of Manitoba sector focused cyclotron, measurements were taken of the differential scattering cross section of protons on ^{24}Mg at incident proton energies of 20.0, 25.0, 30.4, 34.9, 39.9, and 44.9 MeV, in the laboratory angular range 10° to 170°. This was done for scattering from seven different states of ^{24}Mg, namely: 0^+ (0.00 MeV elastic), 2^+ (1.37 MeV), the sum of 4^+ (4.12 MeV) and 2^+ (4.23 MeV), 3^+ (5.23 Mev), 4^+ (6.01 MeV), and 0^+ (6.43 MeV). The differential cross section data, along with data obtained from the literature, were analysed using a standard optical model as well as a coupled channels approach. Since ^{24}Mg is a strongly deformed nucleus it is thought that the optical model is not very suitable and some evidence of this is given in this work. The coupled channels analysis which is used to remedy this situation is also of questionable validity due to the fact that the analysis is limited by computational difficulties. Scattering from only the first three states of ^{24}Mg has been analysed so far using the computer code CHUCK. Work is continuing to include the first five states using the coupled channels code JUPITOR which permits rotational and vibrational states to be coupled together. The data are tabulated at the end of this thesis. Absolute errors of about 3 % for

elastic scattering to 30 % for the 0^+ (6.43 MeV) state are typical.

1.0 INTRODUCTION

This thesis describes the first part of a study made at the University of Manitoba Cyclotron Laboratory on the scattering of protons from ^{24}Mg. The study entailed measurements of the angular distributions of the proton differential scattering cross sections from seven states of ^{24}Mg, at six incident proton energies. The data were subsequently analysed, along with available data from the literature, using an optical model calculation to derive optical model parameters which best agreed with the elastic scattering data at each energy. No attempt was made at this point to arrive at a common set of geometry parameters, nor to observe systematic trends in the optical parameters with changes in energy. The data from the present work were then analysed using a coupled channels approach using the optical model potentials obtained as starting points. Fits to the differential scattering cross sections from the 0^+ (0.00 MeV elastic) and 2^+ (1.37 MeV) states were searched for by varying the strengths of the imaginary parts of the optical model potential. Later the geometry parameters of the imaginary parts of the optical model potential were varied as well. The large changes in the parameters necessary to obtain agreement between theory and experiment seem to indicate that the more accurate coupled channels calculation is better suited for describing the proton - ^{24}Mg interaction.

The justification for the improvement obtained by using the coupled channels approach may be seen by noting that ^{24}Mg is a highly deformed nucleus. Such deformed nuclei have rotational states which are strongly excited during nuclear scattering, thus playing an important role in the scattering process. Hence the optical model cannot be relied upon, since it assumes the inelastic contribution to be small and to be adequately represented by the imaginary terms of the optical model potential. When the inelastic and reaction channels are not negligible compared to the elastic channel these imaginary terms can no longer correctly average the effects of these channels. The coupled channels approach explicitly takes the inelastic channels into consideration, and for this reason is a more realistic theory to be compared with the experimental data.

The energy level scheme (shown in Fig. 1) of ^{24}Mg has been successfully described using a collective or liquid drop model of the nucleus.(1,2,3,4) With this model the two bands indicated, $K=0^+$ and $K=2^+$, are interpreted as being the ground state rotational band and the gamma vibrational band, respectively.

In this thesis the coupled channels calculation is limited to the first two states of ^{24}Mg. A more thorough study is underway to couple the first five states and to include in the analysis data from the literature (which includes polarisation data).

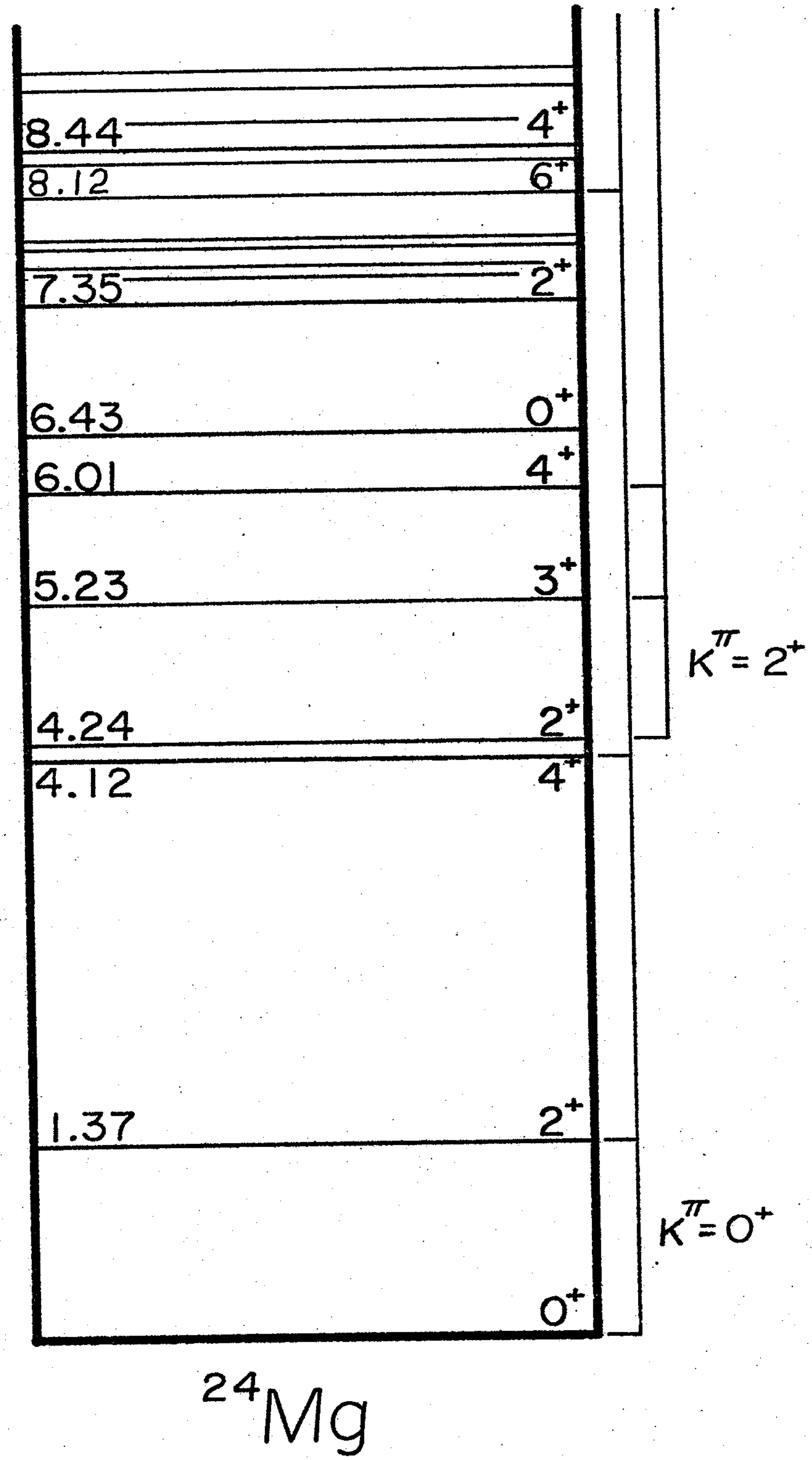

Fig. 1 Energy Levels of ^{24}Mg

2.0 THEORY

In attempting to explain nuclear processes theoretical predictions of physically observable quantities must be made to compare with the experimental data. It is hoped that such quantities can be derived from the solution of the correctly constructed Schrödinger equation. However, the Schrödinger equation must be formulated to properly describe the system composed of the incident projectile and the target nucleus, with all the motions and interactions that are present. Since the target nucleus is usually made up of a number of nucleons this is often very difficult, if not impossible.

Generally the interaction of the projectile with the individual nucleons of the nucleus is replaced by a nucleon-nucleus interaction. In doing this a nonlocal potential is replaced by a local potential . Thus the Schrödinger equation may be written as:

$$(H^1+H^2)\,\Psi = E\,\Psi$$

where H^1 is the Hamiltonian for the nucleon incident on the nucleus, and H^2 describes the states of the target nucleus. E is the total energy and Ψ the total wave function for the system.

For elastic scattering H^2 is usually ignored, since the target nucleus is assumed to be in the ground state and does not change in excitation. This is an approximation since it implies that there is no coupling between the various states of the target nucleus. When coupling is strong H^2 should be included. To obtain theoretical predictions for inelastic scattering (from states other than the ground state) H^2 must be included.

A more detailed description of a possible way of treating these two cases will be given in the following two sections.

2.1 OPTICAL MODEL

For the case where H^2 of the above equation is ignored, all that remains to be specified in the Schrödinger equation is the interaction potential. Numerous forms are possible, but perhaps the most widely used is the optical model potential (OMP). The form of the OMP can be justified from the nucleon-nucleon interaction. It results in inserting in the Schrödinger equation a nucleon-nucleus interaction. This approximation has several drawbacks. It limits the applicable energy range. Firstly, at low energies the incident nucleon is sensitive to compound nucleus effects. Secondly, at high energies the wavelength of the incident nucleon is comparable to the average nucleon separation in the nucleus, and as a result, it "sees" the nucleons in the nucleus as separate entities rather than the nucleus as a whole. Thus the OMP is reasonable only between 10 and 300 MeV.

By replacing the nucleon-nucleon interaction by an effective nucleon- nucleus interaction the characteristics of the former are buried. Adjusting the parameters of the OMP to optimize the fit to the data further hides any discrepancies. The OMP thus tends to be a phenomenological potential that fits the data for a wide range of target nuclei.

By not including H^2 in the calculation, possible processes which would remove incident nucleons from the system are omitted. The OMP corrects for this by introducing imaginary terms. The real part of the potential can account for the elastic scattering and the imaginary part accounts for incident nucleons absorbed or removed by other processes. This is at best an approximation since the inclusion of a single, imaginary potential cannot possibly replace the numerous, complicated processes taking place in the nucleus. However when the other processes are small in magnitude relative to the elastic one this is perhaps a reasonable simplification.

If the inelastic or reaction channels are comparable in cross section to the elastic one, the imaginary potential cannot replace the detailed structure that possibly exists. Also, no consideration is made about possible coupling between the various processes. Nevertheless, the optical model potential is very successful at describing elastic scattering and is useful as a starting point for more exact calculations.

To calculate the theoretical predictions one starts from the Schrödinger equation:

$$\left(-\frac{\hbar^2}{2m}\nabla^2 + V\right)\Psi = E\,\Psi \qquad (2.1.1)$$

where V is the optical model potential describing the interaction, m the reduced mass of the system, E the total energy, and Ψ the wave function for the system. The form of the OMP used in this work is:

$$V_C - V\,f(R,A) - i\left(W - 4AI\ WD\frac{d}{dr}\right) f(RI,AI) + \left(\frac{\hbar}{m_\pi c}\right)^2 (VSO + iWSO) \cdot (\vec{s}\cdot\vec{\ell})\frac{2d}{rdr}\, f(RSO,ASO)$$

$$f(R_i,A_i) = \left\{1 + \exp\left(\frac{r - R_i M_t^{\frac{1}{3}}}{A_i}\right)\right\}^{-1} \qquad (2.1.2)$$

where V_C is the Coulomb potential

$$V_C = \frac{ZZ'e^2}{2r}\left\{3 - \left(\frac{r}{R_C M_t^{\frac{1}{3}}}\right)^2\right\} \quad ; \quad r \leqq R_C M_t^{\frac{1}{3}}$$

$$= \frac{ZZ'e^2}{r} \quad ; \quad r \geqq R_C M_t^{\frac{1}{3}} \qquad (2.1.3)$$

V, W, WD, VSO, and WSO are the potential depths for the real central, imaginary volume, imaginary surface, real spin-orbit, and imaginary spin-orbit potentials respectively. Similarly, R, RI, and RSO are the reduced radii and A, AI, and ASO are the diffuseness parameters for the various potentials. Z and Z' are the charges of the incident projectile and the target nucleus.

Transforming the Schrödinger equation to spherical polar coordinates one obtains:

$$\left(-\frac{\hbar^2}{2m}\frac{1}{r}\frac{d^2}{dr^2}r + \frac{\hbar^2}{2m}\frac{L^2}{r^2} + V\right)\Psi = E\,\Psi \qquad (2.1.4)$$

Here L^2 contains all the angular dependence of ∇^2. If one assumes that the total wave function Ψ can be separated into radial, angular, and spin components (here we do the calculation for a spin 1/2 particle incident on a spin 0 target) one can substitute:

$$\Psi = \sum_{\ell,j}\frac{U_{\ell j}}{r}\sum_{m,m_s}(\ell s m m_s|jM)\;Y_{\ell m}\chi_{sm_s} \qquad (2.1.5)$$

All the radial dependence is contained in $U_{\ell j}/r$. The other two functions are chosen to be eigenfunctions of the operators L^2 and S^2. The $Y_{\ell m}$ are spherical harmonics and the χ_{sm_s} are spin wave functions. The $(\ell s m m_s|jM)$ are Clebsch-Gordan coefficients coupling the angular momentum ℓ and the spin s. After substitution and some algebra one obtains

$$\left(\frac{d^2}{d\rho^2} - \frac{\ell(\ell+1)}{\rho^2} + 1 - \frac{V'}{E}\right)U_{\ell j} = 0 \quad ; \; \rho = \frac{\sqrt{2mE}}{\hbar}\,r \qquad (2.1.6)$$

where the $\ell(\ell+1)$ comes from L^2 operating on $Y_{\ell m}$ V' is here:

$$V' = V_C - V\,f - i(W - 4Ai\;WD\frac{d}{dr})\,f + \left(\frac{\hbar}{m_\pi c}\right)^2(VSO + iWSO)\left\{{\ell \atop -\ell-1}\right\}\frac{2}{r}\frac{d}{dr}\,f \qquad (2.1.7)$$

where ℓ or $-\ell-1$ comes from ℓ operating on $(\ell s m m_s|jM)Y_{\ell m}$, depending on whether $j=\ell+1/2$ or $\ell-1/2$

respectively.

To solve this equation one imposes the following boundary conditions; that $U(r=0)=0$, and that at a radius where the nuclear force is negligible (r_m) the wave function Ψ be matched to a linear combination of regular and irregular Coulomb wave functions, namely

$$\Psi(r_m) = F_\ell(\eta,kr_m) + C_{\ell j}\{ G_\ell(\eta,kr_m) + F_\ell(\eta,kr_m)\} \tag{2.1.8}$$

Here F_ℓ and G_ℓ are respectively the regular and irregular Coulomb wave functions given in the asymptotic limit as:

$$F_\ell(\eta kr_m) = \sin(kr_m - \eta\ln(2kr_m) - \ell\tfrac{\pi}{2} + \sigma_\ell)$$
$$G_\ell(\eta,kr_m) = \cos(kr_m - \eta\ln(2kr_m) - \ell\tfrac{\pi}{2} + \sigma_\ell) \tag{2.1.9}$$

where

$$\eta = \frac{mZZ'e^2}{\hbar^2 k} \tag{2.1.10}$$

and σ_ℓ is the Coulomb phase shift:

$$\sigma_\ell = \arg(\Gamma(\ell+1+i\eta)) \tag{2.1.11}$$

Solving for the coefficients $C_{\ell j}$ permits calculation of the differential cross section, polarisation, and reaction cross section for scattering from the optical model potential. These values are generally compared with experimental data (often in a computer program) and the various parameters of the OMP are adjusted to minimize the difference (χ^2test). Care must be taken in performing such an analysis to avoid producing physically meaningless "fits" to the data.

2.2 COUPLED CHANNELS CALCULATION

The limitations of the optical model potential have been described above and when these limitations are stretched better calculations must be tried. The coupled channels (CC) calculation is such an improvement. For those cases where the elastic scattering process is not the only significant process and/or one wishes to calculate inelastic scattering cross sections as well, the CC calculation treats these other processes explicitly rather than replacing them with a complex potential. Of course not all inelastic scattering processes can be considered, so it is hoped that only a few need be treated in this fashion and that the others, as well as all reactions, can be accounted for in a general manner once more by using a complex potential. The CC calculation thus takes into account contributions that each process makes to the other processes. Correspondingly the calculation is more difficult.

The formulation of the problem requires the Hamiltonian H^2, as well as the wave function for the target nucleus, to be included in the Schrödinger equation. The model used in this work for the target nucleus is the liquid drop model. This model permits the nucleus to be deformed and to oscillate. The different modes of oscillation (rotations and vibrations) corresponding to the various excited states of the nucleus. This model is found to work quite well for a wide range of nuclei. The nuclear surface is given by

$$R = R_0(1 + \sum_{\lambda,\mu} \alpha_{\lambda\mu} Y_{\lambda\mu}) \qquad (2.2.1)$$

where $Y_{\lambda\mu}$ are the spherical harmonics and $\alpha_{\lambda\mu}$ are the deformation parameters.

Since the nucleus may be deformed it follows that the potential describing the interaction between the incident projectile and the nucleus should be conformally deformed. The potential used is the optical model potential, but with its usual radial dependence replaced by

$$R_i = R_{oi}(1 + \sum_{\lambda,\mu} \alpha_{\lambda\mu} Y_{\lambda\mu}) \qquad (2.2.2)$$

To solve, one expands the form factor of the OMP to second order yielding:

$$f(R_i,A_i) = f(R_{oi},A_i) + \frac{R_{oi}}{A_i} e' \; f(R_{oi},A_i)\Sigma + \frac{R_{oi}^2}{A_i} e'(e'-1) \; f(R_{oi},A_i) \; \Sigma^2$$

$$\Sigma = \sum_{\lambda,\mu} \alpha_{\lambda\mu} Y_{\lambda\mu} \quad , \quad e' = \exp(\frac{r-R_{oi}}{A_i}) \qquad (2.2.3)$$

Similarly, the Coulomb potential must be expanded:

$$V_c = \frac{ZZ'e^2}{2r}(3 - \frac{r}{R_c}) + \sum_{\lambda,\mu} \frac{3ZZ'e^2}{(2\ \ +1)}(\frac{r^\lambda}{R_c^{\lambda+1}}) \; (\alpha_{\lambda\mu} Y_{\lambda\mu}) + \ldots ; \quad r \leqq R_c$$

$$= \frac{ZZ'e^2}{2r} + \sum_{\lambda,\mu} \frac{3ZZ'e^2}{(2\ \ +1)} \; (\frac{R_c^\lambda}{r^{\lambda+1}}) \; (\alpha_{\lambda\mu} Y_{\lambda\mu}) + \ldots \quad ; \quad r \geqq R_c \qquad (2.2.4)$$

Substitution yields the deformed optical model potential. The expression is quite complicated but one observes that the potential has two parts; one equivalent to the standard optical model potential and another containing the deformation terms. It is this second part which determines the contributions from all the different states. Thus the deformed OMP can be considered as a standard OMP plus a potential describing the coupling. The Schrödinger equation becomes:

$$\left(\frac{d^2}{d\rho^2} - \frac{L^2}{\rho^2} + V_{omp} + V_{coup}\right) \Psi = (E - H^2)\, \Psi \qquad (2.2.5)$$

The exact expression for H^2 is not important since we only need to know the eigenvalues which result from it operating on the total wave function. Again we choose Ψ to be separable into radial, angular, spin, and now target nucleus wave functions.

$$H^2 \Phi_{I_n M_n} = \omega_n \Phi_{I_n M_n} \qquad (2.2.6)$$

$$\Psi = \sum_{J_n j_n \ell_n} \frac{U_{J_n j_n \ell_n}}{r} \sum_{M_n m_\ell m_s} (\ell_n s m_\ell m_s | j_n m_j)(j_n I_n m_j M_n | J_n M_n) Y_{\ell_n m}\, \chi_{s m_s} \Phi_{I_n M_n} \qquad (2.2.7)$$

where ω_n are the energy levels of the states considered. After substituting and some lengthy algebra (see Tamura's paper[7]):

$$\left(\frac{d^2}{d\rho_n^2} - \frac{\ell_n(\ell_n+1)}{\rho_n^2} - \frac{1}{E_n} V_{omp} + 1\right) U_{J_n j_n \ell_n} = \frac{1}{E_n} \sum_{J_{n'} j_{n'} \ell_{n'}} \langle \Psi_{J_n j_n \ell_n} | V_{coup} | \Psi_{J_n j_{n'} \ell_{n'}} \rangle\, U_{J_n j_n \ell_n} \qquad (2.2.8)$$

$$;\ n = 1, \ldots, n_c$$

where n_c is the number of nuclear states coupled together, and $\langle \psi' | V_{coup} | \psi \rangle$ is the expectation value of V_{coup} coupling ψ' to ψ .

Solving these n_c coupled differential equations one again imposes the boundary conditions that $U(r=0)$ is finite and that in the asymptotic limit it matches with a linear combination of regular and irregular Coulomb wave functions as before. Once the coefficients $C_{Jj\ell}$ (note that there are now different coefficients for each state, ℓ_n, j_n, J_n value) are determined the differential cross sections, etc. can be calculated. As can be seen CC calculations are considerably more difficult.

The formulation introduces only a few new parameters, i.e. the deformation parameters. (In the present work one new parameter $\beta_2 = \alpha_{20}$ was used, thus the expansion used was $R=R_0(1+\beta_2 Y_{20})$; this was a limitation imposed by the computer code CHUCK and will be improved upon in later work.). With this, plus the optical model parameters, many more data is available for comparison. This imposes greater restrictions on the parameters than before, thus reducing possible ambiguities.

By explicitly treating the inelastic channels it should be possible to reduce the strength of the imaginary parts in the OMP. Ideally, if all the inelastic and reaction channels were treated; the imaginary parts could be removed entirely and the potential could be strictly real. This is not feasible, but perhaps the agreement with data will become less dependent on the imaginary potential strengths, leading to better defined real strengths, when a number of channels are treated. This would simplify the understanding of the nuclear interaction greatly.

The fact that in this approach scattering channels are coupled permits the calculation of processes which do nct occur directly. Such multi-step processes cannot be calculated by using other approaches, such as the distorted wave Born approximation (DWBA), which do not have coupling.

However the theory described above is not complete in that only elastic and inelastic scattering is considered. This excludes a variety of reactions, such as knockout or pick up reactions, which should be taken into account. The magnitude of these processes are expected to be sufficiently small when compared with the inelastic ones to permit their omission.

3.0 EXPERIMENTAL APPARATUS

3.1 EXPERIMENTAL LAYOUT

In performing this experiment the proton beam facility of the University of Manitoba sector focused cyclotron was used. The relevant experimental layout is shown in Fig. 2 . Magnetic quadrupole doublets (Q1, Q2, and Q3) were used to focus the proton beam through the system. Slits 1 and 2 served to collimate and to define the proton beam in momentum, respectively. In order to monitor the beam transport through the system, screens were lowered into the beamline and observed through closed circuit television. Steering magnets (S1, S2, and S3) were available to centre the proton beam on axis (mostly to correct for motion off the median plane). The switching magnet bent the proton beam into the left 45° beamline which was used in this experiment. The switching magnet also served to momentum analyse the proton beam.

After traversing the scattering chamber the protons were collected in the Faraday cup. During an experimental run the total charge collected was integrated and used as a normalization.

To reduce the amount of background radiation due to gamma rays produced at the second set of slits lead shielding was arranged around the entrance to the scattering chamber. Also, a 10 cm cylinder of lead with a 4 cm diameter hole was placed in the beamline before the chamber. The Faraday cup was heavily shielded with steel bricks to similarly reduce the background created by the stopping protons.

3.2 SCATTERING CHAMBER

A layout of the scattering chamber used is shown in Fig. 3. The chamber itself is a cylinder of mild steel approximately 1.17 m in diameter and 0.60 m deep. The interior is machine finished and a number of ports exist for viewing, pumping, proton beam entrance and exit, etc. A turntable is mounted at the bottom of the chamber and this is driven by an external motor. An external deci-track shaft encoder provides digital angular read out of the turntable position. Before the start of the experiment this system was carefully aligned to within 0.02° (see Appendix 10.2).

The beam of protons enters the scattering chamber from the left, passes through the centre of the chamber, and exits through a 0.075 mm KAPTON H foil. It then travels through about 3 cm of air before entering the Faraday cup through another KAPTON H foil.

Targets are lowered into the centre of the chamber through a target lock in the centre of the top lid. The targets are mounted on a target ladder capable of supporting five targets. It is also possible to raise the target ladder into an air tight cylinder which can either be evacuated or filled with an inert gas. This feature is necessary when working with targets (like Magnesium) which are chemically reactive. When the target ladder is lowered into the scattering chamber an aluminum cylinder serves to centre the targets. Notches on the shaft of the ladder outside the chamber indicate the vertical position of the targets. The angle of the targets with respect to the incident beam is given by a scale on the outside of the target ladder assembly.

Mounted at 15° on either side of the proton beam axis are two NaI(Tl) detectors. Since the differential elastic scattering cross sections vary rapidly with angle at the forward angles, any asymmetry in the number of counts received by these two detectors would indicate that the beam was passing through the chamber at an angle. The alignment and symmetry of these detectors were verified before the experiment by using the detector array at overlapping settings.

Rigidly mounted to the turntable is the housing for the array of eight detectors and the slit and anti-scattering baffle system. (see Fig. 4) The array housing holds eight NaI(Tl) detectors which detect protons scattered into the solid angle defining slits. These slits are mounted at 10.00° ± 0.02° intervals along the face of the array. Between the detector housing and the target there is a system of slits which restricts particles scattered from objects other than the target from reaching the detectors.

During the experiment the chamber was operated at a pressure of 6 - 8 * 10^{-6} torr.

3.3 ELECTRONICS

Electrical connections to the eight detectors are made by coaxial cables with vacuum feed-throughs in a port in the centre of the bottom lid of the scattering chamber. Immediately outside the chamber the signals from the detectors are pre-amplified. From there the cables pass through a grounded metal cable conduit (to reduce background electrical noise) to the amplifiers in the control room. A schematic diagram for two detectors is given in Fig. 5.

The output from the amplifiers was fed into a single channel analyser (SCA) and through a delay to a linear gate operated in the normally closed mode. The SCA was used to set thresholds and to provide the gating pulse for the linear gate. The number of such gating signals was recorded by a scaler and used as the total number of events detected. The delay on the linear signal from the amplifier and the width of the gating signal from the SCA were adjusted so that the gating pulse overlapped the linear signal. Thus, when a valid event (above threshold) occurred; the linear signal was transmitted to the dual sum and invert amplifier (DSI).

For this experiment four analogue to digital converters (ADC) were used. Thus a pair of detectors fed into one DSI, which in turn fed into one ADC. A PDP 15/20 computer was used on-line to store the experimental data in spectra of 512 channels corresponding to each detector. Differentiating between two detectors providing signals to one ADC was accomplished by using the 'busy' output from the linear gates as a flag to instruct the computer as to which detector produced a given signal.

The two 15° monitor detectors were handled in a similar fashion, except that the SCA was used to set an energy window around the elastically scattered proton peak; the ADC was used only during set up and disconnected during a run. The two scaler values served to monitor the alignment of the incident proton beam.

The charge collected by the Faraday cup was also transported to the control room where it was integrated using a Brookhaven Current Integrator. The digitised output was also recorded by a scaler.

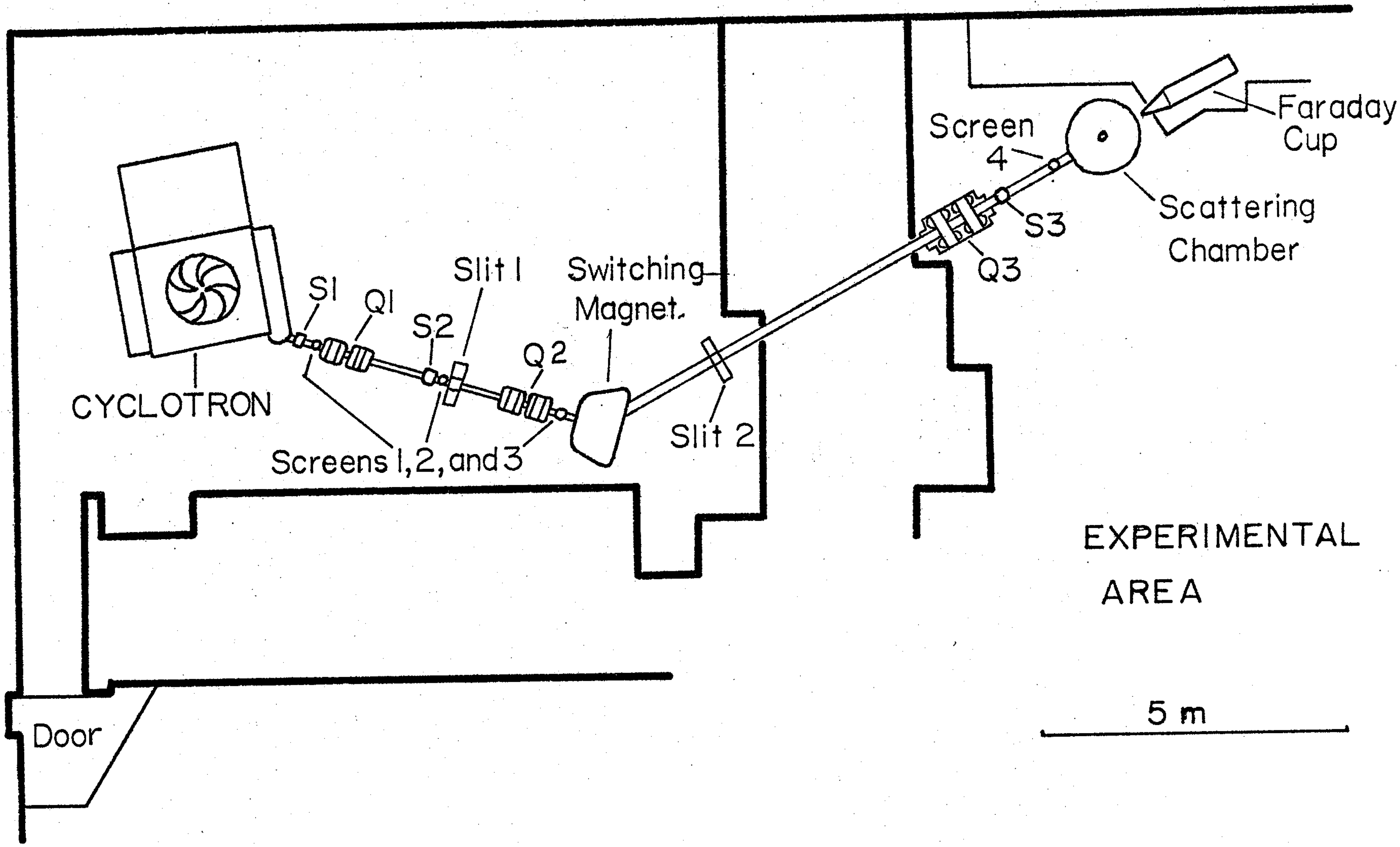

Fig. 2 Experimental Layout

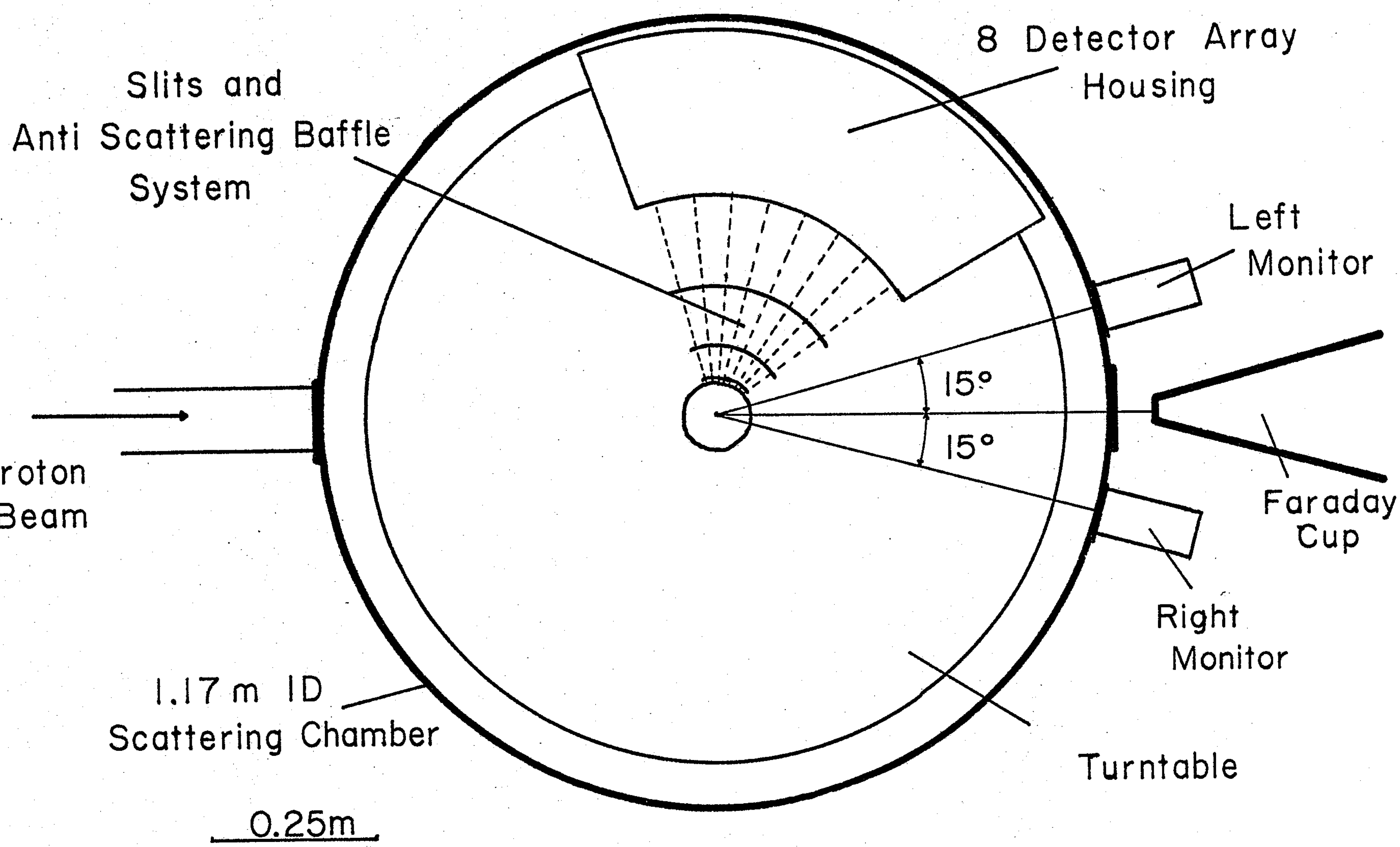

Fig. 3 Scattering Chamber

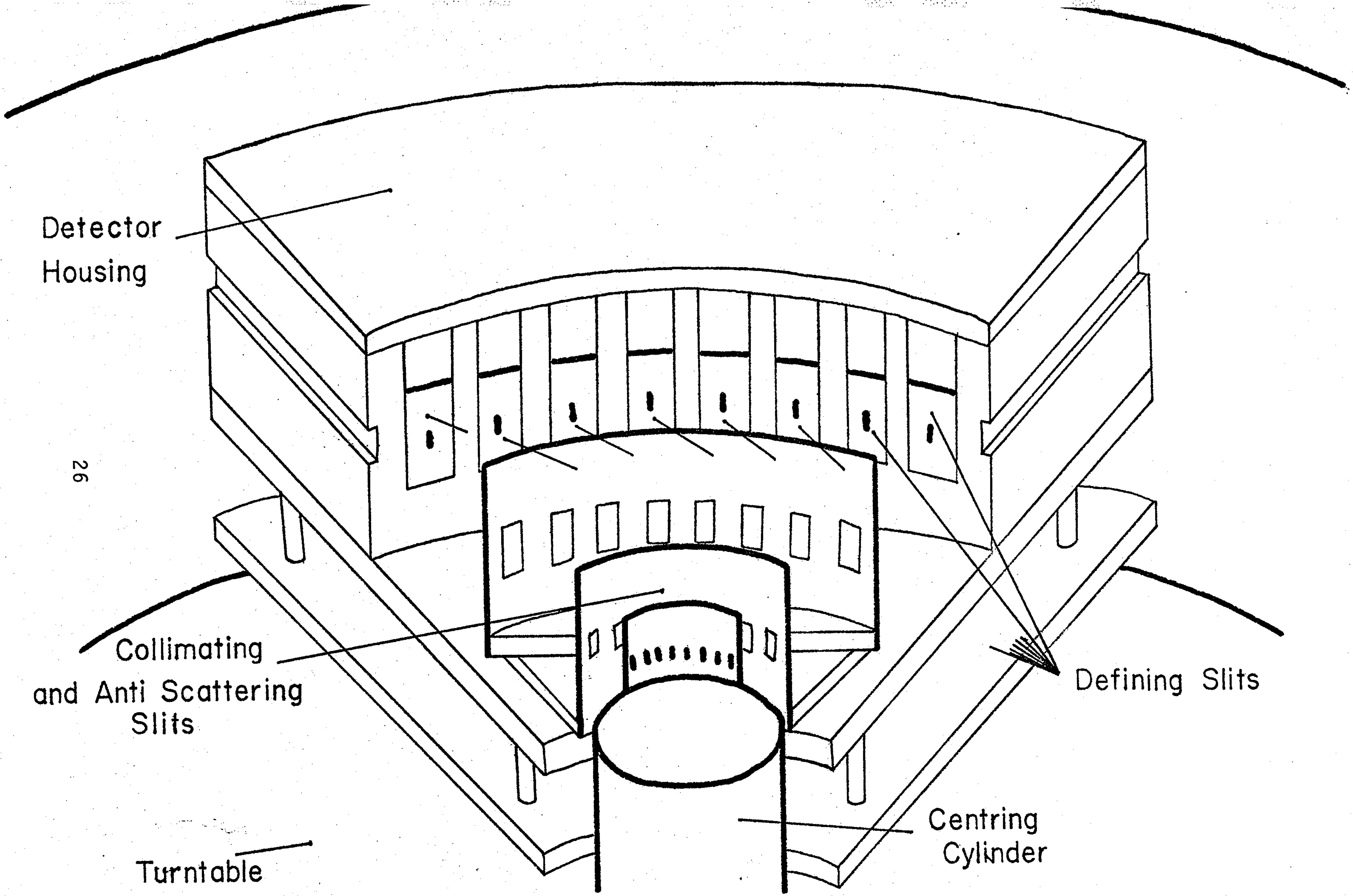

Fig.4 Detector and Slit System

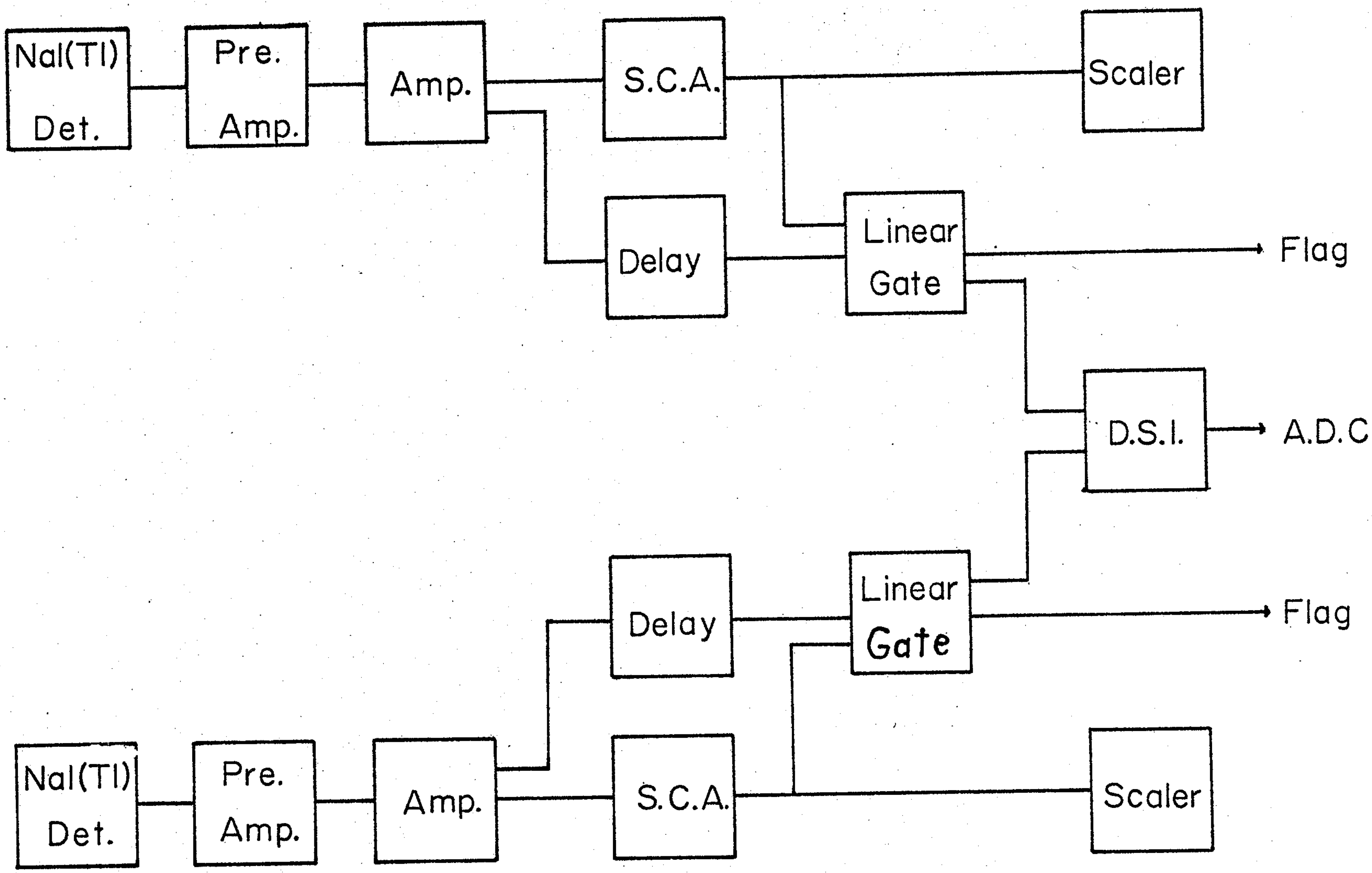

Fig. 5 Electronics

4.0 EXPERIMENTAL METHOD

4.1 PROTON BEAM TRANSPORT

In order to obtain a well defined proton beam the magnetic quadrupole doublet Q1 was used to produce a horizontal waist at the first set of slits. These slits were set at a separation of about 1.0 cm vertical and 0.5 cm horizontal. The magnetic quadrupole doublet Q2 had calculated settings to give an energy focus at the second set of slits. The switching magnet bent the proton beam through 45° to the left. An NMR probe in the switching magnet was used to measure the field strength and, using a previous calibration (see Appendix 10.3), the mean proton beam energy was determined to within 100 kev.

Slit 2 had settings of 1.0 cm (vertical) and 0.5 cm (horizontal). Q3 was used to produce a waist in the proton beam at the centre of the scattering chamber. Typically the beam spot had dimensions of 0.8 cm vertically and 0.4 cm horizontally.

The proton beam could be observed on screens 1-4 and on a plastic scintillator mounted on the target ladder which could be lowered into the centre of the chamber. Steering magnets (S1, S2, and S3) were available to centre the proton beam on axis but this was avoided if possible. Two additional checks on the proton beam alignment were imposed. Firstly, the beam was required to be not steered by the quadrupole lens. Secondly, the ratio of count rates observed by the two 15# monitor detectors was required to be 1.00 ± 0.03.

Typical beam currents obtained were 10-100 nA into the Faraday cup.

4.2 TARGETS

Two isotopically enriched targets of ^{24}Mg were purchased from ORNL for the experiment. They were shipped in small, sealed jars in an inert atmosphere. All handling of the targets for weighing, mounting on the target ladder, and transporting had to be done without exposing the targets to air. To accomplish this a large glove box filled with argon gas was used. The target ladder could be directly attached to the glove box for mounting the targets and then evacuated for carrying to the experimental scattering chamber.

This method produced ^{24}Mg targets virtually free of oxygen contamination, thus simplifying the analysis. Weighing and measuring the area of the targets indicated thicknesses in agreement with the manufacturer's values. However, analysis of the experimental data showed an oxygen contamination of approximately 0.04 mg/cm^2 in both targets. The thicknesses used for the calculations were 4.928 ± 0.125 and 10.108 ± 0.250 mg/cm². In the error calculation 0.5 % was included to account for nonuniformity in the targets and 2 % for uncertainty in determining the area of the targets.

During the experiment the thin target was used for incident proton energies below 35 MeV and the thick target was used at 35 MeV and higher.

4.3 DATA ACQUISITION

Once a good proton beam with the desired energy had been obtained, the detector array was set at a specified angle and the experimental run started. These runs consisted of accumulating data in the form of spectra for the eight detectors corresponding to eight angles separated by 10° . The criterion for finishing a run was to have more than 5000 counts (for good statistics) in each elastic peak. At the end of a run the spectra were stored on magnetic tape for later analysis and the scaler values for the detectors and Faraday cup were recorded. The detector array was then moved to the next angle and the process repeated. The sequence of angles was such that measurements were taken at complementary angles left and right of the incident beam axis. Thus when the left and right measurements were averaged any errors due to instrumental asymmetries were cancelled to first order. This process was continued until satisfactory data had been collected both left and right of the beam axis for angles from 10° to 90° in 2.5° steps, and from 90° to 170° in 5.0° steps.

The two 15° monitor detectors were checked regularly to verify that the beam was still on axis. Fluctuations in the ratio left to right (of the number of protons elastically scattered from ^{24}Mg) of up to 3 % were allowed before the beam transport parameters were adjusted.

To ensure that the target ladder did not obstruct the detector's view of the target, the targets were rotated 30° from perpendicular to the incident beam so as to face the detector array. This had the additional effect of increasing the apparent thickness by a factor of 1/cos30°.

In this manner data was obtained at six incident proton energies, namely: 20.0, 25.0, 30.4, 34.9, 39.9, and 44.9 MeV, as calculated at the effective target centre. An example of a typical spectrum collected is shown in Fig. 6.

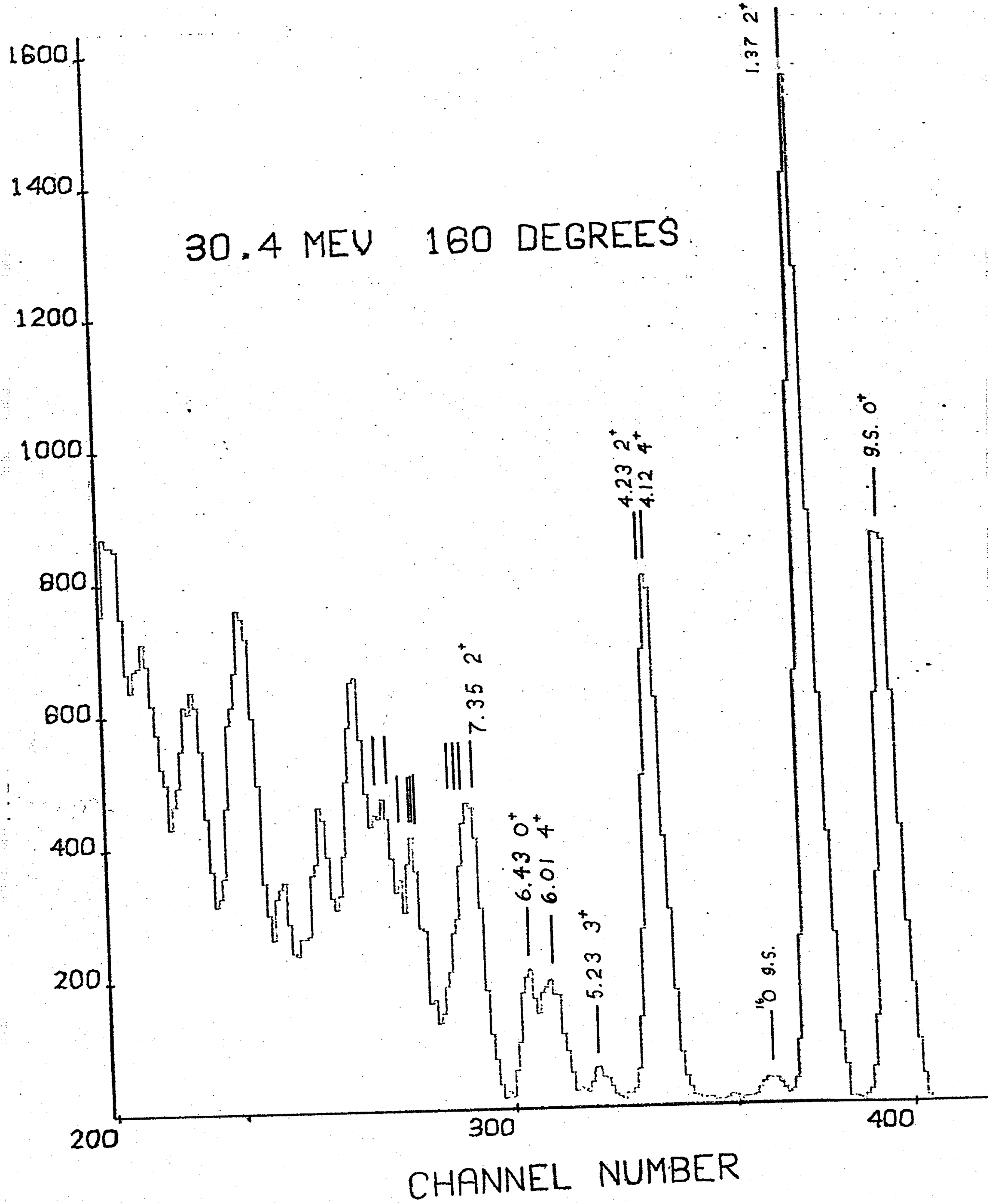

30.4 MEV 160 DEGREES
1600
1400
1200
1000
800
600
400
200
200
300
400
CHANNEL NUMBER
1.37 2+
9.S. 0+
4.23 2+
4.12 4+
7.35 2+
6.43 0+
6.01 4+
5.23 3+
16O g.s.

Fig. 6

5.0 DATA REDUCTION AND ERROR ANALYSIS

5.1 CALCULATION OF THE DIFFERENTIAL CROSS SECTION

The differential cross section for elastic and inelastic scattering was calculated from the formula:

$$\frac{d\sigma}{d\Omega} = \frac{Y\varepsilon}{Nnd\Omega} \tag{5.1.1}$$

Y - number of protons observed in the peaks of interest

N - number of incident protons

n - number of target nuclei per unit area

$d\Omega$-solid angle subtended by the detector

ε - corrections for deadtime, reactions in the detector, and finite geometry

A computer program was written to take the results of the spectra analyses, along with the scaler values for each run, and to calculate the differential cross sections for each detector. The program applied a number of corrections (see 5.3) and averaged the data for the same absolute angle and energy. The formula used to find the mean differential cross section was:

$$\frac{\sum_{i=1}^{N} \frac{x_i}{\sigma_i}}{\sum_{i=1}^{N} \frac{1}{\sigma_i}} \tag{5.1.2}$$

N - number of independent measurements

x_i- differential cross section

σ_i - uncertainty in x_i

Certain corrections required knowledge of the differential cross section. The program did a preliminary calculation, applied the corrections, and calculated the final differential cross sections.

The 0+ (6.43 MeV) state was not always clearly resolved from the 4^+ (6.01 MeV) state owing to its small cross section at forward angles. In the computer analysis of the spectra its yield was thus small and not statistically useful. To overcome this problem the yields of these two states were added together for calculating the differential cross section and the cross section for the 4^+ (6.01 MeV) was subtracted from it. This improved the determination of the 0^+ (6.43 MeV) cross section considerably.

5.2 COMPUTER ANALYSIS OF SPECTRA

A computer program was written to analyse the spectra produced. Analysis consisted of identifying the peaks of interest, subtracting the background, subtracting the oxygen contamination, unfolding the peaks, and calculating the number of events detected in each peak.

A typical spectrum is shown in Fig. 6. It shows the number of events observed as a function of the energy of the scattered proton (channel number). The peak furthest to the right thus corresponds to elastically scattered protons from ^{24}Mg. The other peaks are due to various inelastic scattering processes. A small peak due to elastic scattering from ^{16}O is also visible. The peaks of interest are 0^+ (0.00 MeV elastic), 2^+ (1.37 MeV), 4^+ (4.12 MeV), 2^+ (4.23 MeV), 3^+ (5.23 MeV), 4^+ (6.01 MeV), and 0^+ (6.43 MeV). The 4.12 MeV and 4.23 MeV states could not be resolved in this experiment but the sum of their cross sections was determined. Other peaks corresponding to higher states are visible, but since these peaks are made up of numerous states, they were not considered here.

The program started from the elastic peak and, using relativistic kinematics, located the other peaks of interest. The background was computed assuming that the background at any particular channel was due to the background produced by higher channels. The contribution that each of these higher peaks made was assumed to be proportional to its amplitude. Since the region of interest is above the three particle breakup continuum threshold this was considered to be reasonable.

The program then used the elastic peak as the characteristic peak shape in calculating the number of events in each of the peaks of interest. The contribution due to the oxygen contamination was accounted for by introducing the differential cross section for elastic scattering of protons by oxygen[28] interpolated to this energy and angle. The program then calculated the expected yield.

The uncertainty in the yield was taken as:

$$\sqrt{A + 2B} \tag{5.2.1}$$

where:

A - yield determined by the program

B - amount subtracted due to background and other peaks

If the oxygen peak contributed to the background of a peak an additional 10 % of this amount was added to account for any uncertainty in the oxygen contamination. Generally the oxygen yield was only 1 % of the elastic yield.

5.3 CORRECTIONS

The formula used in 5.1 assumes that Y was the total number of protons scattered into the solid angle $d\Omega$. However the yield as determined by the analysis of the spectra is only the number of relevant events as seen by the computer. Corrections must be made for the losses due to the finite deadtime of the electronics, and for proton reactions in the NaI(Tl) detector. The finite size and divergence of the incident proton beam and the finite size of the solid angle defining collimators must also be considered.

The deadtime of the electronics was calculated assuming that the scalers recorded the correct number of protons entering the detector. By integrating the spectra the total number of events recorded was found. The difference between these two numbers would then be the number of events lost due to deadtime. The number of events lost from the yield would then be this difference times the ratio of the yield to the integral of the spectra. This is equivalent to multiplying the yield from the analysis of the spectra by the ratio of scaler counts to computer counts. The deadtime correction was usually less than 1 % .

Losses in events due to the protons undergoing nuclear reactions in the NaI(Tl) detectors was accounted for by using the recent results of Sourkes et. al.[8] For each measurement the energy of the proton entering the detector was calculated, and the percentage loss due to reactions was interpolated to this value and used to correct the yield. The correction was always less than 2.0 %.

The finite beam geometry correction used the formula as derived by Wilmes.[9] In this formulation the incident protons are assumed to originate from a source area, strike an area of the target , and scatter into the detector. A given event can originate from anywhere on the source, scatter from anywhere on the target, and impinge anywhere on the detecting surface. Thus scattering angles are different from those expected and the detector subtends a larger effective solid angle. The calculation however requires knowledge of the first and second derivatives of the differential cross section with respect to angle. These quantities are calculated from preliminary cross section angular distributions.

Once all the corrections have been applied and the errors (see next section) taken into account the final differential cross sections are calculated.

5.4 UNCERTAINTIES

For each measurement made, the differential cross section and the uncertainty in the measurement was calculated. The uncertainty was determined as the square root of the sum of the squares of the relative uncertainties arising from the various components of the measurement. Using this result as a weighting factor, the mean differential cross section for a given incident energy and absolute angle was calculated. The uncertainty in this mean value was then calculated using:

$$\frac{\sum_{i=1}^{N} \frac{(x_i-\mu)^2}{\sigma_i^2}}{(N-1)\sum_{i=1}^{N} \frac{1}{\sigma_i^2}} \qquad (5.4.1)$$

where:

μ - mean differential cross section

x_i-individual measurement of the differential cross section

σ_i- uncertainty in the individual measurement

N - number of individual measurements taken

Added in quadrature to the uncertainty in the mean were the absolute uncertainties to obtain the absolute error in the mean values.

Table 1 shows the uncertainty used for each component or how it was determined. Some of these values reflect the limitations of the instruments or the methods used, while others are estimates of the uncertainty involved. The possible error due to the uncertainty in the incident proton beam energy and detector angle was calculated using the derivative of the cross section with respect to energy and angle respectively.

Due to the small cross sections of the highest three states for which measurements were made; statistics were poor. In addition the unfolding of the peaks from one another is likely to have introduced additional errors not considered. For these reasons an additional 10 % uncertainty was added in quadrature with the uncertainties of the 3^+ (5.23 MeV), and 4^+ (6.01 MeV) states. Similarly the subtraction method used in determining the 0^+ (6.43 MeV) cross section is of limited accuracy, and a 30 % uncertainty was incorporated here to cover this.

Table 1 Uncertainties

Yield (statistics)	$\sqrt{Y + 2 * BGD}$	rel.
Solid Angle	1 %	abs.
Target Angle	0.5°	abs.
Target Thickness	0.125 mg/cm² thin target	abs.
	0.25 mg/cm² thick target	abs.
Current Integration	1 %	abs.
Deadtime Correction	5 % of correction	rel.
Reactions in NaI(Tl)	5 % of correction	rel.
Finite Geometry	5 % of correction	rel.
Detector Angle	0.02°	rel.
Proton Energy	0.100 MeV	rel.

rel. - relative uncertainty
abs. - absolute uncertainty, magnitude

6.0 EXPERIMENTAL RESULTS

The differential cross sections obtained for protons scattered by ^{24}Mg, both elastically and inelastically, are shown in Fig.'s 7-12. The tabulated data are given in Appendix 10.1. The data shown were collected for proton energies (as calculated at the centre of the target) of 20.0, 25.0, 30.4, 34.9, 39.9, and 44.9 MeV. The excited states of ^{24}Mg for which data is presented are 0^+ (0.00 MeV), 2^+ (1.37 MeV), the sum of 4^+ (4.13 MeV) and 2^+ (4.23 MeV), 3^+ (5.23 MeV), 4^+ (6.01 MeV), and 0^+ (6.43 MeV). Relativistic transformations to the centre of momentum frame were used throughout.

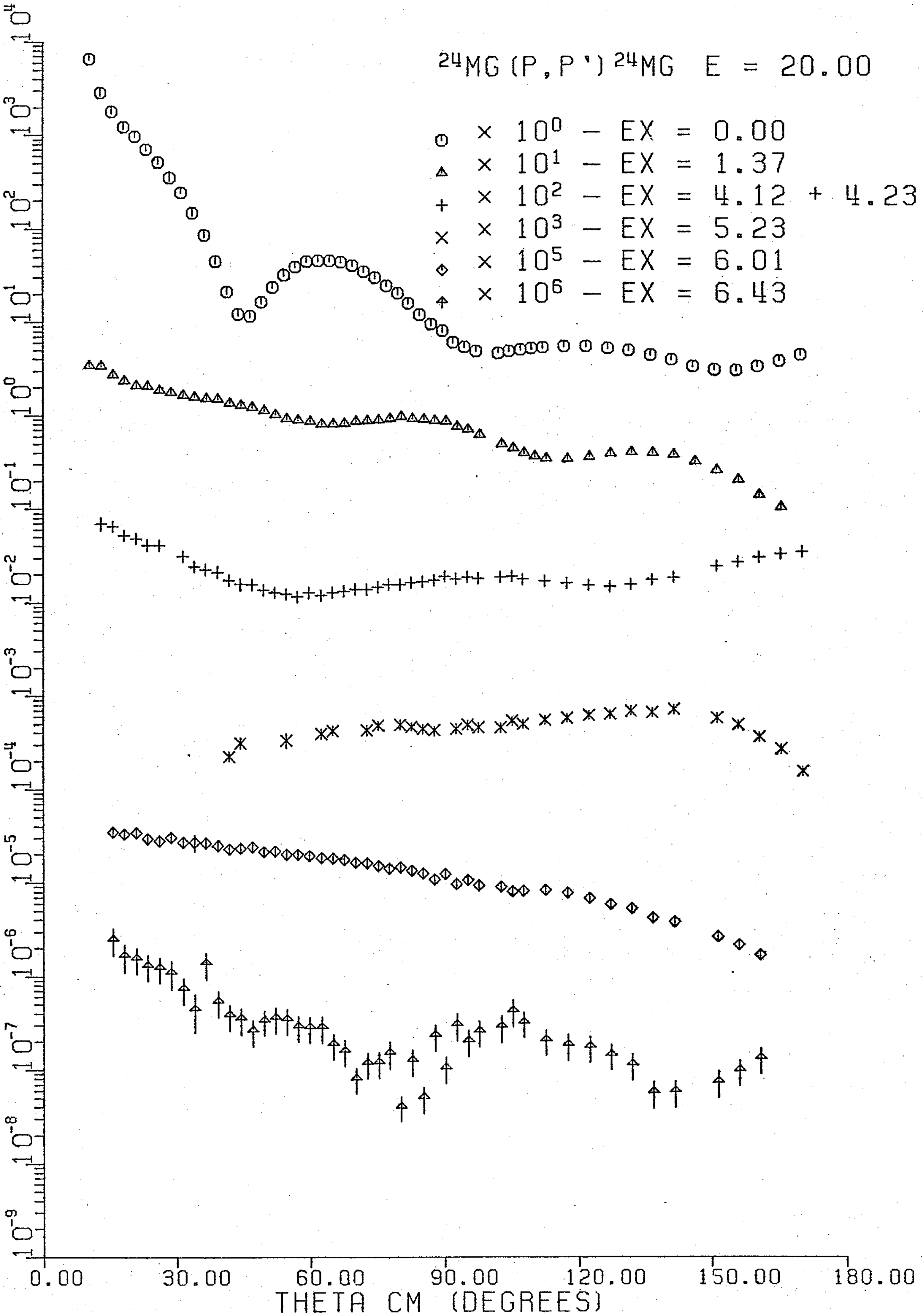
^{24}MG(P,P')^{24}MG E = 20.00
× 10^0 – EX = 0.00
× 10^1 – EX = 1.37
× 10^2 – EX = 4.12 + 4.23
× 10^3 – EX = 5.23
× 10^5 – EX = 6.01
× 10^6 – EX = 6.43
10^4
10^3
10^2
10^1
10^0
10^{-1}
10^{-2}
10^{-3}
10^{-4}
10^{-5}
10^{-6}
10^{-7}
10^{-8}
10^{-9}
0.00
30.00
60.00
90.00
120.00
150.00
180.00
THETA CM (DEGREES)

Fig. 7

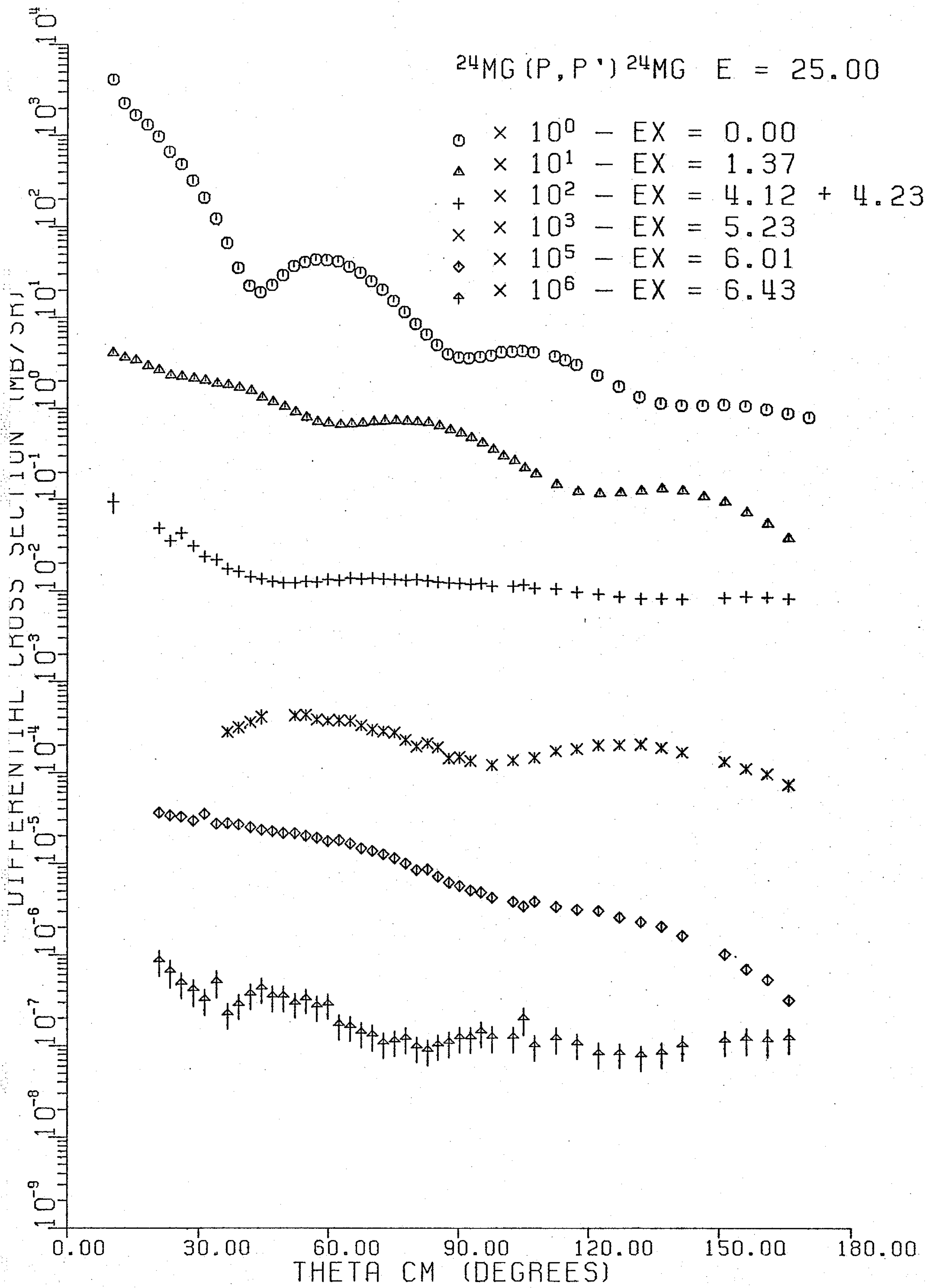

^{24}MG (P,P') ^{24}MG E = 25.00
× 10^0 – EX = 0.00
× 10^1 – EX = 1.37
× 10^2 – EX = 4.12 + 4.23
× 10^3 – EX = 5.23
× 10^5 – EX = 6.01
× 10^6 – EX = 6.43
DIFFERENTIAL CROSS SECTION (MB/SR)
THETA CM (DEGREES)

Fig. 8

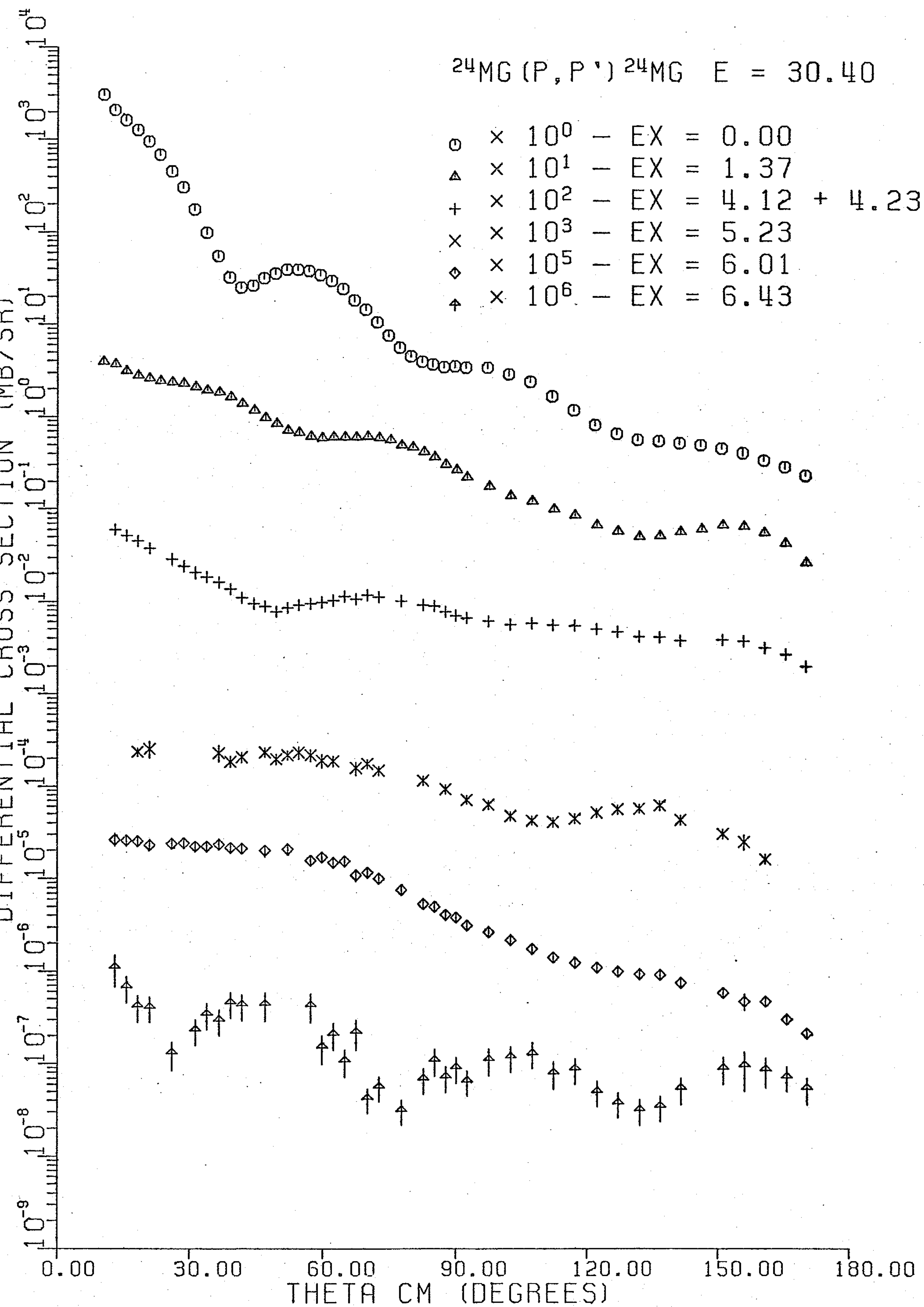
^{24}MG(P,P')^{24}MG E = 30.40
× 10^0 − EX = 0.00
× 10^1 − EX = 1.37
× 10^2 − EX = 4.12 + 4.23
× 10^3 − EX = 5.23
× 10^5 − EX = 6.01
× 10^6 − EX = 6.43
0.00 30.00 60.00 90.00 120.00 150.00 180.00
THETA CM (DEGREES)

Fig. 9

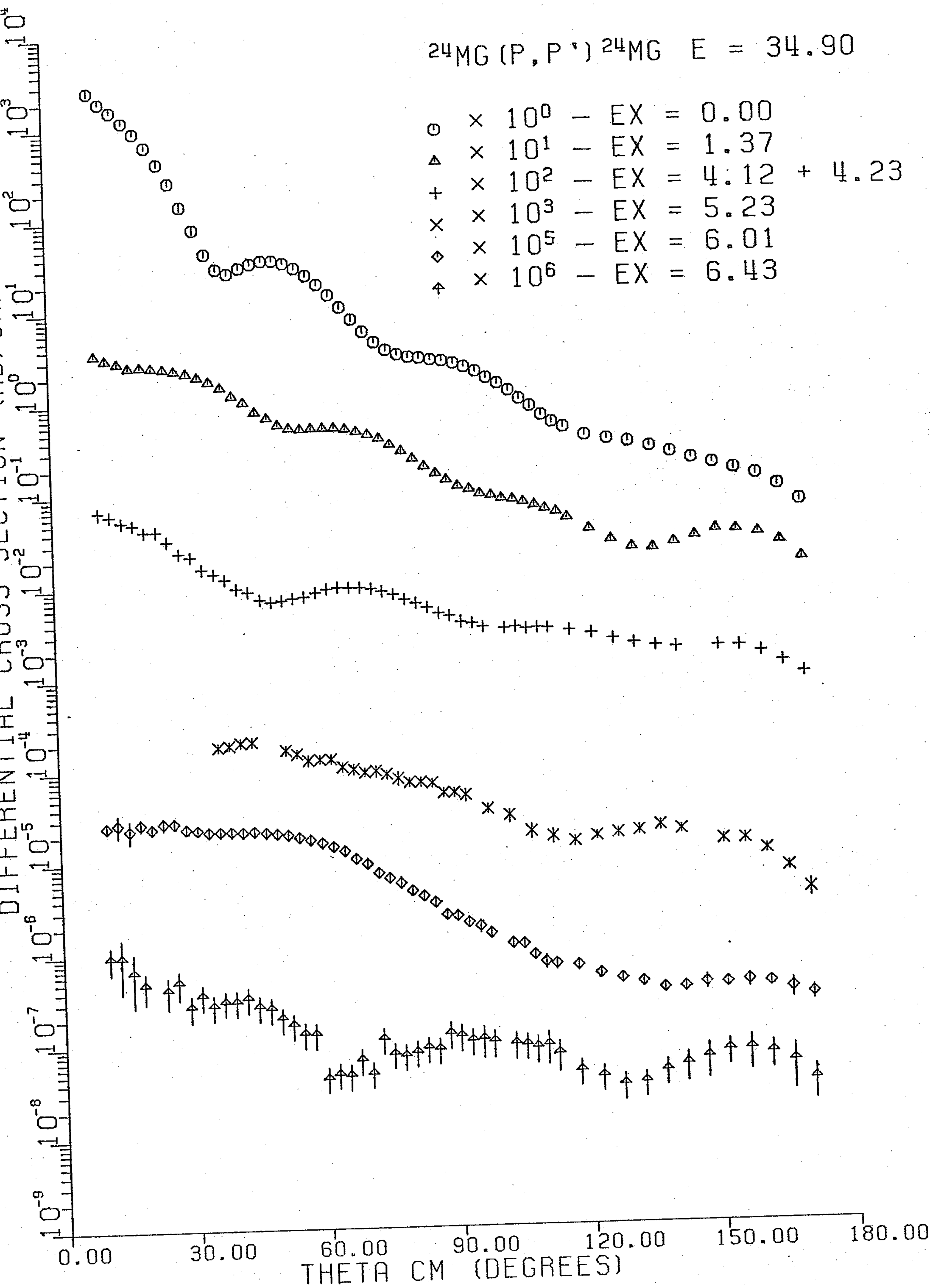

^{24}MG(P,P')^{24}MG E = 34.90
× 10^0 — EX = 0.00
× 10^1 — EX = 1.37
× 10^2 — EX = 4.12 + 4.23
× 10^3 — EX = 5.23
× 10^5 — EX = 6.01
× 10^6 — EX = 6.43
0.00
30.00
60.00
90.00
120.00
150.00
180.00
THETA CM (DEGREES)

Fig. 10

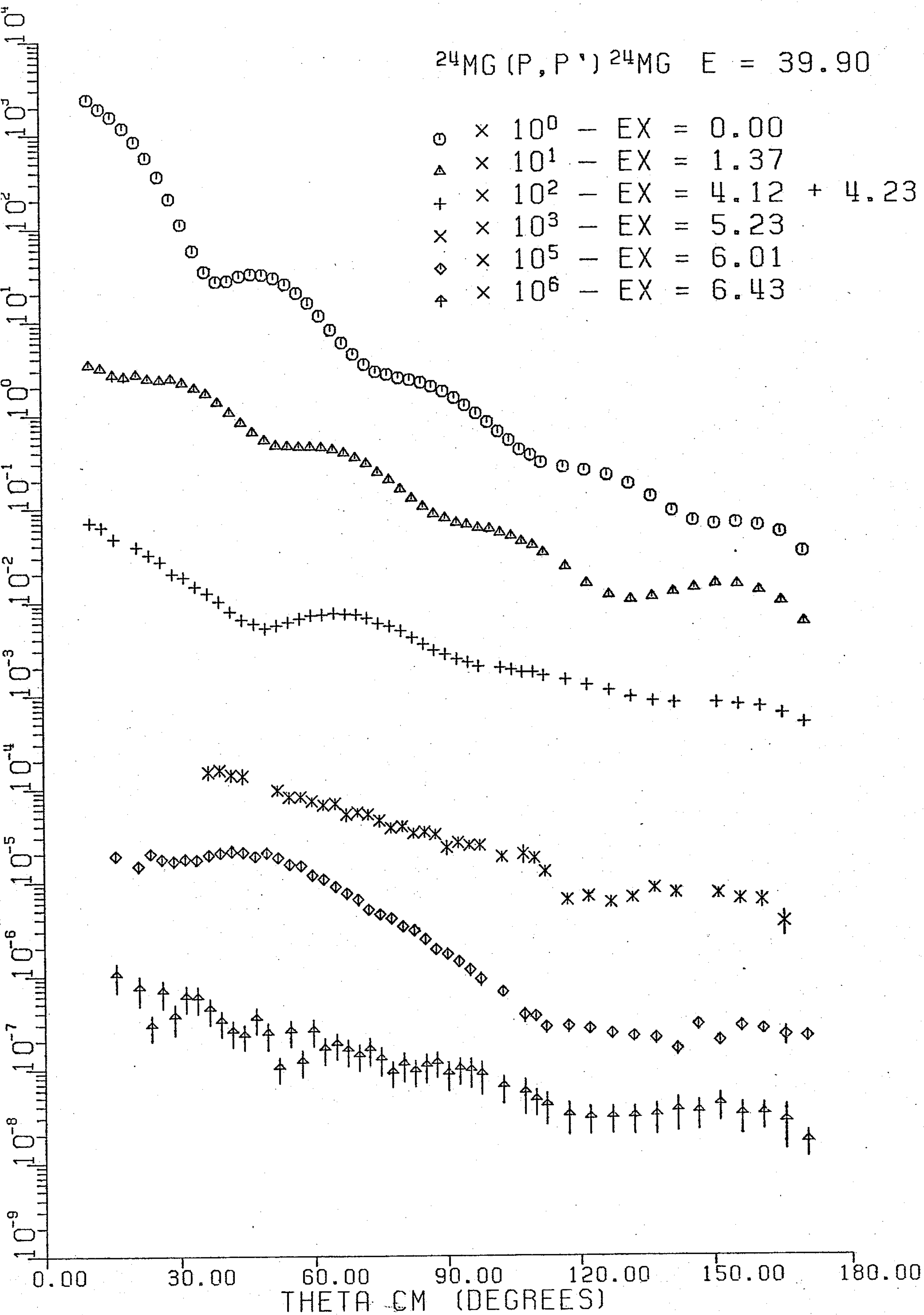

^{24}MG(P,P')^{24}MG E = 39.90
× 10^{0} – EX = 0.00
× 10^{1} – EX = 1.37
× 10^{2} – EX = 4.12 + 4.23
× 10^{3} – EX = 5.23
× 10^{5} – EX = 6.01
× 10^{6} – EX = 6.43
THETA CM (DEGREES)

Fig. 11

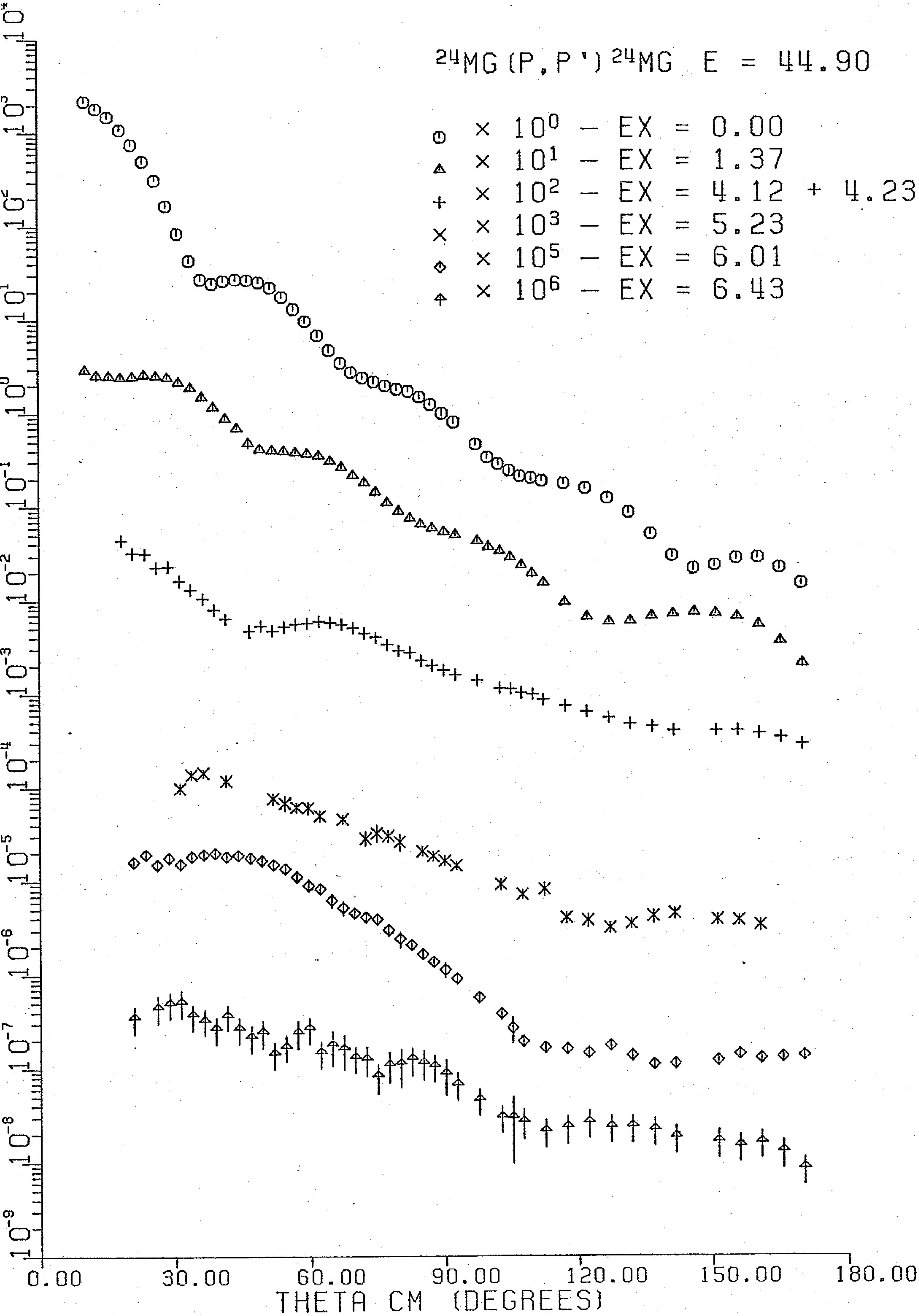
^{24}MG (P,P') ^{24}MG E = 44.90
× 10^0 – EX = 0.00
× 10^1 – EX = 1.37
× 10^2 – EX = 4.12 + 4.23
× 10^3 – EX = 5.23
× 10^5 – EX = 6.01
× 10^6 – EX = 6.43
10^4
10^3
10^2
10^1
10^0
10^{-1}
10^{-2}
10^{-3}
10^{-4}
10^{-5}
10^{-6}
10^{-7}
10^{-8}
10^{-9}
0.00
30.00
60.00
90.00
120.00
150.00
180.00
THETA CM (DEGREES)

Fig. 12

7.0 ANALYSIS

7.1 OPTICAL MODEL

The experimental data plus some data found in the literature were analysed using the optical model search codes SEEK[10] and MAGALI[11]. The form of the optical potential used was as described in section 2.2 . The literature data were included to extend the energy range and to provide polarisation data. The literature data consisted of differential cross sections for protons scattered by ^{24}Mg at energies of 17.5,[12] 49.5,[13] 100,[14] and 155[15] MeV. Polarisation data were available at 17.5,[16] 20.3,[17] 49.5,[18] and 100[19] Mev.

Starting with optical model parameters from the literature, searches were made over the real central, imaginary volume, and imaginary surface parameters to obtain reasonable fits to the data. At the start the spin-orbit parameters were held fixed at the Becchetti - Greenlees parameters.[20] Later fits to data with polarisations were made allowing the spin - orbit parameters to vary. It was found that the values VSO = 6.7 MeV, RSO = 0.96 fm, and ASO = 0.67 fm yielded the best overall fits. Leaving these parameters fixed once more, searches were made to obtain the best agreement with the experimental data.

Throughout the optical model analysis the imaginary volume potential depth was fixed at zero for proton energies below 30 MeV. The Coulomb radius Rc had a fixed value of 1.05 fm, as determined from electron scattering experiments.[1,2,3,19,25]

The first fits were obtained using the program SEEK. Then starting from the parameters determined by SEEK, the program MAGALI was used to incorporate the corrections for the finite width of the detectors and to fit the experimental reaction cross section data.

In order to partially correct for relativistic effects, the incident proton energy used in the above programs was increased so that the programs would calculate the correct relativistic wavenumber. The potential strengths quoted in this paper were also adjusted for relativistic effects.

The optical model fits to the data are shown as the solid lines in Fig.'s 13-26. In general the fits are quite good but there are some discrepancies at the backward angles. The parameters obtained for the best fits are given in Table 2. Also given are the experimental reaction cross sections[21] and the values as calculated from the optical potential. It appears that, while the trends in the values are similar, the results of the experimental measurements are consistently lower than the optical model predictions.

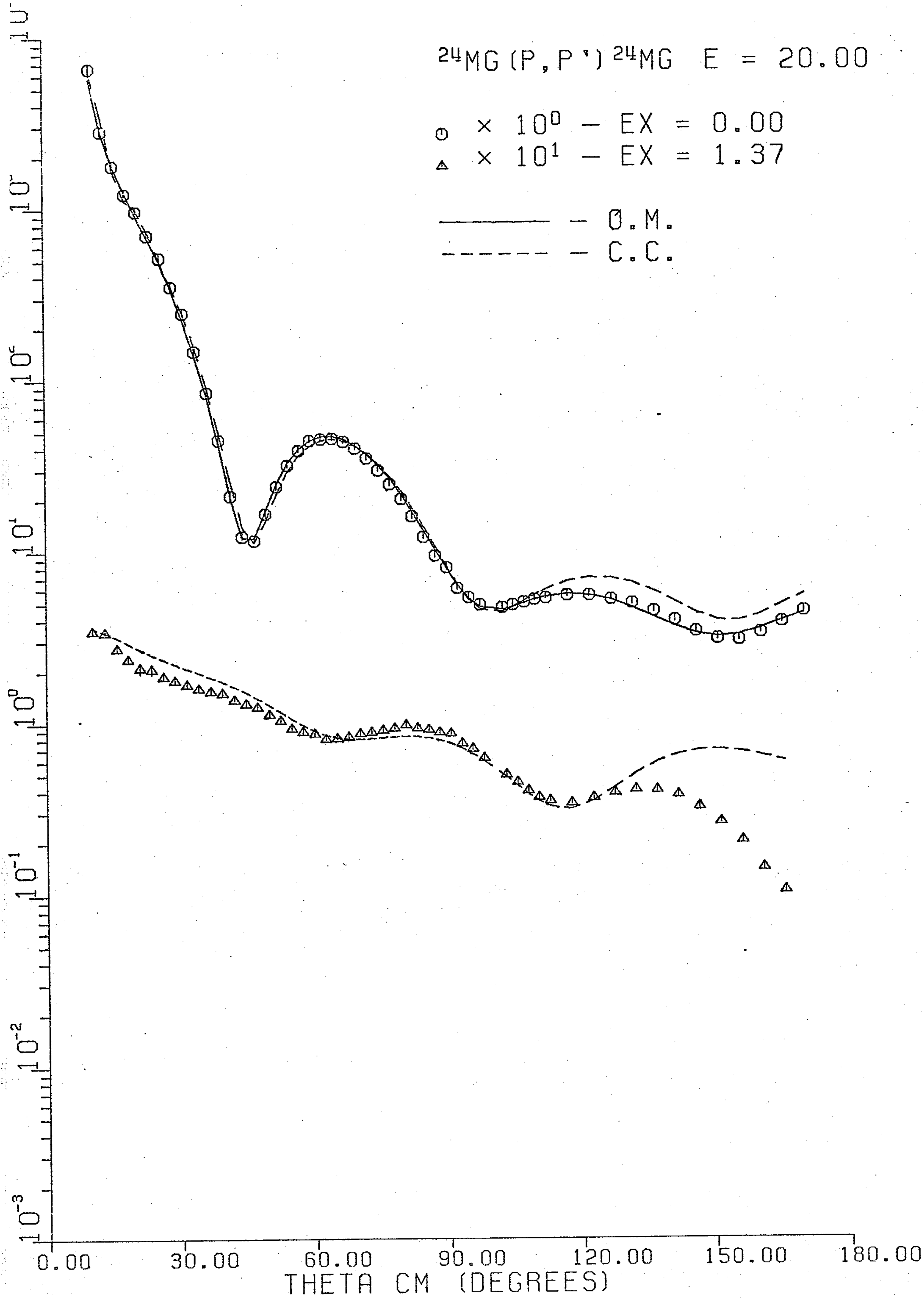

24MG(P,P')24MG E = 20.00
× 10⁰ – EX = 0.00
× 10¹ – EX = 1.37
– Ø.M.
– C.C.
10⁻³
10⁻²
10⁻¹
10⁰
10¹
0.00
30.00
60.00
90.00
120.00
150.00
180.00
THETA CM (DEGREES)

Fig. 13

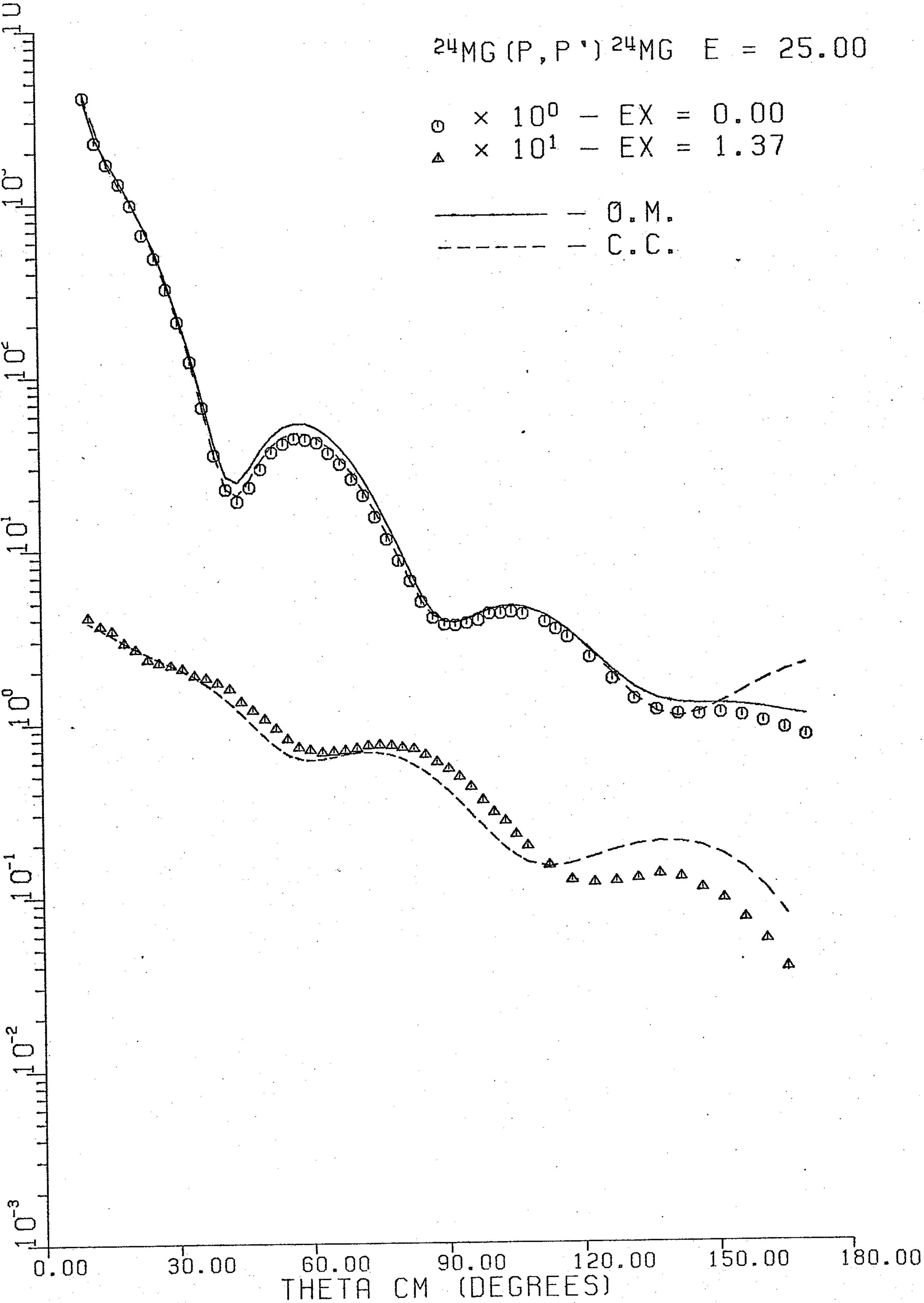

24MG(P,P')24MG E = 25.00
× 10⁰ — EX = 0.00
× 10¹ — EX = 1.37
— O.M.
— C.C.
0.00
30.00
60.00
90.00
120.00
150.00
180.00
THETA CM (DEGREES)

Fig. 14

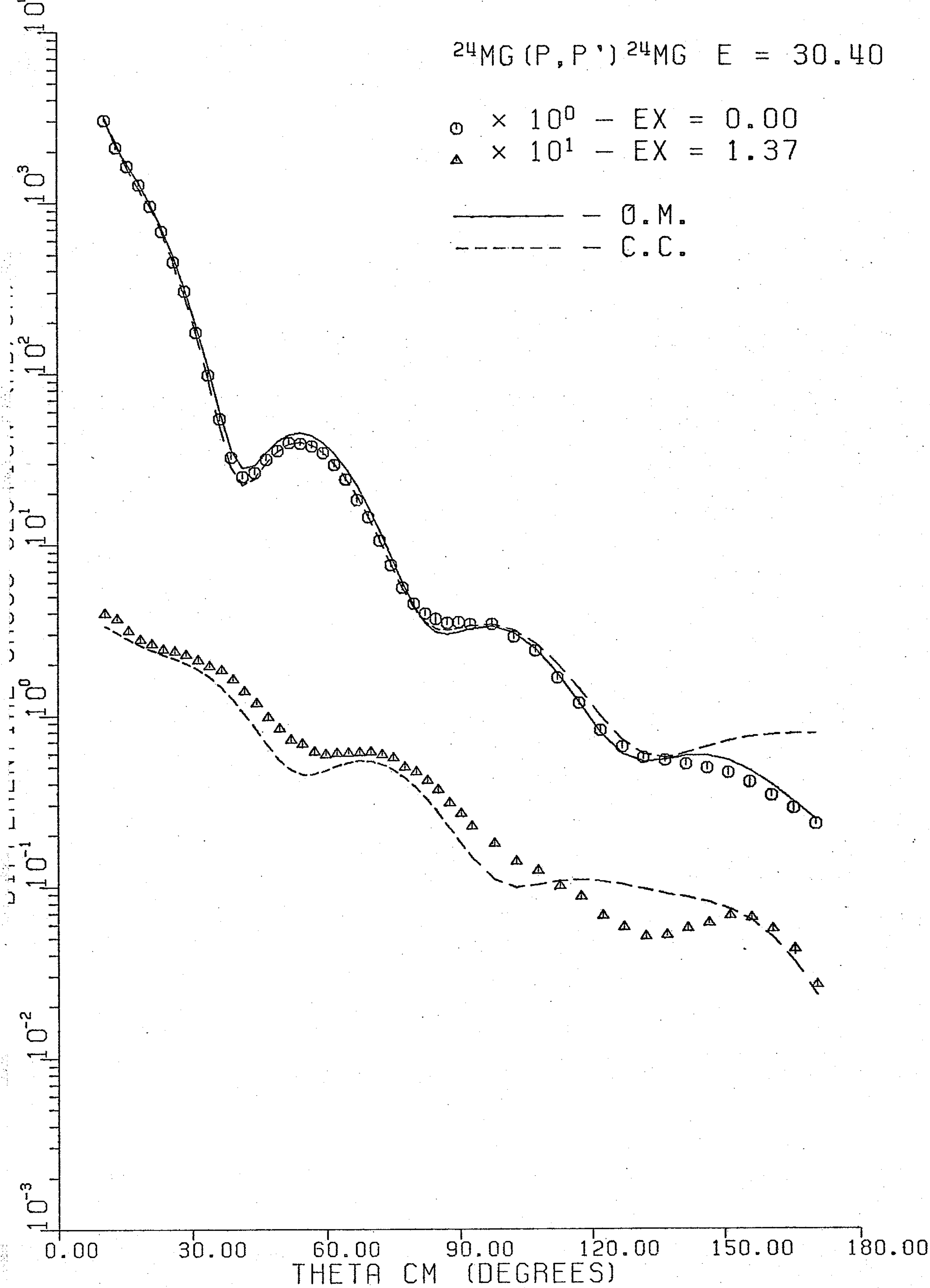

24MG(P,P')24MG E = 30.40
× 10^0 — EX = 0.00
× 10^1 — EX = 1.37
— O.M.
— C.C.
10^4
10^3
10^2
10^1
10^0
10^-1
10^-2
10^-3
0.00
30.00
60.00
90.00
120.00
150.00
180.00
THETA CM (DEGREES)

Fig. 15

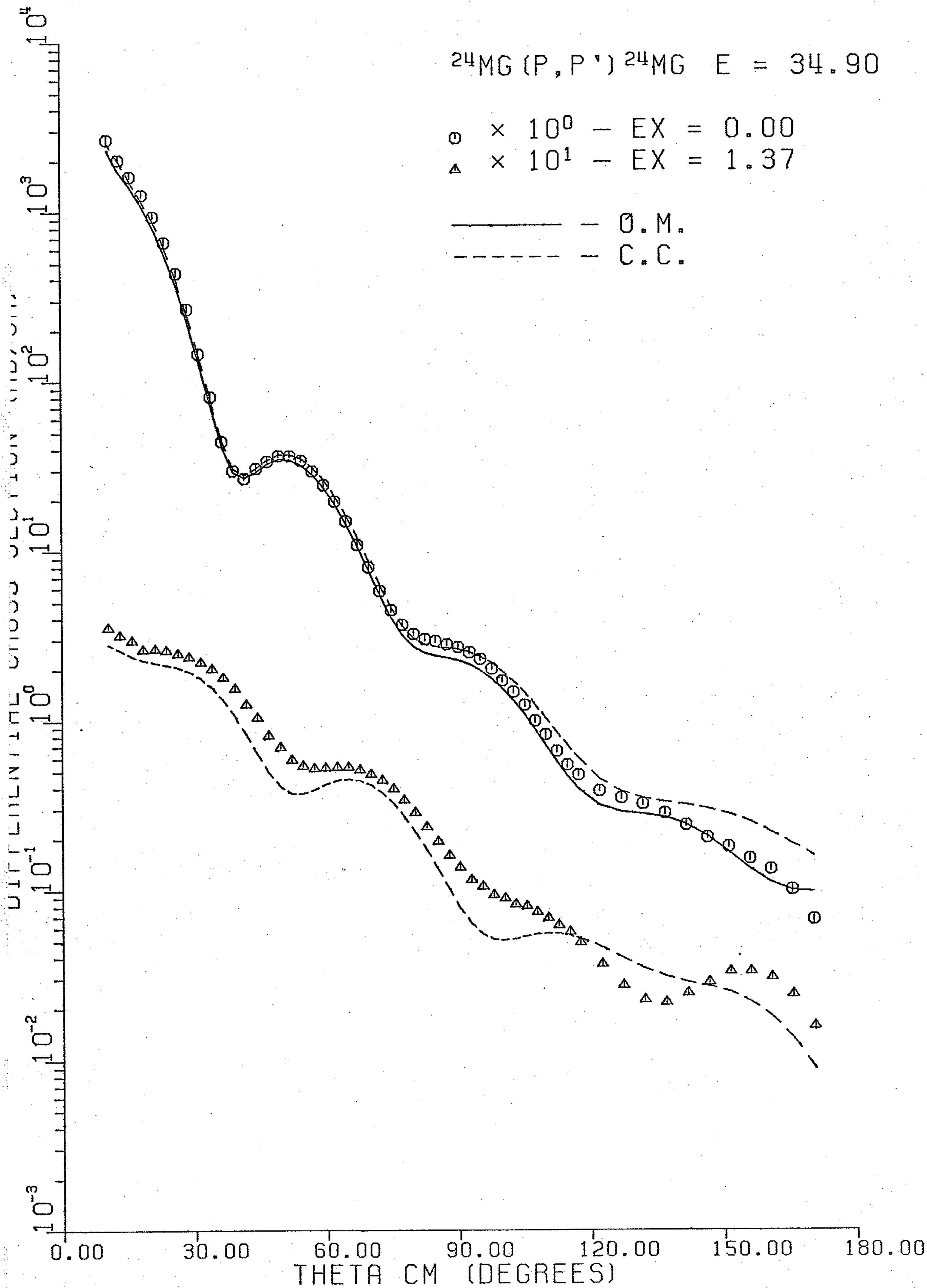

²⁴MG(P,P')²⁴MG E = 34.90
× 10⁰ − EX = 0.00
× 10¹ − EX = 1.37
Ø.M.
C.C.
10⁴
10³
10²
10¹
10⁰
10⁻¹
10⁻²
10⁻³
0.00
30.00
60.00
90.00
120.00
150.00
180.00
THETA CM (DEGREES)

Fig. 16

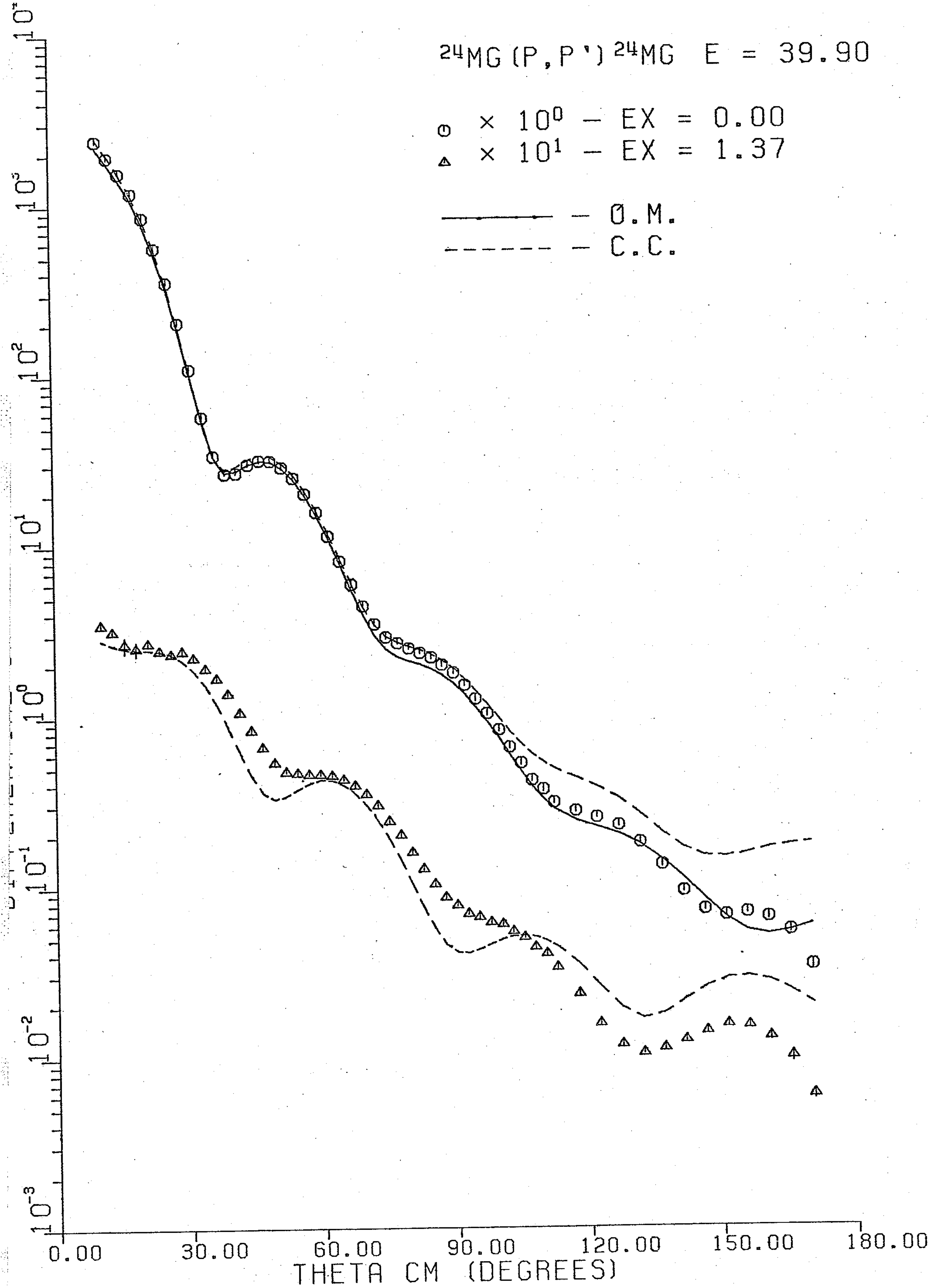

^{24}MG(P,P')^{24}MG E = 39.90
× 10^0 — EX = 0.00
× 10^1 — EX = 1.37
— Ø.M.
— C.C.
10^{-3}
10^{-2}
10^{-1}
10^0
10^1
10^2
10^3
10^4
0.00
30.00
60.00
90.00
120.00
150.00
180.00
THETA CM (DEGREES)

Fig. 17

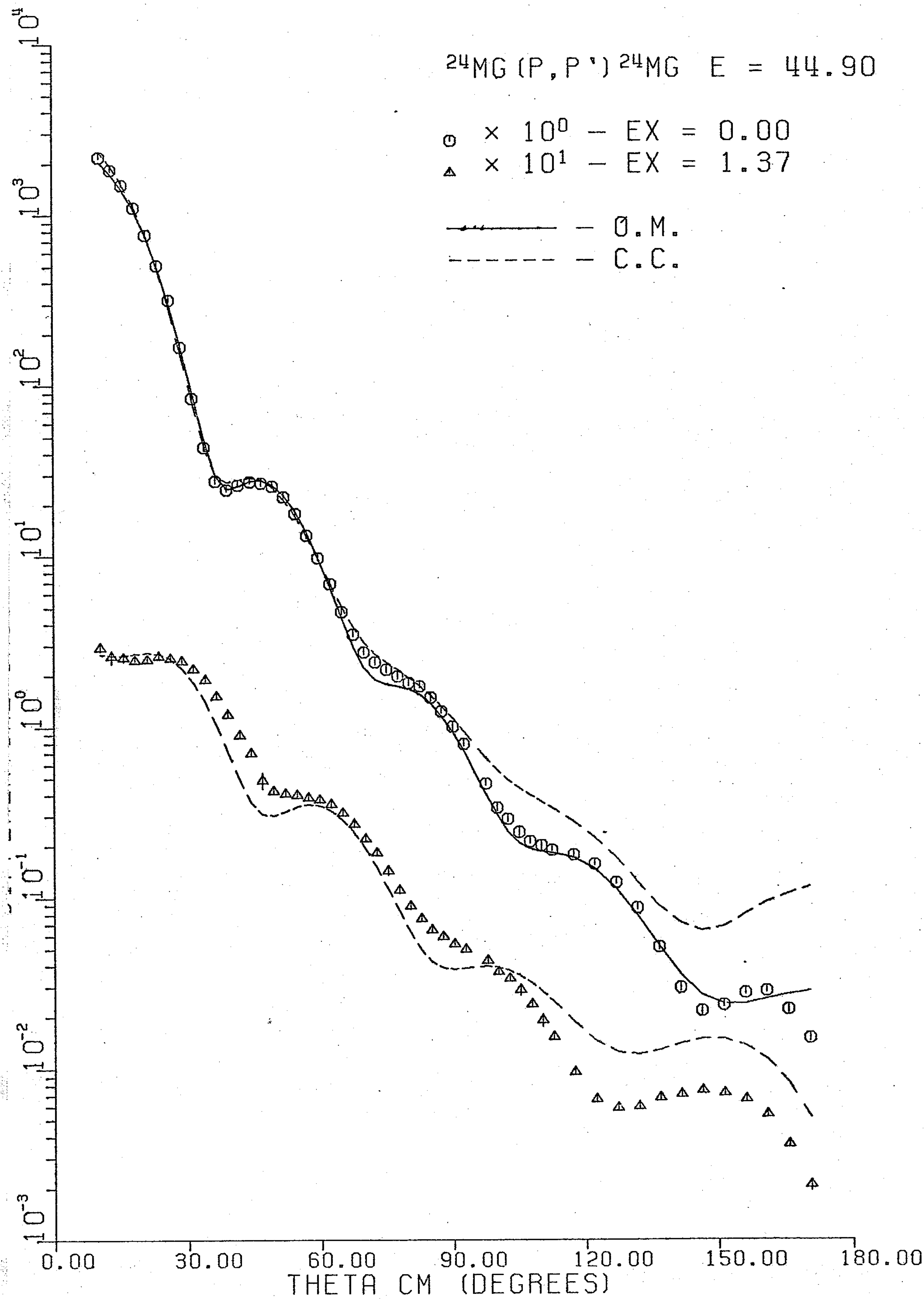
^{24}MG (P,P') ^{24}MG E = 44.90
× 10^0 – EX = 0.00
× 10^1 – EX = 1.37
– O.M.
– C.C.
10^4
10^3
10^2
10^1
10^0
10^{-1}
10^{-2}
10^{-3}
0.00
30.00
60.00
90.00
120.00
150.00
180.00
THETA CM (DEGREES)

Fig. 18

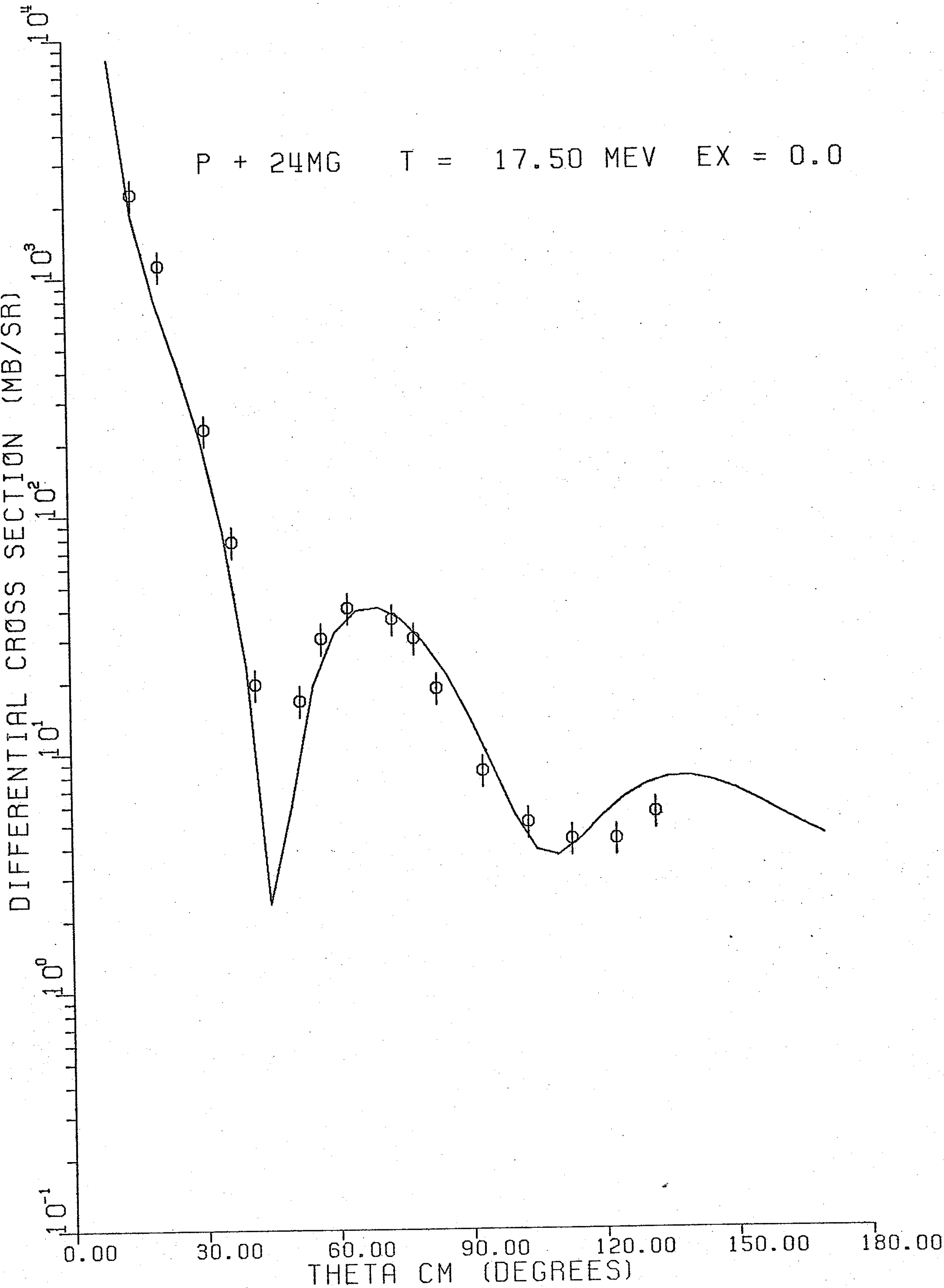
P + 24MG T = 17.50 MEV EX = 0.0
DIFFERENTIAL CROSS SECTION (MB/SR)
THETA CM (DEGREES)
0.00
30.00
60.00
90.00
120.00
150.00
180.00
10^{-1}
10^{0}
10^{1}
10^{2}
10^{3}
10^{4}

Fig. 19

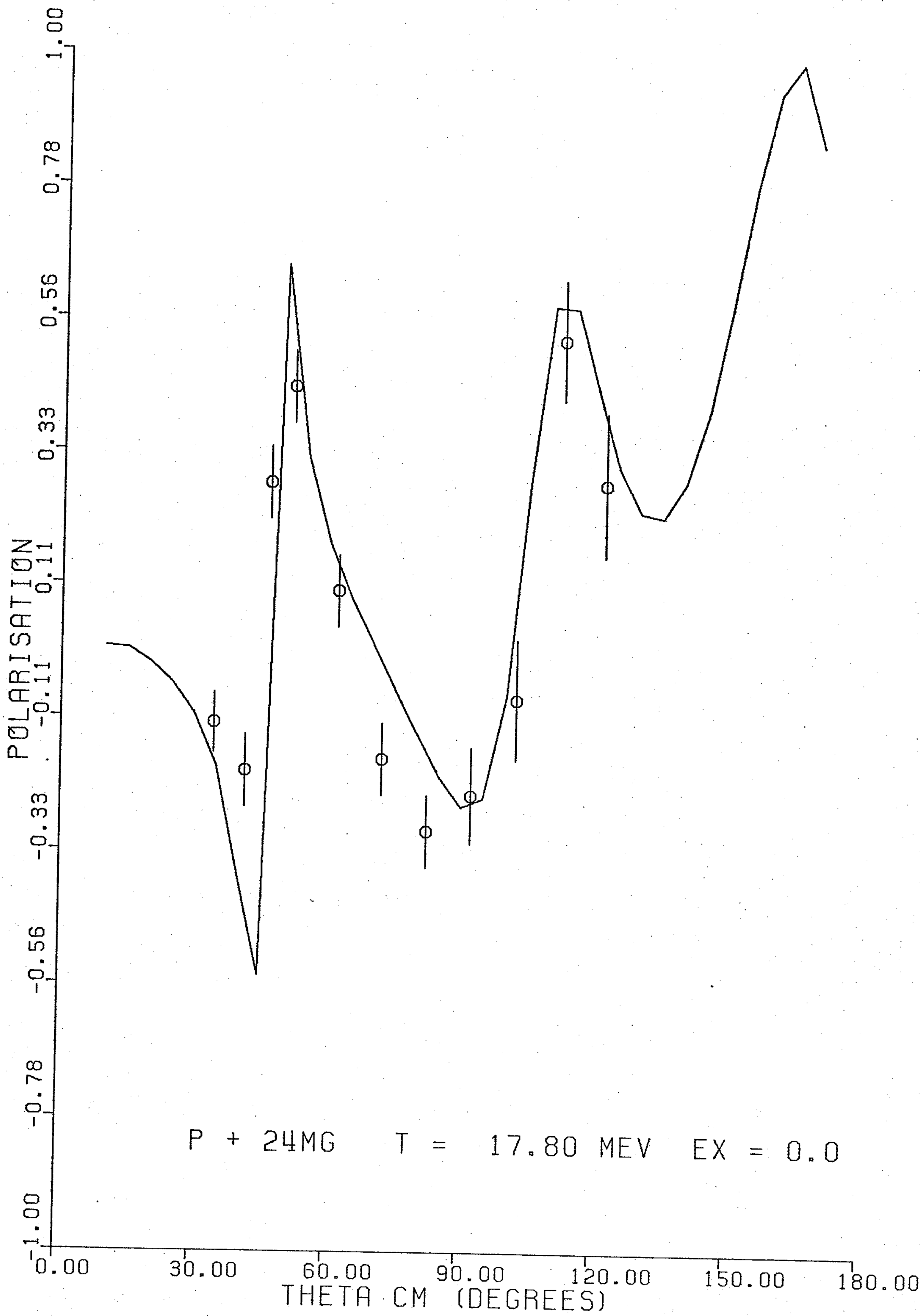
1.00
0.78
0.56
0.33
0.11
-0.11
-0.33
-0.56
-0.78
-1.00
PØLARISATIØN
P + 24MG T = 17.80 MEV EX = 0.0
0.00
30.00
60.00
90.00
120.00
150.00
180.00
THETA CM (DEGREES)

Fig. 20

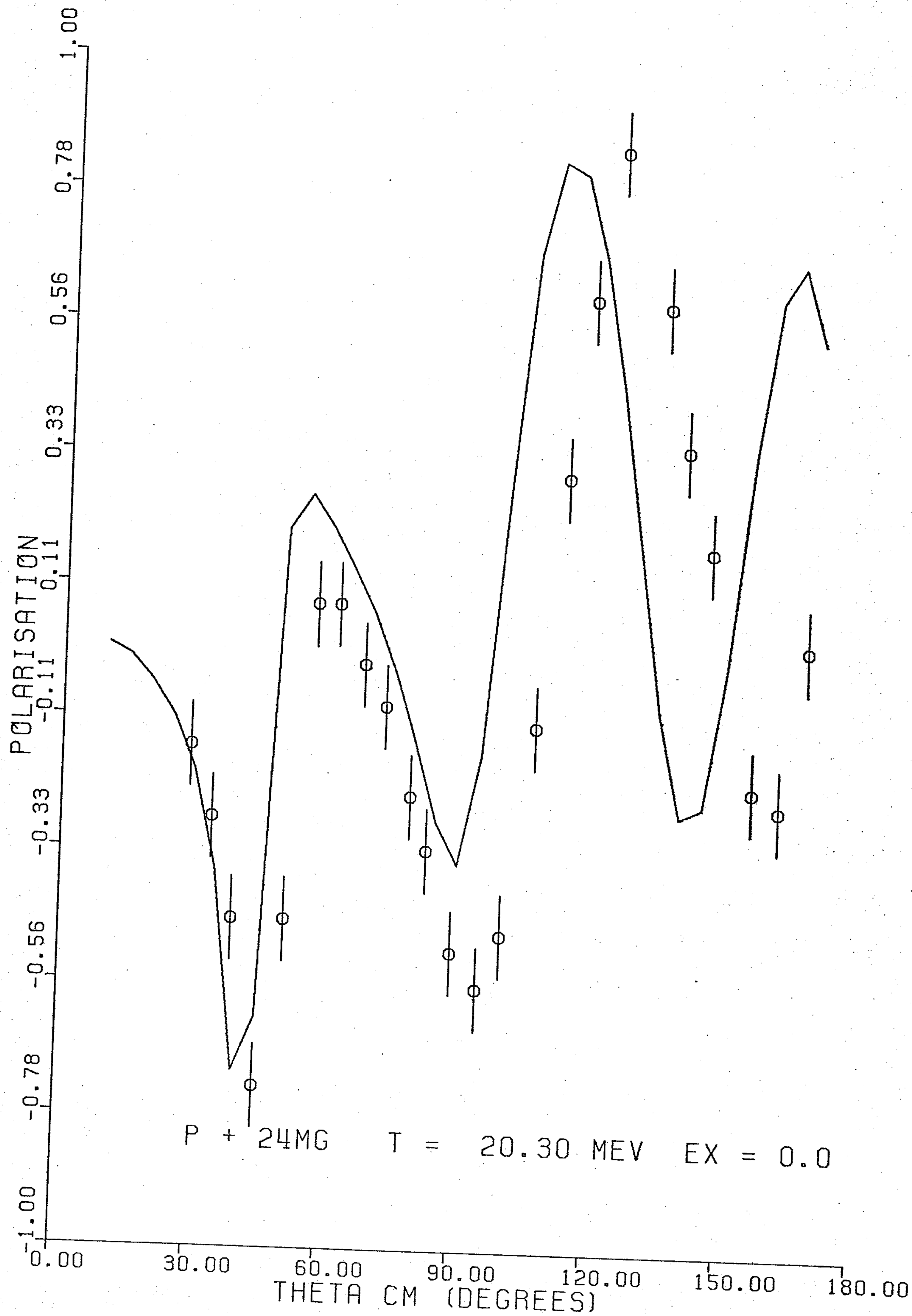
P + 24MG T = 20.30 MEV EX = 0.0
POLARISATION
THETA CM (DEGREES)
1.00
0.78
0.56
0.33
0.11
-0.11
-0.33
-0.56
-0.78
-1.00
0.00
30.00
60.00
90.00
120.00
150.00
180.00

Fig. 21

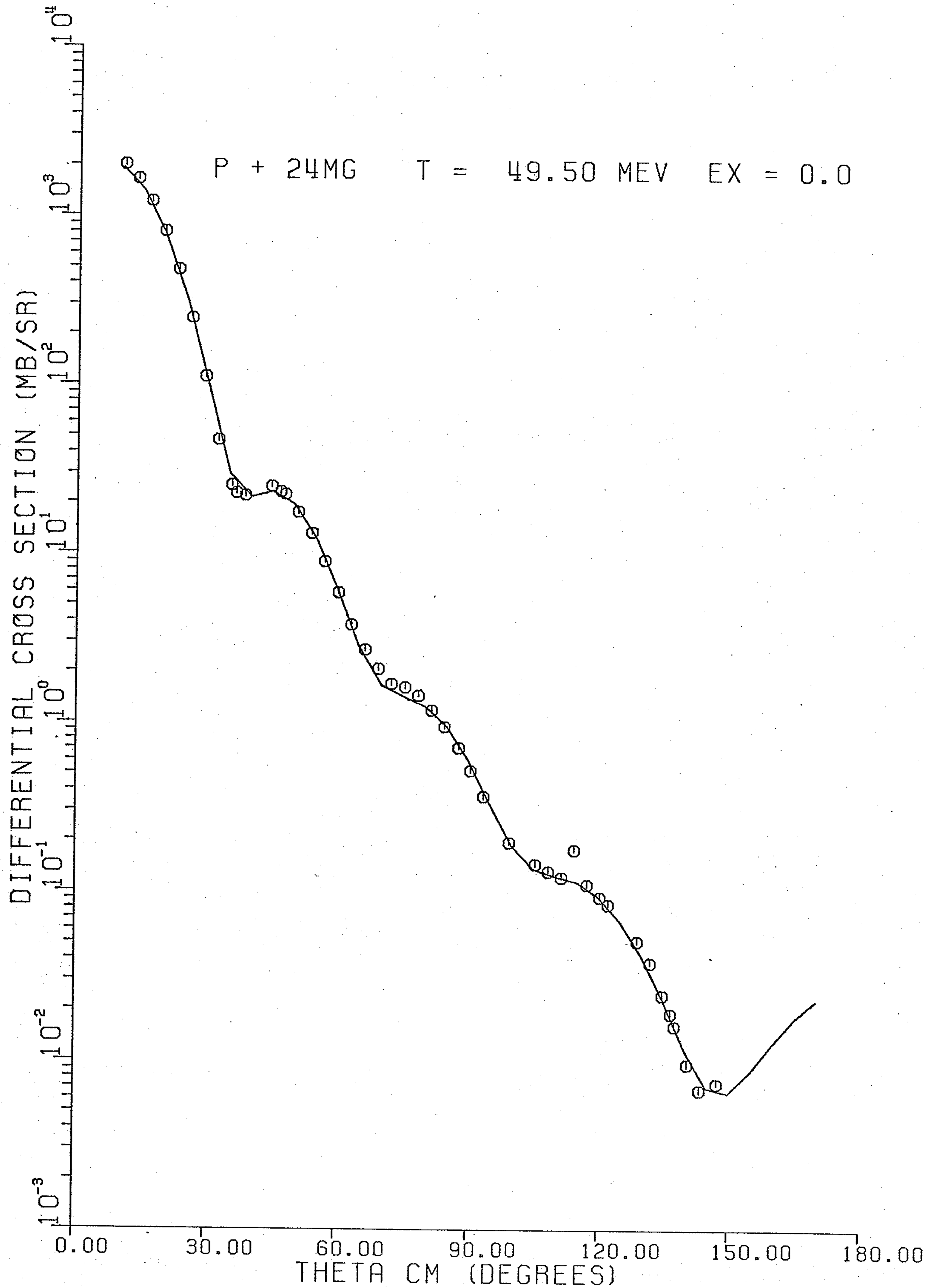
P + 24MG T = 49.50 MEV EX = 0.0
DIFFERENTIAL CRØSS SECTIØN (MB/SR)
THETA CM (DEGREES)
0.00
30.00
60.00
90.00
120.00
150.00
180.00

Fig. 22

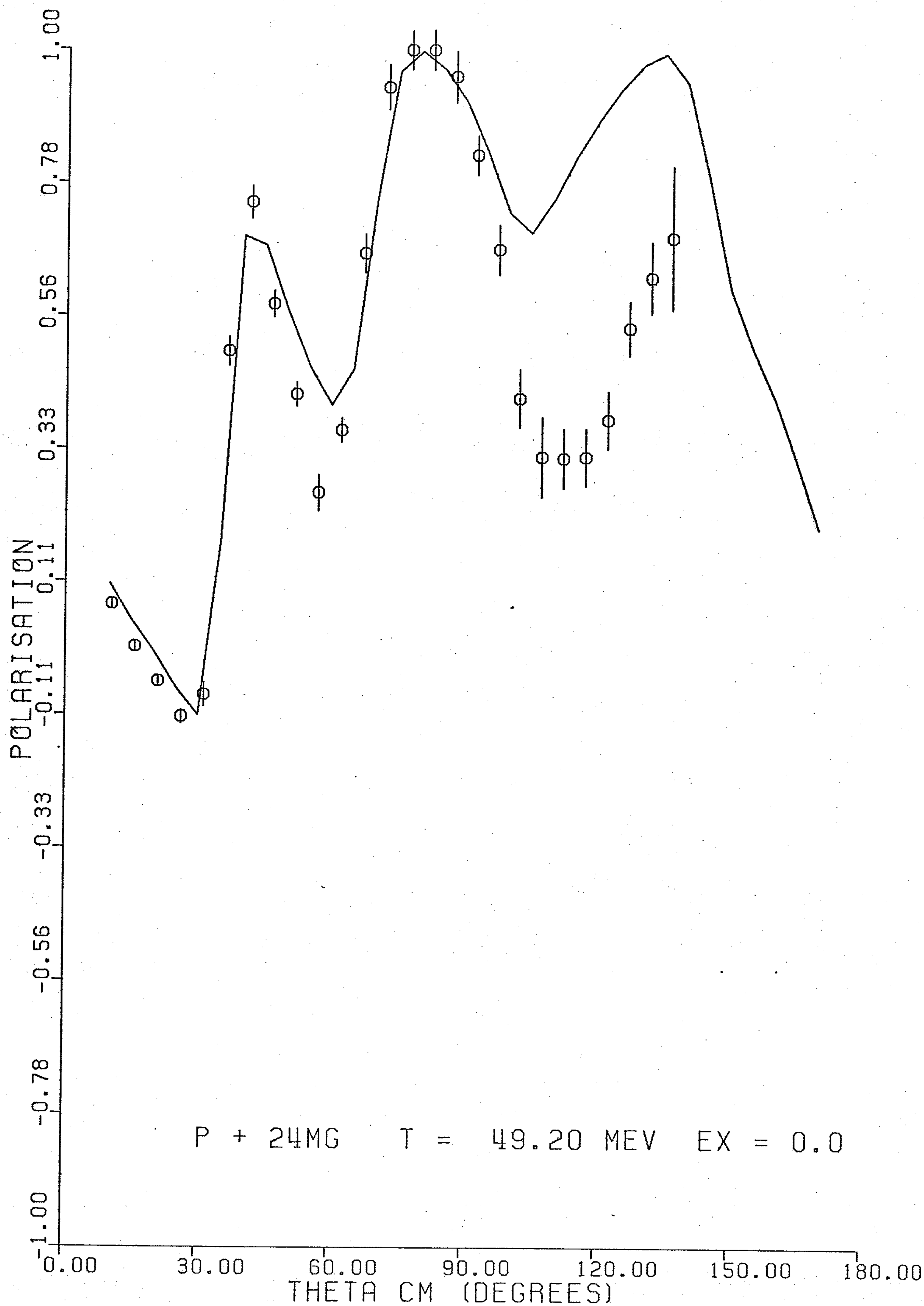
1.00
0.78
0.56
0.33
0.11
-0.11
-0.33
-0.56
-0.78
-1.00
POLARISATION
P + 24MG T = 49.20 MEV EX = 0.0
0.00
30.00
60.00
90.00
120.00
150.00
180.00
THETA CM (DEGREES)

Fig. 23

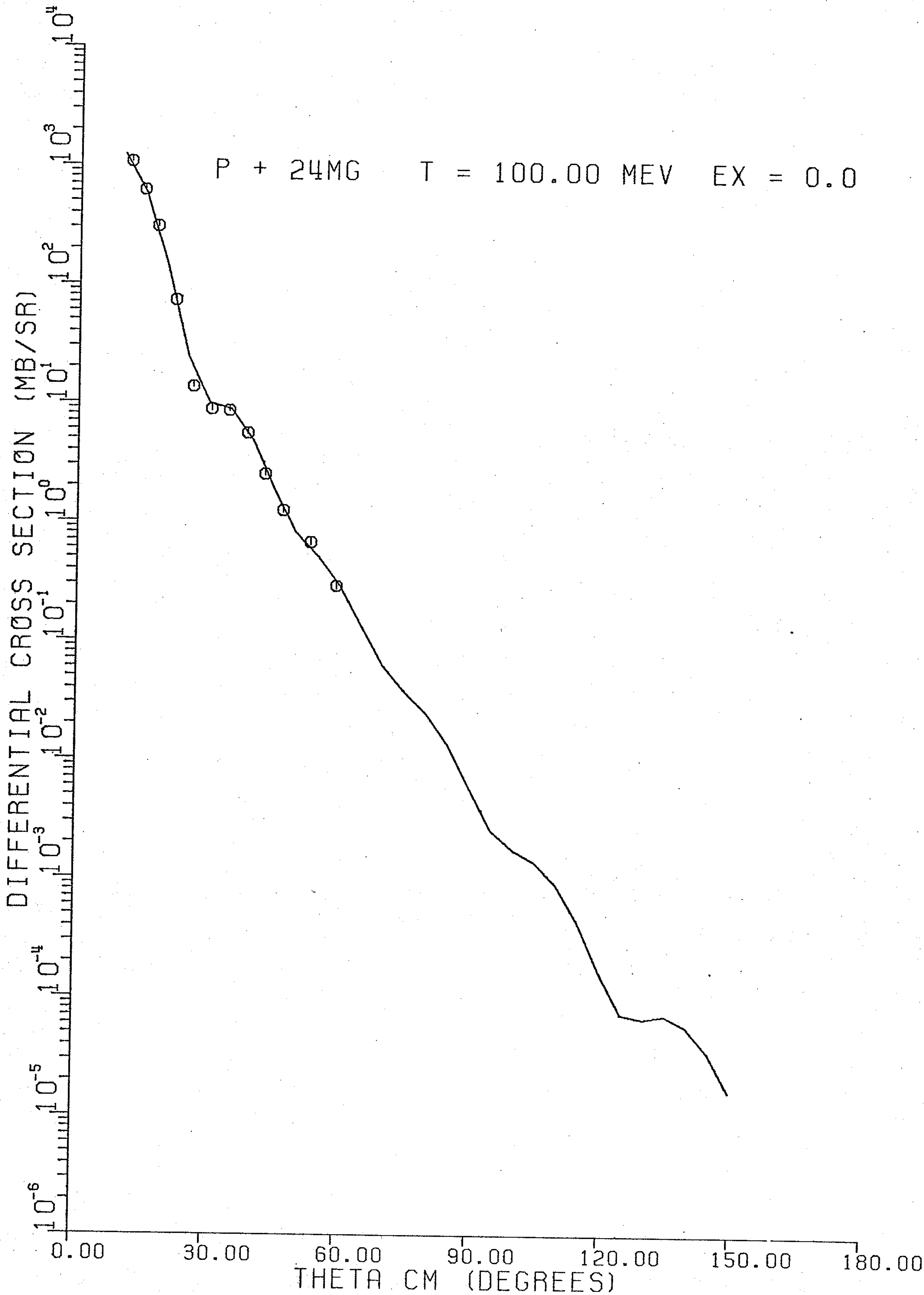
P + 24MG T = 100.00 MEV EX = 0.0
DIFFERENTIAL CROSS SECTION (MB/SR)
THETA CM (DEGREES)
0.00
30.00
60.00
90.00
120.00
150.00
180.00

Fig. 24

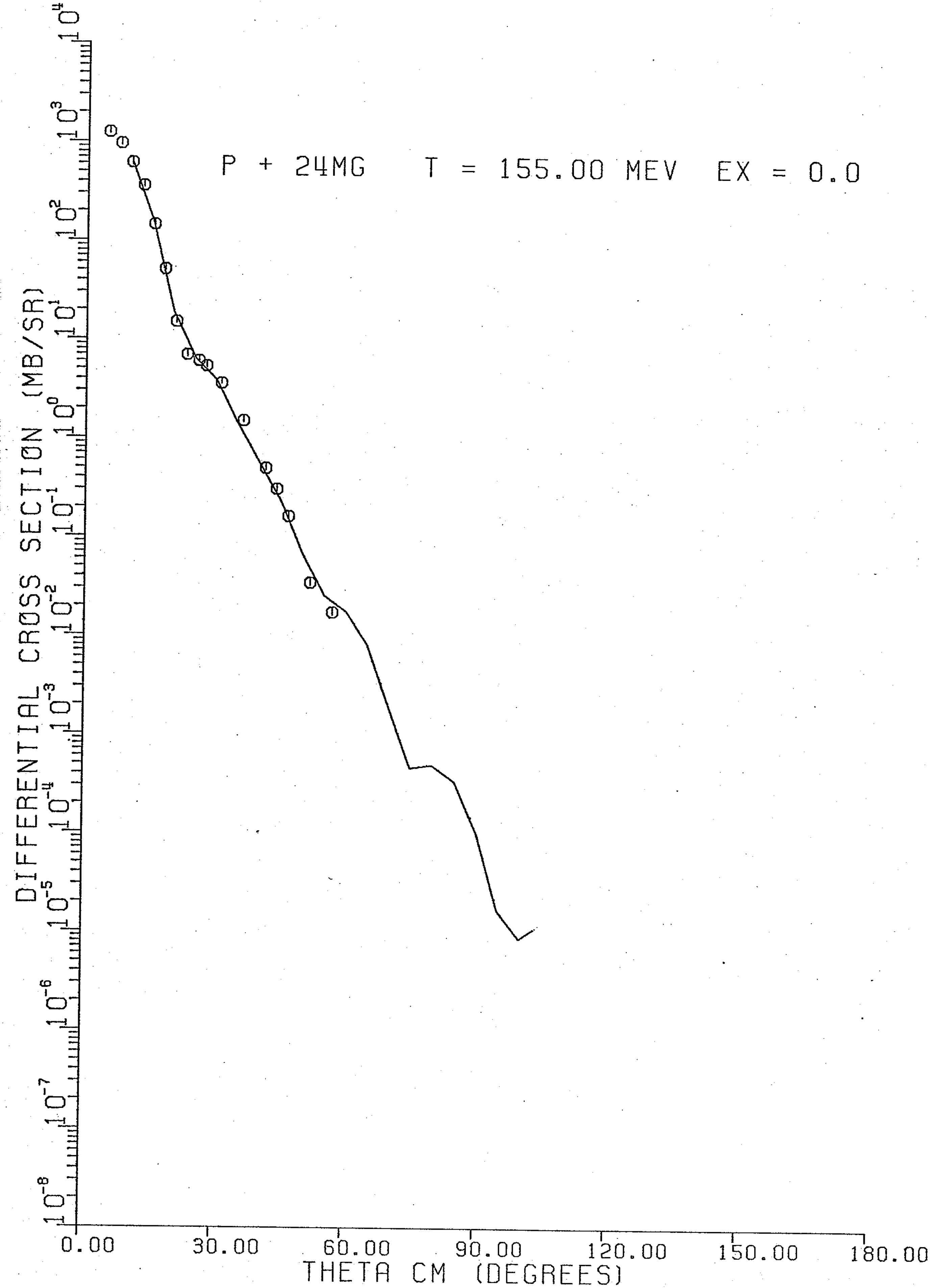
P + 24MG T = 155.00 MEV EX = 0.0
DIFFERENTIAL CROSS SECTION (MB/SR)
THETA CM (DEGREES)
0.00
30.00
60.00
90.00
120.00
150.00
180.00

Fig. 25

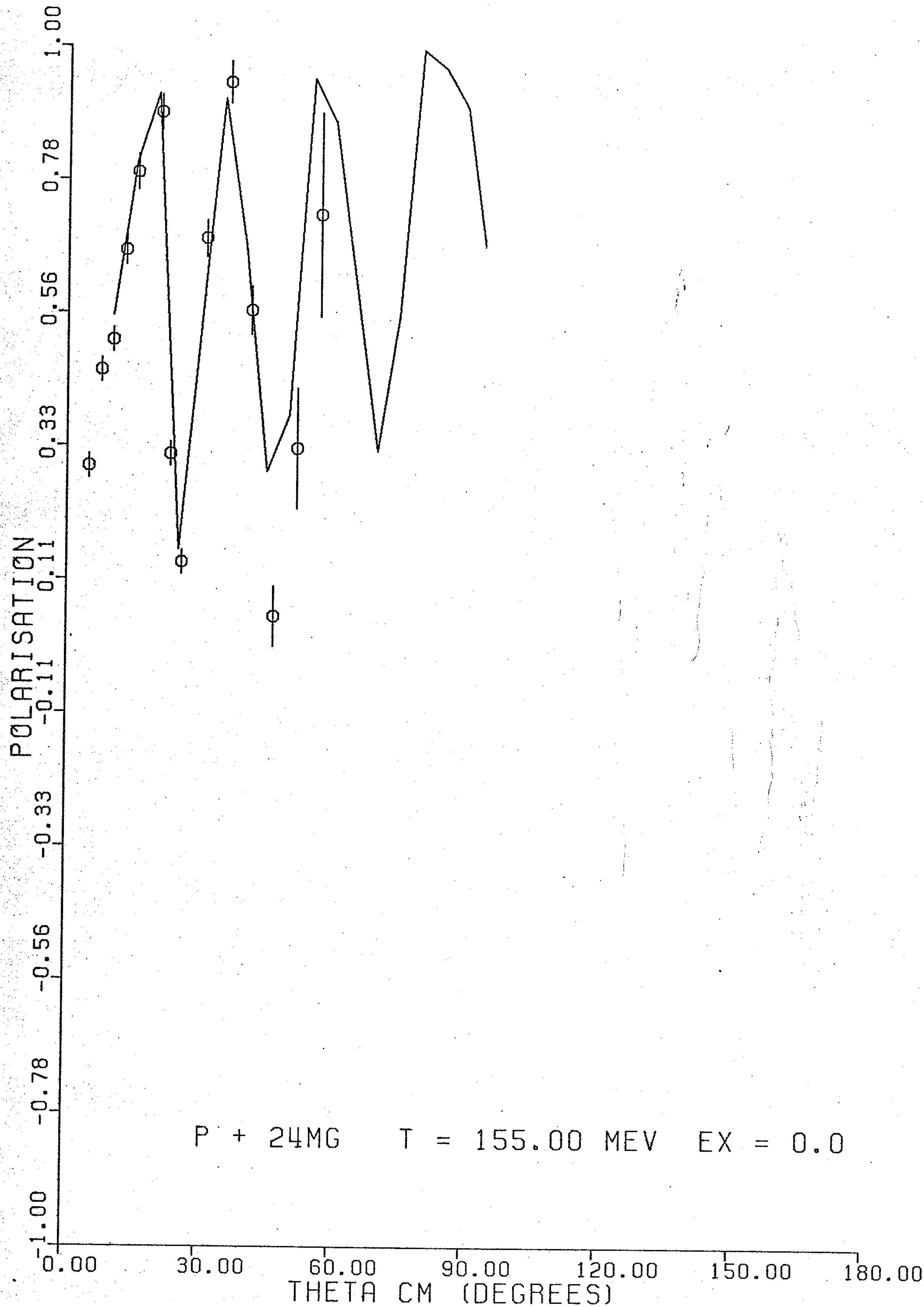
1.00
0.78
0.56
0.33
0.11
-0.11
-0.33
-0.56
-0.78
-1.00
POLARISATION
P + 24MG T = 155.00 MEV EX = 0.0
0.00
30.00
60.00
90.00
120.00
150.00
180.00
THETA CM (DEGREES)

Fig. 26

Table 2 Optical Model Potential Parameters

T	20.0	25.0	30.4	34.9	39.9	44.9
V	46.6	47.2	47.3	50.8	48.6	44.8
R	1.21	1.15	1.13	1.05	1.07	1.09
A	0.58	0.67	0.66	0.74	0.73	0.72
W	0.00	0.00	0.40	6.04	5.69	5.08
WD	6.21	6.92	6.23	0.58	0.00	0.00
RI	1.25	1.41	1.37	1.56	1.67	1.71
AI	0.60	0.46	0.51	0.51	0.51	0.34
VSO	6.70	6.70	6.70	6.70	6.70	6.70
RSO	0.96	0.96	0.96	0.96	0.96	0.96
ASO	0.67	0.67	0.67	0.67	0.67	0.67
χ^2/N	7.4	13	18	15	22	19
N	52	53	49	54	53	52
$\sigma_{r_{th}}$	717	686	652	654	636	563
$\sigma_{r_{exp}}$	820	775	725	670	650	620

N = number of data points

7.2 COUPLED CHANNELS

The coupled channels analysis of the data was done using the computer program CHUCK.[22] Since this program only permitted coupling between members of the ground state rotational band, only the first three states of ^{24}Mg were used in the calculations. Furthermore, since the third state was not resolved in this work, we were unable to compare the theoretical calculations with experimental results. The third state was included in the calculations strictly for completeness, since it makes a small contribution, through coupling, to the second state. Thus the coupling scheme used in these calculations was $0^+-2^+-4^+$ and the theoretical calculations for the differential cross sections of the first two states were compared to the experimentally measured values to determine the goodness of the agreement.

The starting parameters used in specifying the interaction potential for the coupled channels calculation were taken from the results of the optical model analysis as described above. It should be noted here that the computer code does not optimise any of the parameters, it merely performs a single calculation based on the input parameters. Even so, the time required and the computer services cost is quite prohibitive. The method used to obtain the final coupled channels parameters was as follows. Choosing the 30.4 MeV data as typical, numerous computations were performed starting from one fixed set of parameters, varying one parameter at a time and noting its effect on the results. Then, assuming that the effect of changing a particular parameter value does not depend severely on the value of the other parameters one was able to make good estimates of parameter values to provide the best agreement with the experimental data. For example: if it was noted that one choice of parameters yielded elastic scattering cross section values which were too high at backward angles, and inelastic cross sections which were slightly high also, then increasing the strength of the imaginary potentials could improve the fit. In such a manner satisfactory agreement to the experimental data was obtained at the six energies measured for the first two states of ^{24}Mg Fig. 13 - 18.

The value for β_2 , the coupling or deformation parameter, was taken from the literature(1,2,23,24) (mostly electron scattering data) which consistently gave a value of 0.47. This value was used throughout and was not varied in any attempt to improve the fit to the data.

The effect of changing the various parameters of the interaction potential was the following. As stated above increasing W had the effect of lowering the back angle elastic cross sections and uniformly lowering the inelastic cross sections. Increasing WD similarly lowered the elastic results at back angles, but had greater effect on the inelastic results, lowering the 2^+ and deepening its minima, and drastically lowering the 4^+ cross section. Lowering the real potential strength, V, lowered the elastic cross section slightly and shifted the minima to the right. The 2^+ cross section was lower and the 4^+ more so. Increasing the imaginary radius parameter RI shifted the minima of the 0^+ cross sections slightly to the left and lowered the cross sections of the inelastic states. The elastic results could be increased at back angles by decreasing the imaginary diffuseness parameter AI. This also had the effect of increasing the 2^+ and 4^+ cross sections. An increase in R , the real radius parameter, would shift the elastic minima to the left, lower the 2^+ values, and drastically lower the 4^+ values. Finally, increasing the real diffuseness parameter A had the effect of filling in the minima of the elastic cross section, raising the 2^+ values and lowering the 4^+ differential cross section slightly. The parameters describing the spin-orbit interaction were not changed from those values used in the optical model analysis, since to this point the polarisation data have not been compared with the coupled channels predictions.

The parameters obtained by this method for the coupled channels interaction potential are shown in Table 3. The dashed lines in Fig.'s 13-18 are the calculated cross sections as determined using these parameter values.

Table 3 Coupled Channels Potential Parameters

T	20.0	25.0	30.4	34.9	39.9	44.9
V	46.6	47.2	47.3	50.8	48.6	44.8
R	1.21	1.15	1.13	1.05	1.07	1.09
A	0.58	0.67	0.66	0.74	0.73	0.72
W	0.0	0.0	2.48	2.98	3.00	3.00
WD	3.67	4.43	2.48	2.24	1.87	1.25
RI	1.25	1.41	1.50	1.56	1.67	1.71
AI	0.60	0.60	0.60	0.51	0.51	0.60
VSO	6.70	6.70	6.70	6.70	6.70	6.70
RSO	0.96	0.96	0.96	0.96	0.96	0.96
ASO	0.67	0.67	0.67	0.67	0.67	0.67
$\sigma_{r_{th}}$	688	741	713	662	670	657
$\sigma_{r_{exp}}$	820	775	725	670	650	620

8.0 DISCUSSION

The data obtained appear to follow smooth curves and the errors associated with the cross sections are sufficient to account for any fluctuations from these curves, with the possible exception of the 6.43 MeV data. The cross section for the state at 6.43 MeV may contain some structure, but then uncertainties are large and not all the data fall on a simple, smooth curve.

It is interesting to note how the back angle differential elastic scattering cross section is dependent upon the incident proton energy. At 170° from 20.0 MeV to 44.9 MeV there is a decrease of 2.5 orders of magnitude. For the inelastic cross sections the change ranges from only 1.0 to 1.7 orders of magnitude. Thus from a simplistic point of view, as the incident proton energy increases, inelastic contributions to the scattering process become more important.

Even without this energy enhancement, the inelastic processes are comparable with the elastic scattering. Backward of about 30° the 2^+ (1.37 MeV) differential cross section is of the same magnitude as the elastic one. The differential cross sections for exciting the other states, with the possible exception of the 3^+ (5.23 MeV) state, are not much lower, being usually within an order of magnitude of the elastic scattering differential cross section. At far backward angles the summed cross sections of the 4^+ (4.12 MeV) and 2^+ (4.23 MeV) states are greater than the elastic scattering differential cross section. Clearly the inelastic channels are important in any theory trying to describe scattering from ^{24}Mg.

The 3^+ (5.23 MeV) state has a fairly small differential cross section. This is not unreasonable, as it is an unnatural parity state. It cannot therefore be populated directly, but only through some complicated process. Work has been done[5] to explain the non-negligible size of unnatural parity states on the basis of i) compound nucleus formation, ii) spin - orbit interactions between the projectile and target nucleons, iii) exchange processes, and iv) multi-step scattering processes. The most plausible explanation is the fourth one, that is a multi - step scattering process takes place, i.e., the 3^+ state is populated through coupling to other states.

The optical model analysis seems to fit the data quite well, except perhaps at backward angles and at higher incident proton energies. This may be due to the increasing effect of inelastic scattering processes. However the optimisation of the parameters of the OMP may have hidden many of the discrepancies.

This may account for the fluctuations in the parameters obtained. For this reason no attempt was made to search for a set of parameters having a common geometry. Since the optical model analysis is thought to be of doubtful validity in this case a coupled channels calculation was performed.

The coupled channels calculations appear to follow the trend of the experimental differential cross section values fairly well. However, exact agreement cannot be expected, considering the inefficient means by which the parameters are optimised. Also the program CHUCK which was used is not entirely suitable in this case, since it does not permit members of the gamma vibrational band to be included in the calculations. With ^{24}Mg this may be a serious drawback and limit its usefulness.

In addition, since only two states are available for comparison with experimental data, the restrictions on the parameters are not as stringent as might be. Improved calculations to include the gamma vibrational band are needed. This would permit the theoretical predictions for the 4^+ and 2^+ states (of the gamma vibrational band) to be added together and then to be compared with the cross section measured in this work for the sum of the two states. Also the predictions for the excitation of the 3^+ state may provide further testing of the choice of the potential parameters.

By comparing the potential parameters determined in the optical model analysis with those of the coupled channels analysis we can see that outside of a few small changes in the geometry, the prominent difference is in that the imaginary strengths are decreased by approximately 50% in the case of the coupled channels analysis. This is rather pleasing, in that it indicates that the imaginary part of the interaction potential, which was originally introduced to correct for inelastic and reaction processes, is of lesser importance in the CC calculation. Thus the explicit inclusion of certain inelastic processes has lead to a better description of the interaction.

9.0 CONCLUSIONS

Based on the observation that the potential parameters changed significantly between the optical model and the coupled channels calculations (mostly the strengths of the imaginary terms, but also some of the geometry parameters), it would appear that the optical model is a less accurate means of describing the proton - ^{24}Mg interaction. While it certainly can fit the elastic scattering data (once the potential parameters are suitably optimised), it would appear that these fits are misleading and that the potential thus derived is not a good approximation to the true interaction. If this were not the case then the more accurate and physically more correct coupled channels calculation would not have required such significant changes in the parameters.

Even so, the coupled channels analysis made to this point is inadequate in that it only shows that there is room for improvement. A more thorough analysis is required, incorporating more than the first two states of ^{24}Mg in the calculation and subsequent comparison with measured results. Such an analysis is of course limited by the necessity of keeping the computation within a reasonable time and thus restricting the number of coupled states.

Work is continuing in this direction using the computer code JUPITOR[26] which is more suitable to this particular scattering problem. The program JUPITOR will permit the coupling $0^{+}-2^{+}-4^{+}-2^{+}-3^{+}$. After these calculations have been made it will be possible to compare theory and experiment for four of the angular distributions presented in this thesis. In addition the literature data (which includes polarisation data) can be compared to the theory. It is hoped that such restrictions on the results of the calculations will better determine the proton - ^{24}Mg interaction in this energy range.

10.0 APPENDIX

10.1 TABULATED DATA

The following tables contain the differential cross sections for protons scattered by ^{24}Mg at incident energies of 20.0, 25.0, 30.4, 34.9, 39.9, and 44.9 MeV, from the excited states: 0^+ (0.00 MeV elastic), 2^+ (1.37 MeV), the sum of 4^+ (4.12 MeV) and 2^+ (4.23 MeV), 3^+ (5.23 MeV), 4^+ (6.01 MeV), and 0^+ (6.43 MeV). Relativistic transformations to the centre of momentum frame of reference were used throughout. Uncertainties quoted are the absolute percentage errors in the differential cross sections.

ENERGY = 20.00 EX = 0.0

THETA CM (°)	(MB/SR)	% ABS. ERROR
10.43	6599.	3.1
13.03	2855.	7.2
15.64	1790.	4.3
18.24	1235.	5.7
20.84	973.2	3.0
23.44	706.0	4.1
26.04	520.1	4.6
28.63	353.9	7.3
31.23	246.7	3.8
33.82	148.7	6.9
36.41	85.28	4.8
39.00	45.06	5.2
41.58	21.25	5.3
44.16	12.30	3.7
46.74	11.74	3.9
49.31	16.67	4.6
51.88	24.07	3.9
54.45	32.06	3.8
57.01	39.14	3.1
59.57	44.93	3.4
62.13	45.69	3.0
64.68	45.90	3.0
67.23	43.89	3.1
69.77	40.39	3.0
72.31	35.16	3.0
74.84	30.02	3.0
77.37	24.79	3.2
79.90	20.43	3.2
82.42	16.08	3.4
84.93	12.18	3.2
87.45	9.517	3.7
89.95	8.097	3.8
92.45	6.148	3.2
94.95	5.433	3.0
97.45	4.916	3.0
102.42	4.715	2.9
104.90	4.922	3.0
107.37	5.063	3.0

109.84	5.274	3.4
112.31	5.369	3.0
117.22	5.534	2.9
122.12	5.543	2.9
127.01	5.287	3.0
131.88	4.981	3.0
136.73	4.477	3.1
141.58	3.958	3.0
146.41	3.384	3.7
151.23	3.072	2.9
156.04	3.036	3.1
160.84	3.350	2.9
165.63	3.861	2.9
170.43	4.461	2.9

ENERGY = 20.00 EX = 1.37

THETA CM (°)	(MB/SR)	% ABS. ERROR
10.57	34.72	4.4
13.21	34.12	3.5
15.84	27.33	3.2
18.48	23.82	4.2
21.12	21.06	6.9
23.75	20.81	6.7
26.38	18.88	4.4
29.01	17.80	4.2
31.63	16.82	3.8
34.25	15.96	2.9
36.87	15.45	3.0
39.48	15.05	3.0
42.10	13.78	2.9
44.70	13.02	3.0
47.31	12.44	3.2
49.90	11.30	3.1
52.50	10.38	3.0
55.09	9.370	3.0
57.67	8.962	3.2
60.25	8.684	3.2
62.82	8.115	3.0
65.39	8.214	3.0
67.95	8.351	3.7

70.51	8.676	3.2
73.06	8.849	3.1
75.61	9.094	3.1
78.15	9.396	3.1
80.68	9.796	3.9
83.21	9.381	3.0
85.73	9.181	3.0
88.25	8.873	3.2
90.76	8.745	3.2
93.26	7.626	3.1
95.76	7.110	3.1
98.25	6.274	3.1
103.21	4.993	3.1
105.68	4.519	3.1
108.15	4.028	3.3
110.61	3.693	3.8
113.06	3.526	3.0
117.95	3.414	2.9
122.82	3.646	2.9
127.67	3.911	3.0
132.50	4.083	3.1
137.30	4.022	3.1
142.09	3.785	3.0
146.87	3.222	4.2
151.63	2.612	3.0
156.38	2.038	3.0
161.11	1.412	3.5
165.84	1.039	3.9

ENERGY = 20.00 EX = 4.20

THETA CM (°)	(MB/SR)	% ABS. ERROR
13.12	7.021	15.5
15.74	6.501	8.8
18.36	5.265	6.1
20.98	4.856	4.0
23.60	4.089	4.7
26.21	4.103	6.7
31.43	3.135	5.3
34.04	2.437	3.2
36.64	2.249	4.8

39.24	2.091	3.3
41.84	1.736	3.7
44.44	1.579	3.8
47.03	1.569	4.6
49.61	1.373	3.6
52.19	1.268	3.8
54.77	1.242	3.9
57.35	1.164	5.1
59.92	1.272	4.4
62.48	1.201	4.7
65.04	1.277	3.5
67.60	1.326	4.6
70.15	1.381	4.1
72.69	1.381	3.3
75.23	1.466	3.8
77.77	1.550	3.9
80.30	1.565	4.1
82.82	1.644	3.4
85.34	1.666	3.6
87.85	1.718	3.4
90.36	1.910	5.1
92.86	1.797	3.2
95.36	1.882	3.2
97.85	1.809	3.2
102.82	1.863	3.1
105.30	1.893	3.2
107.77	1.792	3.3
112.69	1.703	3.2
117.59	1.605	2.9
122.48	1.538	3.0
127.34	1.490	3.0
132.19	1.564	4.6
137.02	1.741	3.7
141.84	1.842	3.1
151.43	2.441	3.1
156.21	2.708	3.2
160.98	3.018	3.4
165.74	3.308	2.9
170.50	3.448	3.1

ENERGY = 20.00 EX = 5.23

THETA CM (°)	(MB/SR)	% ABS. ERROR

41.84	.2263	12.0
44.44	.3118	11.7
54.77	.3373	17.1
62.48	.3936	12.8
65.04	.4261	11.2
72.69	.4289	12.6
75.23	.4797	10.6
80.30	.4938	11.9
82.82	.4697	10.7
85.34	.4421	10.6
87.85	.4266	11.7
92.86	.4473	11.5
95.36	.4927	11.1
97.85	.4584	10.5
102.82	.4590	10.9
105.30	.5382	10.5
107.77	.5011	10.6
112.69	.5545	10.5
117.59	.5820	10.4
122.48	.6198	10.5
127.34	.6361	10.4
132.19	.6902	10.9
137.02	.6669	10.4
141.84	.7148	11.1
151.43	.5771	10.7
156.21	.4905	10.4
160.98	.3640	10.6
165.74	.2687	10.8
170.50	.1560	10.9

ENERGY = 20.00 EX = 6.01

THETA CM (°)	(MB/SR)	% ABS. ERROR
15.74	3.474	11.4
18.36	3.325	12.0
20.98	3.413	10.5
23.60	2.949	10.4
26.21	2.811	10.4
28.82	3.045	12.5
31.43	2.740	10.5

34.04	2.706	19.1
36.64	2.668	11.0
39.24	2.486	10.5
41.84	2.312	10.5
44.44	2.352	10.5
47.03	2.403	10.7
49.61	2.172	10.6
52.19	2.180	10.7
54.77	2.023	10.6
57.35	2.016	10.5
59.92	1.943	10.7
62.48	1.863	10.8
65.04	1.816	10.5
67.60	1.778	10.6
70.15	1.660	10.5
72.69	1.622	10.8
75.23	1.522	10.5
77.77	1.427	11.8
80.30	1.470	10.4
82.82	1.343	10.6
85.34	1.262	10.8
87.85	1.093	11.0
90.36	1.254	11.1
92.86	.9727	11.6
95.36	1.066	10.8
97.85	.9440	10.8
102.82	.9057	12.2
105.30	.8096	11.3
107.77	.8251	10.5
112.69	.8335	10.6
117.59	.7788	10.5
122.48	.6865	10.7
127.34	.5911	10.4
132.19	.5317	10.9
137.02	.4247	11.0
141.84	.3812	11.7
151.43	.2635	11.5
156.21	.2181	11.0
160.98	.1703	10.8

ENERGY = 20.00 EX = 6.43

THETA CM (°)	(MB/SR)	% ABS. ERROR

15.74	2.444	31.7
18.36	1.630	32.5
20.98	1.536	30.4
23.60	1.279	30.2
26.21	1.223	30.2
28.82	1.087	33.2
31.43	.7197	30.4
34.04	.4429	43.9
36.64	1.352	31.0
39.24	.5262	30.4
41.84	.3760	30.4
44.44	.3481	30.4
47.03	.2581	30.6
49.61	.3332	30.4
52.19	.3560	30.7
54.77	.3438	30.4
57.35	.2876	30.4
59.92	.2812	30.7
62.48	.2818	30.8
65.04	.1838	30.4
67.60	.1574	30.4
70.15	.0796	30.4
72.69	.1153	30.7
75.23	.1178	30.4
77.77	.1502	32.1
80.30	.0397	30.2
82.82	.1237	30.6
85.34	.0497	30.7
87.85	.2295	31.1
90.36	.1042	31.2
92.86	.2986	31.8
95.36	.2004	30.8
97.85	.2541	30.8
102.82	.2869	32.8
105.30	.4209	31.4
107.77	.3165	30.3
112.69	.2058	30.6
117.59	.1818	30.4
122.48	.1740	30.6
127.34	.1421	30.2
132.19	.1125	31.0
137.02	.0566	31.0
141.84	.0576	32.0
151.43	.0734	31.7
156.21	.0970	31.1
160.98	.1298	30.8

ENERGY = 25.00 EX = 0.0

THETA CM (°)	(MB/SR)	% ABS. ERROR
10.43	4118.	4.7
13.03	2264.	3.5
15.64	1693.	3.9
18.24	1308.	4.5
20.84	982.5	2.9
23.44	661.8	4.5
26.04	485.5	4.1
28.64	320.0	6.3
31.23	207.6	5.3
33.83	122.5	5.0
36.42	66.31	4.8
39.00	35.27	5.1
41.59	22.23	3.2
44.17	19.02	3.8
46.75	22.88	3.7
49.32	29.18	3.2
51.89	36.59	3.2
54.46	40.66	3.5
57.02	43.44	3.0
59.58	42.91	3.2
62.14	41.29	3.0
64.69	35.95	3.4
67.24	31.04	3.0
69.78	25.30	3.7
72.32	20.35	3.5
74.85	15.29	3.8
77.38	11.41	4.0
79.91	8.513	4.7
82.43	6.535	3.5
84.95	4.967	4.0
87.46	3.998	3.2
89.96	3.642	2.9
92.47	3.611	3.1
94.96	3.722	3.2
97.46	3.847	2.9
99.95	4.201	3.2
102.43	4.220	3.2
104.91	4.275	3.2
107.38	4.174	3.0
112.32	3.758	3.2
114.78	3.411	3.6
117.23	3.049	3.3
122.13	2.331	3.3

127.02	1.754	3.3
131.89	1.342	3.3
136.74	1.147	3.1
141.58	1.089	3.0
146.41	1.078	3.2
151.23	1.095	3.2
156.04	1.062	3.3
160.84	.9826	3.4
165.64	.8925	4.5
170.43	.8096	3.5

ENERGY = 25.00 EX = 1.37

THETA CM (°)	(MB/SR)	% ABS. ERROR
10.53	41.03	3.3
13.16	36.55	3.5
15.79	34.33	6.2
18.42	29.16	4.8
21.04	26.79	5.0
23.67	23.36	3.1
26.29	22.37	3.3
28.91	21.55	3.7
31.52	20.51	3.1
34.14	18.81	3.4
36.75	18.19	3.1
39.35	17.01	3.1
41.96	15.75	3.1
44.56	13.31	3.5
47.15	11.82	3.0
49.75	10.49	3.1
52.33	9.234	3.1
54.92	8.032	3.5
57.50	7.209	3.0
60.07	6.946	3.5
62.64	6.737	3.0
65.20	6.776	2.9
67.76	6.923	2.9
70.31	7.103	3.2
72.86	7.331	3.0
75.40	7.390	3.1
77.94	7.315	3.1

80.47	7.162	3.1
83.00	7.040	3.0
85.52	6.495	3.2
88.03	5.882	3.1
90.54	5.384	3.0
93.04	4.812	3.2
95.54	4.230	3.0
98.03	3.532	3.3
100.52	3.013	3.5
103.00	2.661	3.5
105.47	2.229	4.5
107.94	1.920	3.4
112.86	1.477	3.7
117.76	1.219	3.1
122.64	1.170	3.0
127.49	1.194	2.9
132.33	1.240	3.0
137.15	1.302	3.0
141.96	1.246	3.2
146.74	1.080	3.6
151.52	.9364	3.5
156.29	.7201	3.4
161.04	.5423	4.7
165.79	.3760	5.1

ENERGY = 25.00 EX = 4.20

THETA CM (°)	(MB/SR)	% ABS. ERROR
10.48	9.391	25.2
20.95	4.802	7.9
23.56	3.534	4.6
26.17	4.306	7.9
28.78	3.073	3.7
31.39	2.376	3.2
33.99	2.164	3.0
36.59	1.738	3.7
39.19	1.607	4.0
41.79	1.417	3.8
44.38	1.346	4.6
46.96	1.268	4.2
49.55	1.217	3.1

52.13	1.225	3.4
54.70	1.250	3.8
57.28	1.242	3.7
59.84	1.312	3.6
62.41	1.308	3.5
64.96	1.368	3.5
67.52	1.338	3.0
70.07	1.356	3.7
72.61	1.349	3.0
75.15	1.329	3.2
77.68	1.294	3.5
80.21	1.316	3.3
82.73	1.275	3.2
85.25	1.232	3.4
87.77	1.215	3.1
90.27	1.196	3.0
92.78	1.175	3.3
95.27	1.203	3.5
97.77	1.115	3.1
102.73	1.112	3.2
105.21	1.164	3.5
107.68	1.058	3.0
112.61	1.041	3.5
117.52	.9703	3.0
122.40	.9171	2.9
127.27	.8526	3.0
132.13	.8157	3.1
136.96	.8178	3.1
141.78	.8034	3.1
151.39	.8284	2.9
156.17	.8621	3.3
160.95	.8443	3.0
165.72	.8209	3.7

ENERGY = 25.00 EX = 5.23

THETA CM (°)	(MB/SR)	% ABS. ERROR
36.59	.2790	11.0
39.19	.3113	13.3
41.79	.3601	10.4
44.38	.4113	17.0

52.13	.4237	11.0
54.70	.4273	12.8
57.28	.3848	10.4
59.84	.3716	10.4
62.41	.3735	13.2
64.96	.3718	12.5
67.52	.3278	10.6
70.07	.2967	13.9
72.61	.2858	11.2
75.15	.2726	10.6
77.68	.2296	11.1
80.21	.1948	10.5
82.73	.2097	10.5
85.25	.1888	10.5
87.77	.1441	11.8
90.27	.1471	13.6
92.78	.1347	12.2
97.77	.1205	12.2
102.73	.1360	10.8
107.68	.1466	11.8
112.61	.1735	10.8
117.52	.1821	10.5
122.40	.1995	10.5
127.27	.2016	10.6
132.13	.2040	10.4
136.96	.1874	10.5
141.78	.1668	10.6
151.39	.1325	10.5
156.17	.1105	10.4
160.95	.0956	10.6
165.72	.0732	14.3

ENERGY = 25.00 EX = 6.01

THETA CM (°)	(MB/SR)	% ABS. ERROR
20.95	3.632	11.0
23.56	3.349	12.0
26.17	3.266	10.7
28.78	2.940	11.7
31.39	3.481	11.1
33.99	2.717	11.3

36.59	2.752	10.7
39.19	2.653	10.5
41.79	2.499	10.5
44.38	2.333	10.5
46.96	2.262	10.6
49.55	2.167	11.0
52.13	2.148	10.5
54.70	2.024	10.6
57.28	1.912	10.5
59.84	1.778	10.7
62.41	1.809	10.5
64.96	1.663	10.5
67.52	1.474	10.5
70.07	1.364	10.8
72.61	1.274	10.5
75.15	1.145	10.5
77.68	1.001	11.0
80.21	.8441	10.7
82.73	.8595	10.4
85.25	.7221	10.7
87.77	.6165	11.0
90.27	.5690	10.4
92.78	.5040	11.1
95.27	.4796	10.7
97.77	.4255	10.9
102.73	.3828	11.0
105.21	.3418	12.1
107.68	.3814	10.7
112.61	.3369	11.1
117.52	.3150	10.8
122.40	.3043	10.9
127.27	.2583	10.6
132.13	.2299	10.4
136.96	.2020	10.4
141.78	.1606	10.6
151.39	.1005	11.1
156.17	.0684	11.9
160.95	.0529	13.0
165.72	.0313	10.8

ENERGY = 25.00 EX = 6.43

THETA CM (°)	(MB/SR)	% ABS. ERROR

20.95	.8425	31.1
23.56	.6447	32.5
26.17	.4765	30.7
28.78	.4016	32.1
31.39	.3145	31.2
33.99	.4953	31.5
36.59	.2199	30.6
39.19	.2773	30.4
41.79	.3602	30.4
44.38	.4182	30.4
46.96	.3431	30.5
49.55	.3414	31.0
52.13	.2871	30.3
54.70	.3227	30.5
57.28	.2662	30.4
59.84	.2814	30.6
62.41	.1667	30.3
64.96	.1606	30.4
67.52	.1369	30.4
70.07	.1274	30.8
72.61	.1047	30.4
75.15	.1103	30.4
77.68	.1188	31.0
80.21	.0951	30.7
82.73	.0877	30.2
85.25	.1004	30.7
87.77	.1071	31.1
90.27	.1210	30.2
92.78	.1204	31.1
95.27	.1393	30.6
97.77	.1231	30.9
102.73	.1226	31.0
105.21	.1944	32.7
107.68	.0989	30.7
112.61	.1188	31.2
117.52	.1031	30.8
122.40	.0813	31.0
127.27	.0811	30.5
132.13	.0763	30.2
136.96	.0817	30.3
141.78	.0988	30.5
151.39	.1107	31.2
156.17	.1166	32.3
160.95	.1119	34.0
165.72	.1175	30.7

ENERGY = 30.40 EX = 0.0

THETA CM (°)	(MB/SR)	% ABS. ERROR
10.43	3052.	2.9
13.04	2096.	3.0
15.64	1645.	3.2
18.25	1278.	3.0
20.85	953.3	3.0
23.45	684.2	3.0
26.05	451.3	4.8
28.65	304.1	3.1
31.24	175.3	3.4
33.83	98.49	4.0
36.42	54.56	3.4
39.01	32.49	3.1
41.59	24.91	3.0
44.18	26.32	2.9
46.75	31.71	3.0
49.33	35.56	3.5
51.90	39.37	3.0
54.47	39.32	3.2
57.03	37.78	3.2
59.59	34.56	3.1
62.15	29.42	3.1
64.70	24.15	3.3
67.25	18.30	4.0
69.79	14.55	3.1
72.33	10.59	3.0
74.87	7.618	3.4
77.40	5.613	3.5
79.92	4.514	3.3
82.44	3.956	3.4
84.96	3.688	7.0
87.47	3.486	3.1
89.98	3.516	3.9
92.48	3.441	3.5
97.47	3.422	3.2
102.44	2.898	3.9
107.39	2.391	2.9
112.33	1.658	3.5
117.25	1.184	3.6
122.15	.8208	3.6
127.03	.6545	3.3
131.90	.5673	3.4
136.75	.5459	3.0
141.59	.5195	3.5

146.42	.4922	3.5
151.24	.4592	4.0
156.05	.4066	6.5
160.85	.3410	3.3
165.64	.2882	5.5
170.43	.2320	3.0

ENERGY = 30.40 EX = 1.37

THETA CM (°)	(MB/SR)	% ABS. ERROR
10.51	39.56	5.0
13.13	36.96	3.0
15.76	31.44	4.9
18.38	27.92	3.1
21.00	26.13	3.1
23.62	24.32	3.1
26.24	23.68	2.9
28.85	22.73	2.9
31.46	21.08	3.0
34.07	19.55	3.1
36.68	18.48	3.3
39.28	16.36	3.0
41.88	13.86	3.0
44.48	11.80	2.9
47.07	9.768	3.8
49.66	8.410	4.3
52.24	7.205	3.1
54.82	6.836	5.1
57.40	6.130	3.5
59.97	5.948	3.0
62.53	6.016	3.0
65.09	6.052	3.0
67.65	6.066	3.6
70.20	6.139	3.0
72.75	5.948	3.0
75.29	5.660	3.3
77.82	5.000	3.4
80.35	4.697	3.3
82.88	4.194	3.4
85.40	3.671	4.7
87.91	3.087	3.5

90.42	2.680	3.9
92.92	2.251	4.1
97.91	1.780	3.4
102.88	1.396	3.9
107.82	1.235	2.9
112.75	1.005	3.5
117.65	.8691	3.3
122.53	.6741	3.5
127.39	.5776	3.3
132.24	.5084	3.3
137.06	.5206	3.0
141.88	.5672	3.7
146.67	.6122	3.1
151.46	.6734	3.5
156.23	.6534	4.6
161.00	.5603	3.1
165.76	.4294	6.9
170.51	.2645	4.2

ENERGY = 30.40 EX = 4.20

THETA CM (°)	(MB/SR)	% ABS. ERROR
13.09	5.990	5.9
15.71	5.186	3.0
18.32	4.517	5.1
20.93	3.748	6.5
26.15	2.904	4.1
28.76	2.388	3.0
31.36	2.086	3.1
33.96	1.840	3.0
36.56	1.603	7.0
39.16	1.364	3.1
41.75	1.108	3.3
44.34	.9425	3.3
46.93	.8827	4.7
49.51	.7704	8.5
52.09	.8562	4.1
54.66	.9228	3.8
57.23	.9533	3.8
59.80	.9813	3.9
62.36	1.038	4.2

64.92	1.136	3.9
67.47	1.070	4.8
70.02	1.176	3.1
72.56	1.128	3.0
77.63	1.006	2.9
82.68	.9227	3.3
85.20	.8942	4.1
87.71	.7767	3.2
90.22	.7065	4.8
92.72	.6655	3.8
97.71	.6116	3.4
102.68	.5668	4.1
107.63	.5822	2.9
112.56	.5573	3.7
117.47	.5490	3.1
122.36	.5028	3.5
127.23	.4677	3.2
132.09	.4179	3.6
136.92	.4123	3.0
141.75	.3776	3.8
151.36	.3842	4.0
156.15	.3705	6.1
160.93	.3154	2.9
165.70	.2674	8.2
170.47	.1996	5.9

ENERGY = 30.40 EX = 5.23

THETA CM (°)	(MB/SR)	% ABS. ERROR
18.32	.2345	10.4
20.93	.2536	19.4
36.56	.2291	20.2
39.16	.1856	13.7
41.75	.2079	12.8
46.93	.2320	11.1
49.51	.1969	13.3
52.09	.2167	11.6
54.66	.2323	15.2
57.23	.2176	13.8
59.80	.1899	16.5
62.36	.1872	13.4

67.47	.1572	15.8
70.02	.1737	11.1
72.56	.1479	11.7
82.68	.1149	11.1
87.71	.0927	10.4
92.72	.0719	10.5
97.71	.0632	10.9
102.68	.0478	10.5
107.63	.0427	10.7
112.56	.0410	11.1
117.47	.0449	11.4
122.36	.0516	10.9
127.23	.0568	11.1
132.09	.0577	10.8
136.92	.0622	11.9
141.75	.0434	12.0
151.36	.0307	11.8
156.15	.0250	18.3
160.93	.0163	12.3

ENERGY = 30.40 EX = 6.01

THETA CM (°)	(MB/SR)	% ABS. ERROR
13.09	2.652	15.1
15.71	2.600	11.3
18.32	2.544	11.0
20.93	2.318	10.5
26.15	2.397	13.0
28.76	2.435	10.7
31.36	2.242	10.6
33.96	2.214	11.5
36.56	2.342	10.7
39.16	2.139	11.1
41.75	2.121	11.0
46.93	2.012	13.5
52.09	2.094	10.5
57.23	1.583	13.3
59.80	1.716	12.9
62.36	1.500	11.5
64.92	1.537	11.8
67.47	1.094	14.0

70.02	1.172	10.5
72.56	1.003	10.6
77.63	.7522	10.4
82.68	.5350	10.4
85.20	.4973	11.7
87.71	.4112	10.5
90.22	.3831	10.7
92.72	.3122	10.5
97.71	.2634	12.0
102.68	.2169	10.8
107.63	.1747	10.5
112.56	.1416	11.9
117.47	.1228	10.7
122.36	.1098	10.6
127.23	.0987	10.5
132.09	.0930	10.6
136.92	.0919	10.5
141.75	.0754	10.7
151.36	.0583	11.6
156.15	.0474	20.1
160.93	.0473	13.9
165.70	.0302	10.4
170.47	.0212	11.9

ENERGY = 30.40 EX = 6.43

THETA CM (°)	(MB/SR)	% ABS. ERROR
13.09	1.071	37.3
15.71	.6637	31.5
18.32	.4093	31.1
20.93	.4000	30.4
26.15	.1278	34.0
31.36	.2257	30.4
33.96	.3399	31.8
36.56	.2896	30.7
39.16	.4478	31.2
41.75	.4223	31.0
46.93	.4340	34.7
57.23	.4186	34.4
59.80	.1480	33.7
62.36	.2048	31.8

64.92	.1056	32.2
67.47	.2163	35.5
70.02	.0412	30.4
72.56	.0554	30.5
77.63	.0310	30.2
82.68	.0671	30.3
85.20	.1068	32.0
87.71	.0703	30.4
90.22	.0897	30.7
92.72	.0644	30.4
97.71	.1091	32.5
102.68	.1155	30.7
107.63	.1271	30.3
112.56	.0783	32.3
117.47	.0863	30.6
122.36	.0493	30.5
127.23	.0371	30.4
132.09	.0313	30.4
136.92	.0338	30.3
141.75	.0531	30.6
151.36	.0877	31.9
156.15	.0933	45.8
160.93	.0848	35.3
165.70	.0707	30.2
170.47	.0529	32.3

ENERGY = 34.90 EX = 0.0

THETA CM (°)	(MB/SR)	% ABS. ERROR
10.43	2672.	6.4
13.04	2039.	3.0
15.65	1626.	3.2
18.25	1260.	3.2
20.85	942.3	3.2
23.45	660.5	4.3
26.05	434.0	4.0
28.65	267.5	4.2
31.25	146.5	8.8
33.84	81.37	7.9
36.43	44.25	4.9
39.02	29.96	3.4

41.60	26.87	3.3
44.18	30.66	3.1
46.76	33.82	3.0
49.34	36.42	3.0
51.91	36.45	2.9
54.48	34.10	3.0
57.04	29.69	3.1
59.60	24.67	3.3
62.16	19.64	3.5
64.71	14.98	3.6
67.26	10.90	3.5
69.80	8.009	4.2
72.34	5.816	3.9
74.88	4.490	3.6
77.41	3.670	3.8
79.93	3.259	3.2
82.45	3.024	3.1
84.97	2.937	2.9
87.48	2.808	3.2
89.99	2.721	3.1
92.49	2.517	3.1
94.99	2.309	3.1
97.48	2.029	3.1
99.97	1.727	3.5
102.45	1.480	3.1
104.93	1.234	3.2
107.40	.9989	3.7
109.87	.8252	6.0
112.34	.6620	3.2
114.80	.5465	4.2
117.26	.4788	3.2
122.15	.3873	3.1
127.04	.3485	2.9
131.91	.3212	3.0
136.76	.2835	3.1
141.60	.2429	3.2
146.43	.2043	3.0
151.24	.1808	3.3
156.05	.1538	4.7
160.85	.1330	4.0
165.64	.1008	5.1
170.43	.0671	6.2

ENERGY = 34.90 EX = 1.37

THETA CM (°)	(MB/SR)	% ABS. ERROR
10.50	35.66	3.1
13.12	31.96	5.4
15.74	29.58	5.1
18.36	26.11	3.1
20.98	26.46	3.1
23.60	25.95	4.6
26.21	24.92	4.3
28.82	23.81	3.3
31.43	22.11	3.2
34.04	20.17	3.1
36.64	17.94	3.1
39.24	15.47	3.2
41.84	12.45	3.2
44.43	10.41	4.0
47.02	8.214	4.6
49.61	6.983	3.0
52.19	5.847	3.1
54.77	5.429	3.0
57.35	5.221	2.9
59.91	5.271	3.0
62.48	5.315	2.9
65.04	5.325	2.9
67.59	5.117	2.9
70.14	4.829	3.5
72.69	4.450	3.1
75.23	3.966	3.2
77.76	3.393	3.7
80.29	2.860	3.8
82.82	2.363	3.1
85.34	1.927	3.8
87.85	1.597	3.5
90.36	1.366	3.3
92.86	1.152	3.4
95.36	1.052	3.1
97.85	.9372	3.0
100.34	.8987	3.4
102.82	.8300	3.1
105.29	.8021	2.9
107.76	.7408	3.1
110.23	.6818	3.5
112.69	.6224	3.1
115.14	.5678	4.1
117.59	.4913	3.3
122.48	.3645	3.3
127.34	.2739	3.5
132.19	.2248	3.1

137.02	.2180	3.1
141.84	.2467	3.0
146.64	.2869	3.0
151.43	.3328	3.0
156.21	.3319	3.7
160.98	.3058	3.1
165.74	.2428	4.4
170.50	.1575	5.7

ENERGY = 34.90 EX = 4.20

THETA CM (°)	(MB/SR)	% ABS. ERROR
10.47	6.915	14.4
13.08	6.264	8.2
15.70	5.474	8.0
18.31	5.086	11.7
20.92	4.255	5.7
23.53	4.261	11.0
26.14	3.310	3.1
28.75	2.447	3.5
31.35	2.205	3.5
33.95	1.611	5.8
36.55	1.426	3.9
39.14	1.231	5.1
41.74	.9784	5.6
44.32	.8977	6.1
46.91	.7359	3.1
49.49	.6877	2.9
52.07	.7105	3.4
54.64	.7489	3.0
57.21	.7822	5.8
59.78	.8564	3.4
62.34	.9256	3.2
64.90	.9571	3.6
67.45	.9513	3.5
69.99	.9409	3.2
72.54	.9118	3.0
75.07	.8605	3.2
77.61	.7933	3.1
80.14	.6937	2.9
82.66	.6272	3.0

85.18	.5553	3.3
87.69	.4820	3.0
90.20	.4449	3.0
92.70	.3781	3.4
95.20	.3698	3.2
97.69	.3312	3.1
102.66	.3165	3.0
105.13	.3296	4.4
107.61	.3105	3.2
110.07	.3168	4.1
112.53	.3111	3.3
117.44	.2932	3.1
122.34	.2659	3.1
127.21	.2309	3.3
132.07	.2040	3.1
136.91	.1897	3.3
141.73	.1796	3.3
151.35	.1829	3.0
156.14	.1785	3.5
160.92	.1549	3.4
165.70	.1210	6.0
170.47	.0887	6.9

ENERGY = 34.90 EX = 5.23

THETA CM (°)	(MB/SR)	% ABS. ERROR
36.55	.1838	11.2
39.14	.1906	10.4
41.74	.2033	10.8
44.32	.2078	12.1
52.07	.1668	12.0
54.64	.1516	11.0
57.21	.1275	12.7
59.78	.1300	10.5
62.34	.1305	11.7
64.90	.1061	11.4
67.45	.1001	13.9
69.99	.0922	10.4
72.54	.0945	13.4
75.07	.0864	10.6
77.61	.0778	16.5

80.14	.0705	11.0
82.66	.0700	11.0
85.18	.0680	10.5
87.69	.0528	11.1
90.20	.0525	10.9
92.70	.0491	15.1
97.69	.0345	11.7
102.66	.0289	15.8
107.61	.0193	17.3
112.53	.0167	16.6
117.44	.0146	12.1
122.34	.0166	10.9
127.21	.0176	10.7
132.07	.0187	12.1
136.91	.0207	11.9
141.73	.0187	10.8
151.35	.0142	10.6
156.14	.0143	12.9
160.92	.0109	10.9
165.70	.0070	11.0
170.47	.0040	20.9

ENERGY = 34.90 EX = 6.01

THETA CM (°)	(MB/SR)	% ABS. ERROR
10.47	2.529	12.6
13.08	2.704	27.3
15.70	2.353	27.0
18.31	2.717	14.7
20.92	2.429	11.4
23.53	2.760	14.9
26.14	2.752	12.8
28.75	2.367	11.9
31.35	2.292	10.5
33.95	2.208	11.0
36.55	2.186	10.4
39.14	2.188	10.4
41.74	2.161	10.5
44.32	2.198	10.8
46.91	2.117	10.5
49.49	2.054	10.5

52.07	1.992	10.4
54.64	1.848	10.5
57.21	1.744	10.6
59.78	1.595	10.4
62.34	1.454	10.4
64.90	1.279	10.6
67.45	1.053	10.5
69.99	.9228	10.5
72.54	.7353	10.8
75.07	.6398	10.4
77.61	.5559	10.9
80.14	.4588	11.1
82.66	.3997	10.6
85.18	.3411	10.5
87.69	.2488	12.3
90.20	.2385	11.5
92.70	.2024	11.0
95.20	.1831	15.1
97.69	.1542	11.7
102.66	.1178	11.5
105.13	.1156	11.2
107.61	.0870	11.9
110.07	.0727	15.9
112.53	.0688	14.4
117.44	.0660	10.9
122.34	.0532	10.6
127.21	.0462	11.2
132.07	.0417	10.5
136.91	.0352	11.0
141.73	.0363	13.9
146.55	.0399	17.7
151.35	.0393	11.0
156.14	.0410	16.7
160.92	.0391	12.2
165.70	.0338	23.2
170.47	.0290	17.0

ENERGY = 34.90 EX = 6.43

THETA CM (°)	(MB/SR)	% ABS. ERROR
10.47	.9486	33.4

13.08	.9520	58.9
15.70	.6589	58.4
18.31	.4741	36.7
23.53	.4180	37.0
26.14	.5032	33.7
28.75	.2718	32.3
31.35	.3610	30.4
33.95	.2755	31.0
36.55	.3061	30.2
39.14	.3038	30.3
41.74	.3297	30.4
44.32	.2666	30.7
46.91	.2538	30.4
49.49	.1966	30.4
52.07	.1666	30.3
54.64	.1324	30.3
57.21	.1308	30.5
59.78	.0432	30.3
62.34	.0477	30.3
64.90	.0459	30.5
67.45	.0670	30.3
69.99	.0477	30.4
72.54	.1123	30.7
75.07	.0772	30.3
77.61	.0729	31.0
80.14	.0795	31.2
82.66	.0870	30.5
85.18	.0845	30.4
87.69	.1251	32.9
90.20	.1171	31.8
92.70	.1039	31.1
95.20	.1077	37.4
97.69	.0994	32.0
102.66	.0939	31.7
105.13	.0907	31.3
107.61	.0842	32.3
110.07	.0891	38.7
112.53	.0714	36.3
117.44	.0461	31.0
122.34	.0393	30.4
127.21	.0316	31.4
132.07	.0332	30.3
136.91	.0443	31.0
141.73	.0512	35.3
146.55	.0606	41.6
151.35	.0721	31.1
156.14	.0727	40.0
160.92	.0663	32.7
165.70	.0532	51.2
170.47	.0335	40.4

ENERGY = 39.90 EX = 0.0

THETA CM (°)	(MB/SR)	% ABS. ERROR
10.43	2427.	3.3
13.04	1941.	3.1
15.65	1568.	3.0
18.25	1193.	3.0
20.86	858.2	3.3
23.46	568.8	4.2
26.06	359.0	3.3
28.66	206.5	3.6
31.25	110.5	3.9
33.85	58.14	5.5
36.44	34.30	3.4
39.02	26.95	3.1
41.61	27.14	3.0
44.19	30.47	3.3
46.77	32.06	3.2
49.35	31.92	3.1
51.92	29.21	3.2
54.49	25.27	3.2
57.05	20.30	3.4
59.61	15.82	3.2
62.17	11.50	3.5
64.72	8.169	4.1
67.27	5.955	4.2
69.81	4.447	3.5
72.35	3.481	3.1
74.89	2.915	3.1
77.42	2.691	2.9
79.94	2.510	3.0
82.46	2.360	2.9
84.98	2.208	3.2
87.49	2.007	3.2
90.00	1.792	3.1
92.50	1.524	3.1
95.00	1.254	3.8
97.49	1.029	3.7
99.98	.8254	3.2
102.46	.6534	3.3
104.94	.5298	4.1

107.42	.4195	3.5
109.88	.3679	3.5
112.35	.3087	3.4
117.27	.2732	2.9
122.16	.2515	3.0
127.05	.2251	3.2
131.91	.1792	3.2
136.77	.1315	4.2
141.61	.0924	3.5
146.43	.0718	3.5
151.25	.0660	3.9
156.06	.0687	3.3
160.85	.0646	4.6
165.65	.0540	4.9
170.43	.0336	6.5

ENERGY = 39.90 EX = 1.37

THETA CM (°)	(MB/SR)	% ABS. ERROR
10.49	34.80	3.7
13.11	31.79	2.9
15.73	26.91	11.1
18.35	25.56	9.6
20.96	27.28	3.9
23.58	24.61	3.5
26.19	23.55	4.0
28.80	24.32	3.3
31.41	22.31	3.7
34.01	19.26	4.4
36.62	16.87	3.1
39.22	13.70	3.3
41.81	10.64	3.2
44.40	8.352	3.6
46.99	6.573	3.6
49.58	5.391	3.3
52.16	4.743	3.0
54.74	4.660	3.1
57.31	4.585	3.0
59.88	4.585	3.0
62.44	4.472	2.9
65.00	4.268	3.0

67.55	3.929	3.1
70.10	3.507	3.2
72.65	2.995	3.2
75.19	2.418	3.4
77.72	2.009	3.8
80.25	1.589	3.2
82.77	1.271	3.1
85.29	1.034	3.2
87.81	.8676	3.4
90.31	.7796	3.0
92.82	.6926	3.0
95.31	.6581	3.5
97.80	.6137	3.1
100.29	.5969	2.9
102.77	.5414	3.0
105.25	.5010	2.9
107.72	.4357	4.0
110.18	.3984	3.1
112.64	.3308	3.3
117.55	.2322	3.7
122.44	.1545	3.4
127.30	.1161	3.5
132.15	.1035	2.9
136.99	.1100	3.0
141.81	.1231	3.5
146.61	.1377	4.1
151.41	.1508	3.6
156.19	.1486	4.0
160.96	.1268	4.8
165.73	.0984	7.4
170.49	.0582	6.6

ENERGY = 39.90 EX = 4.20

THETA CM (°)	(MB/SR)	% ABS. ERROR
10.47	7.073	4.2
13.08	6.340	7.7
15.69	4.764	12.0
20.92	3.865	4.0
23.53	3.167	3.9
26.13	2.707	8.3

28.74	2.015	9.4
31.34	1.838	3.1
33.94	1.463	10.8
36.54	1.245	3.1
39.13	1.011	4.0
41.72	.7924	3.5
44.31	.6502	2.9
46.90	.5841	3.0
49.48	.5196	4.2
52.06	.5525	3.1
54.63	.6059	3.2
57.20	.6621	3.1
59.76	.7089	3.2
62.32	.7290	3.1
64.88	.7544	3.4
67.43	.7368	3.1
69.98	.7300	3.1
72.52	.6716	3.2
75.06	.5887	3.8
77.59	.5459	3.7
80.12	.4853	3.0
82.64	.4109	3.1
85.16	.3503	3.5
87.67	.3028	3.6
90.18	.2703	4.6
92.68	.2439	3.4
95.18	.2233	3.4
97.67	.2033	3.3
102.64	.1940	3.1
105.12	.1854	4.5
107.59	.1734	4.1
110.06	.1727	3.1
112.52	.1606	3.4
117.43	.1459	3.2
122.32	.1272	3.1
127.19	.1104	3.5
132.05	.0939	3.1
136.89	.0855	3.3
141.72	.0814	3.4
151.34	.0811	3.0
156.13	.0766	8.5
160.92	.0732	3.0
165.69	.0615	6.3
170.46	.0487	4.5

ENERGY = 39.90 EX = 5.23

THETA CM (°)	(MB/SR)	% ABS. ERROR
36.54	.1508	15.5
39.13	.1581	12.9
41.72	.1409	14.6
44.31	.1370	16.9
52.06	.0967	11.9
54.63	.0809	13.7
57.20	.0817	11.8
59.76	.0732	10.4
62.32	.0670	11.6
64.88	.0691	12.6
67.43	.0526	15.2
69.98	.0558	10.6
72.52	.0525	12.5
75.06	.0453	13.3
77.59	.0382	11.7
80.12	.0390	10.5
82.64	.0332	10.6
85.16	.0342	12.5
87.67	.0323	12.0
90.18	.0234	16.9
92.68	.0262	12.3
95.18	.0248	10.5
97.67	.0246	12.3
102.64	.0184	10.9
107.59	.0197	20.5
110.06	.0178	13.3
112.52	.0129	13.2
117.43	.0064	12.4
122.32	.0069	14.2
127.19	.0060	11.8
132.05	.0067	11.5
136.89	.0085	11.4
141.72	.0076	13.4
151.34	.0074	11.9
156.13	.0065	14.6
160.92	.0063	18.8
165.69	.0037	29.4

ENERGY = 39.90 EX = 6.01

THETA CM (°)	(MB/SR)	% ABS. ERROR
15.69	1.919	12.5
20.92	1.487	13.3
23.53	2.005	11.1
26.13	1.770	12.0
28.74	1.676	14.4
31.34	1.767	11.1
33.94	1.745	11.8
36.54	1.965	10.8
39.13	2.066	10.5
41.72	2.116	10.7
44.31	2.077	10.4
46.90	1.890	10.8
49.48	2.035	11.1
52.06	1.817	10.5
54.63	1.551	10.7
57.20	1.496	11.2
59.76	1.184	11.2
62.32	1.075	11.3
64.88	.8879	11.1
67.43	.7601	11.3
69.98	.6528	10.9
72.52	.5044	11.5
75.06	.4523	12.4
77.59	.4054	10.5
80.12	.3363	12.7
82.64	.3009	10.5
85.16	.2443	12.6
87.67	.1916	10.7
90.18	.1699	12.6
92.68	.1408	10.8
95.18	.1149	13.6
97.67	.0915	15.4
102.64	.0667	11.9
107.59	.0378	16.9
110.06	.0366	10.6
112.52	.0281	15.1
117.43	.0286	15.0
122.32	.0266	12.2
127.19	.0238	12.1
132.05	.0222	11.6
136.89	.0213	14.6
141.72	.0163	16.0
146.54	.0295	13.5
151.34	.0197	12.7
156.13	.0283	15.0
160.92	.0262	11.9

165.69	.0227	22.4
170.46	.0217	11.1

ENERGY = 39.90 EX = 6.43

THETA CM (°)	(MB/SR)	% ABS. ERROR
15.69	1.004	33.2
20.92	.7227	34.4
23.53	.2866	31.1
26.13	.6673	32.5
28.74	.3586	36.2
31.34	.5858	31.2
33.94	.5721	32.1
36.54	.4336	30.8
39.13	.3206	30.4
41.72	.2491	30.6
44.31	.2267	30.3
46.90	.3410	30.8
49.48	.2358	31.2
52.06	.1024	30.3
54.63	.2479	30.6
57.20	.1186	31.3
59.76	.2559	31.4
62.32	.1610	31.4
64.88	.1823	31.2
67.43	.1563	31.5
69.98	.1368	31.0
72.52	.1599	31.7
75.06	.1268	33.1
77.59	.0910	30.3
80.12	.1099	33.5
82.64	.0932	30.4
85.16	.1065	33.4
87.67	.1152	30.7
90.18	.0874	33.3
92.68	.0987	30.8
95.18	.0960	34.9
97.67	.0858	37.9
102.64	.0636	32.3
107.59	.0546	40.3
110.06	.0459	30.5

112.52	.0400	37.4
117.43	.0313	37.2
122.32	.0294	32.7
127.19	.0298	32.5
132.05	.0300	32.0
136.89	.0310	36.6
141.72	.0351	38.8
146.54	.0338	34.7
151.34	.0408	33.4
156.13	.0318	37.2
160.92	.0324	32.4
165.69	.0270	49.9
170.46	.0163	31.2

ENERGY = 44.90 EX = 0.0

THETA CM (°)	(MB/SR)	% ABS. ERROR
10.44	2190.	3.0
13.04	1837.	3.2
15.65	1492.	2.9
18.26	1101.	3.9
20.86	762.6	3.4
23.46	505.0	4.3
26.06	317.2	3.1
28.66	168.1	4.6
31.26	84.27	4.5
33.85	43.77	5.4
36.44	27.52	3.3
39.03	24.50	3.1
41.62	26.23	3.2
44.20	27.29	3.1
46.78	26.92	4.6
49.36	25.64	3.1
51.93	22.24	3.3
54.50	17.80	3.8
57.06	13.21	4.3
59.62	9.770	4.0
62.18	6.886	4.2
64.73	4.748	4.7
67.28	3.483	3.8
69.82	2.732	3.3

72.36	2.404	3.7
74.90	2.170	4.4
77.43	1.984	4.5
79.95	1.818	4.8
82.48	1.735	3.3
84.99	1.485	4.6
87.50	1.236	3.4
90.01	1.002	5.7
92.51	.7999	4.3
97.50	.4636	3.0
99.99	.3361	4.0
102.47	.2884	4.2
104.95	.2421	6.9
107.43	.2130	3.4
109.90	.2024	6.7
112.36	.1901	3.0
117.28	.1783	3.2
122.17	.1575	3.1
127.06	.1225	3.0
131.92	.0870	3.9
136.77	.0512	3.9
141.61	.0297	4.6
146.44	.0217	5.4
151.25	.0235	3.5
156.06	.0277	3.3
160.86	.0285	3.2
165.65	.0222	5.2
170.44	.0151	5.6

ENERGY = 44.90 EX = 1.37

THETA CM (°)	(MB/SR)	% ABS. ERROR
10.48	29.19	5.0
13.10	25.87	9.7
15.72	25.41	5.6
18.34	24.68	2.9
20.95	24.74	3.2
23.57	26.01	3.3
26.18	25.24	3.0
28.79	24.29	2.9
31.39	21.94	3.2

34.00	18.98	3.3
36.60	15.18	3.1
39.20	11.80	3.1
41.79	8.912	3.7
44.38	7.053	3.7
46.97	4.856	10.5
49.56	4.232	3.7
52.14	4.051	3.2
54.71	3.984	2.9
57.28	3.850	3.1
59.85	3.762	3.3
62.41	3.533	3.5
64.97	3.133	3.5
67.53	2.688	3.7
70.08	2.207	4.2
72.62	1.836	4.5
75.16	1.442	5.8
77.69	1.114	5.1
80.22	.8985	5.2
82.74	.7579	4.3
85.26	.6486	4.2
87.78	.5916	3.1
90.28	.5401	3.3
92.79	.4984	3.0
97.77	.4290	3.1
100.26	.3679	3.4
102.74	.3362	3.6
105.22	.2906	7.8
107.69	.2371	3.7
110.16	.1923	8.7
112.62	.1538	4.2
117.52	.0951	3.1
122.41	.0659	3.3
127.28	.0587	3.0
132.13	.0598	3.0
136.97	.0673	3.2
141.79	.0704	3.2
146.60	.0743	3.5
151.39	.0716	3.3
156.18	.0660	3.1
160.95	.0539	3.5
165.72	.0361	4.5
170.48	.0208	7.6

ENERGY = 44.90 EX = 4.20

THETA CM (°)	(MB/SR)	% ABS. ERROR
18.30	4.435	6.6
20.91	3.263	5.6
23.52	3.199	4.1
26.13	2.289	7.2
28.73	2.336	4.8
31.34	1.642	3.2
33.94	1.321	3.9
36.53	1.062	3.9
39.13	.7992	3.2
41.72	.6487	4.2
46.89	.4790	4.1
49.47	.5378	4.6
52.05	.4755	3.5
54.62	.5336	3.6
57.19	.5625	3.3
59.75	.5750	3.6
62.31	.6079	3.0
64.87	.5861	3.0
67.42	.5528	3.3
69.97	.5113	4.2
72.51	.4504	3.8
75.05	.4086	4.3
77.58	.3387	5.9
80.11	.2887	9.7
82.63	.2778	3.0
85.15	.2277	4.2
87.66	.2033	3.6
90.17	.1809	6.1
92.67	.1590	3.2
97.66	.1395	3.6
102.63	.1155	5.7
105.11	.1130	6.0
107.58	.1023	4.4
110.05	.0992	6.9
112.51	.0862	3.5
117.42	.0741	3.6
122.31	.0642	3.5
127.18	.0554	3.5
132.04	.0477	3.0
136.89	.0442	3.1
141.71	.0405	3.4
151.33	.0403	3.1
156.13	.0403	3.0
160.91	.0376	3.7
165.69	.0340	4.5
170.46	.0289	3.3

ENERGY = 44.90 EX = 5.23

THETA CM (°)	(MB/SR)	% ABS. ERROR
31.34	.1001	11.5
33.94	.1390	10.5
36.53	.1447	10.7
41.72	.1199	13.7
52.05	.0774	13.5
54.62	.0694	17.4
57.19	.0622	11.9
59.75	.0616	14.1
62.31	.0502	12.5
67.42	.0462	11.1
72.51	.0288	16.6
75.05	.0329	19.4
77.58	.0306	14.6
80.11	.0265	20.2
85.15	.0209	12.2
87.66	.0186	11.0
90.17	.0165	11.9
92.67	.0147	10.5
102.63	.0092	12.4
107.58	.0072	10.5
112.51	.0082	16.0
117.42	.0041	12.9
122.31	.0038	14.5
127.18	.0032	12.9
132.04	.0035	10.8
136.89	.0042	14.9
141.71	.0045	13.4
151.33	.0039	12.6
156.13	.0038	11.5
160.91	.0034	14.4

ENERGY = 44.90 EX = 6.01

THETA CM (°)	(MB/SR)	% ABS. ERROR
20.91	1.634	11.7
23.52	1.947	11.4
26.13	1.516	11.6
28.73	1.786	10.6
31.34	1.554	11.0
33.94	1.859	10.4
36.53	1.946	10.4
39.13	2.013	10.5
41.72	1.858	10.4
44.31	1.927	10.9
46.89	1.788	11.6
49.47	1.688	11.8
52.05	1.511	10.8
54.62	1.378	10.7
57.19	1.122	11.8
59.75	.9125	10.8
62.31	.8363	11.4
64.87	.6283	16.6
67.42	.5239	16.4
69.97	.4577	11.1
72.51	.4170	12.8
75.05	.3920	13.3
77.58	.3019	13.7
80.11	.2426	18.7
82.63	.2112	11.8
85.15	.1673	13.0
87.66	.1376	11.4
90.17	.1141	17.0
92.67	.0910	11.3
97.66	.0577	10.7
102.63	.0383	10.6
105.11	.0271	31.8
107.58	.0195	12.9
112.51	.0168	11.5
117.42	.0163	11.8
122.31	.0146	11.1
127.18	.0175	10.5
132.04	.0137	11.4
136.89	.0110	11.9
141.71	.0113	11.6
151.33	.0123	11.9
156.13	.0143	11.1
160.91	.0129	11.7
165.69	.0132	12.1
170.46	.0137	11.2

ENERGY = 44.90 EX = 6.43

THETA CM (°)	(MB/SR)	% ABS. ERROR
20.91	.3464	32.0
26.13	.4489	31.9
28.73	.4912	30.5
31.34	.5140	31.0
33.94	.3703	30.2
36.53	.3273	30.3
39.13	.2664	30.4
41.72	.3676	30.3
44.31	.2683	31.0
46.89	.2180	31.9
49.47	.2454	32.1
52.05	.1441	30.7
54.62	.1719	30.7
57.19	.2410	32.2
59.75	.2688	30.7
62.31	.1489	31.6
64.87	.1787	39.8
67.42	.1621	39.5
69.97	.1307	31.1
72.51	.1274	33.7
75.05	.0829	34.4
77.58	.1085	34.9
80.11	.1123	43.3
82.63	.1258	32.2
85.15	.1144	34.0
87.66	.1047	31.6
90.17	.0883	40.5
92.67	.0676	31.5
97.66	.0457	30.7
102.63	.0303	30.6
105.11	.0297	67.4
107.58	.0270	33.8
112.51	.0213	31.8
117.42	.0234	32.1
122.31	.0266	31.2
127.18	.0234	30.4
132.04	.0239	31.7
136.89	.0220	32.3

141.71	.0185	31.9
151.33	.0165	32.3
156.13	.0149	31.2
160.91	.0161	32.0
165.69	.0129	32.6
170.46	.0085	31.4

10.2 ALIGNMENT

Before starting the experiment the detector and target system were carefully aligned. A theodolite (T2) was positioned and leveled so that it could be rotated in the vertical plane and thus view either the pin in the centre of the switching magnet or the pin in the centre of the scattering chamber. This ensured that the theodolite was centred on the straight line between these two reference pcints. The height was adjusted so that the theodolite was level with the median plane of the switching magnet (and hopefully of the cyclotron). Once the theodolite was properly set up it was used to align the detector and target system.

While looking through the theodolite into the scattering chamber at 0.00°, the turntable was rotated in steps of 10.00° so that each detector was positioned in turn at 0.00°. Taking advantage of scribe markings on the detector defining slits, each detector was verified to be at 0.00° ± 0.01°. In a similar fashion the anti-scattering baffles were aligned. The height was also set so that the detectors were centred about the median plane.

The target ladder was lowered into position and, using the theodolite, verified to be correctly centred.

The angle readout was checked by setting the target at 90° and seeing that it was indeed parallel to the line of sight (0.00°). An approximation is made here since this was done with the chamber at atmospheric pressure. Under vacuum the chamber lid flexed, thus lowering the target ladder slightly. This was not deemed significant.

In order to align the two 15° monitor detectors it was necessary to use the proton beam. First a well-defined proton beam was obtained in the scattering chamber, using the screens to see that it was on centre. The two extreme detectors of the eight detector array were then alternately positioned at 15° and -15°. The number of protons elastically scattered into the two detectors from a nickel target placed perpendicular to the incident proton beam was recorded for a fixed number of incident protons (using the Faraday cup as a normalisation). Thus the ratio of the number of counts of these two detectors indicated whether or not the proton beam was on axis. Adjustments to the beam transport were made until the ratio was 1.00 ± 0.01. Then the detector array was moved out of the way and the 15° monitor detectors were used. Their positions were adjusted until they also yielded a ratio of 1.00 ± 0.01. The detector array was used once more at overlapping positions to verify that the proton beam alignment was still satisfactory.

10.3 CROSS OVER TECHNIQUE

To measure the mean energy of the proton beam bent into the 45° left beamline a kinematic cross over technique[27] was used. This relied on the fact that the angle at which protons are scattered with the same energy from two target nuclei of different masses uniquely determines the incident energy of the protons. For our calibration a piece of plastic sheeting was used to provide carbon and hydrogen nuclei as targets.

First a proton beam of arbitrary energy was obtained in the scattering chamber. By viewing the beam spot on the screens and comparing the count rates of the 15° monitor detectors the proton beam was verified to be on axis and well defined (1.0 by 0.5 cm at the centre of the chamber). The plastic (CH) target was lowered into position. Spectra were collected, both left and right of the beam, for numerous angles in the range of the kinematic cross over. The separation (number of channels) between the spectrum peaks corresponding to the first excited state of carbon and hydrogen was plotted as a function of angle. A quadratic fit was performed, and the cross over angle and thus the beam energy determined.

This process was repeated for proton energies of

25.3, 30.8, 32.1, and 39.0 MeV. Each time the strength of the field of the switching magnet was measured using an NMR technique. A calibration of the mean proton beam energy bent into the 45° left scattering chamber was thus determined as a function of the switching magnet field strength or the NMR readings. This calibration was used to set up the experiments at the desired energies. Uncertainty in determining the mean energy of the proton beam was 100 kev.

10.4 COMPUTER CODES

The two programs used to analyse the spectra and to calculate the differential cross sections have already been discussed in detail in section 5.0. A brief description of the three theoretical analysis programs used, namely: SEEK, MAGALI, and CHUCK, will be given here.

SEEK[10] is a Fortran program used to carry out optical model analyses of elastic scattering data of spin 0 or 1/2, charged or uncharged particles, from complex nuclei with zero spin. It permits searches to be made over the nuclear optical model parameter space to yield optimum fits to differential cross section, polarisation, and total reaction cross section data. The search uses the Oak Ridge - Oxford method in which the chi squared surface is expanded to second order by a Taylor series, approximated by a quadratic function and solved for the minimum. The numerical integration of the Schrodinger equation is carried out with a modified, multi-step Numerov method.

The multi-step technique was a modification made to the original program at the University of Manitoba. Other changes made here include the ability to handle differential cross section and polarisation data at independent angles, spin - orbit geometry independent of real central geometry, increasing to double precision, increasing the maximum number of partial waves to 46 (previously 30), the number of integration steps to 400 (previously 200), and correcting mixed mode expressions. Three versions exist with the following options:

SEEK1 - Gaussian surface potential

SEEK2 - derivative Wood - Saxon potential

SEEK3 - as SEEK2 with new, optional input routine

SEEK3 was used in the present work.

The program MAGALI[11] is an improved version of SEEK using the same methods as described above. However it also handles spin 1 incident projectiles , performs calculations incorporating the finite angular width of the detectors, permits up to 60 partial waves, and is generally more versatile than SEEK. Changes have been made to the original program here again, namely: multi- step method in the integration, conversion to double precision, and numerous small changes to improve the run time. MAGALI was used to obtain final fits for this work.

CHUCK[22] performs coupled channels calculations to yield elastic and inelastic scattering differential cross sections and tensor polarisations. The program can be used to couple reaction processes as well but this was not done here. The expansion of the interaction potential is only to first order in the deformation terms. The coupling to inelastic channels is limited to members of the ground state rotational band, so it was only useful for the first three states. It is important to note that the program does not perform searches but simply does a single calculation based on the input data. This is due to the very long time required for a single calculation.

11.0 REFERENCES

(1) Y. Horikawa, Y. Torizuka, A. Nakada, S. Mitsunobu, Y. Kojema, and M. Kimura, Phys. Letters 36B (1971) 9

(2) A. Nakada, and Y. Torizuka, J. Phys. Soc. Japan 32 (1972) 1

(3) W. J. Thompson, and J. S. Eck, Phys. Letters 67B (1977) 151

(4) P. M. Endt, and C. van der Leun, Nucl. Phys. A214 (1963) 1

(5) T. Tamura, Nucl. Phys. 73 (1965) 241

(6) P. E. Hodgson, Nuclear Reactions and Nuclear Structure Clarendon Press Oxford 1971

(7) T. Tamura, Rev. Mod. Phys. 37 (1965) 679

(8) A. M. Sourkes, M. S. de Jong, C. A. Goulding, W. T. H. van Oers, E. A. Ginkel, R. F. Carlson, A. J. Cox, and D. J. Margaziotis, Nucl. Instr. Meth. 143 (1977) 589

(9) H. Wilmes, Nucl. Instr. Meth. 41 (1966) 122

(10) M. A. Melkanoff, J. Raynal, and T. Sawada, UCLA 66-10

(11) J. Raynal, Service de Physique Theorique, Centre d'Etudes Nucleaires, Saclay DPh-T/69-42

(12) G. M. Crawley, and G. T. Garvey, Phys. Rev. 160 (1967) 981

(13) A. A. Rush, E. J. Burge, V. E. Lewis, D. A.

Smith, and N. K. Ganguly, Nucl. Phys. A104 (1967) 340

(14) Y. S. Horowitz, N. K. Sherman, and R. E. Bell, Nucl. Phys. a134 (1969) 577

(15) A. Willis, B. Geoffrion, N. Marty, M. Morlet, C. Rolland, and B. Tatischeff, NUcl. Phys. A112 (1968) 417

(16) W. A. Blanpied, Phys. Rev. 113 (1959) 1099

(17) A. G. Blair, C. Glashausser, R. de Swiniarski, J. Goudergues, R. Lombard, B. Mayer, J. Thirion, and P. Vaganov, Phys. Rev. C1 (1970) 444

(18) V. E. Lewis, E. J. Burge, A. A. Rush, and D. A. Smith, Nucl. Phys. A101 (1967) 589

(19) C. S. Curran, T. E. Drake, A. Johnston, S. W. Brain, W. A. Gillespie, E. W. Lees, R. P. Singhal, and A. G. Slight, J. Phys. A5 (1972) L39

(20) F. D. Becchetti, and G. W. Greenlees, Phys. Rev. 182 (1969) 1190

(21) N. E. Davison, D. K. Hasell, A. M. Sourkes, W. T. H. van Oers, R. F. Carlson, A. J. Cox, D. J. Margaziotis, to be published

(22) P. D. Kunz, unpublished

(23) J. E. Emmaa, R. K. Cole, C. N. Waddell, H. S. Sandhu, and R. R. Deltman, Nucl. Phys.

A218 (1974) 125

(24) B. Zwieglinski, G. M. Crawley, H. Nann, and J. A. Nolen, Jr. MSUCL-247 1977

(25) G. C. Li, I. Sick, and M. R. Yearian, Phys. Rev. C9 (1974) 1861

(26) T. Tamura ORNL-4152

(27) R. Smyth, Rev. Sci. Instr. 41 (1966) 122

(28) W. T. H. van Oers, and J. M. Cameron, Phys. Rev. 184 (1969) 1061